UNIVERSITAT POLITÈCNICA DE CATALUNYA
BARCELONATECH
Departament d'Enginyeria Electrònica

FAULT DIAGNOSIS AND FAULT TOLERANT CONTROL OF MULTIPHASE VOLTAGE SOURCE CONVERTERS FOR APPLICATION IN TRACTION DRIVES

Thesis submitted in partial fulfillment of the requirement for the PhD degree issued by the Universitat Politècnica de Catalunya, in its Electronic Engineering Program.

Mehdi Salehifar

Director: *Dr. Manuel Moreno Eguilaz*

July 2014

UNIVERSITAT POLITÈCNICA DE CATALUNYA
BARCELONATECH
Escola de Doctorat

Acta de calificación de tesis doctoral

Curso académico:

Nombre y apellidos **Mehdi Salehifar**

Programa de doctorado **Electronic Engineering**

Unidad estructural responsable del programa **Department of Electronic Engineering**

Resolución del Tribunal

Reunido el Tribunal designado a tal efecto, el doctorando / la doctoranda expone el tema de la su tesis doctoral titulada _____

_____.

Acabada la lectura y después de dar respuesta a las cuestiones formuladas por los miembros titulares del tribunal, éste otorga la calificación:

☐ NO APTO ☐ APROBADO ☐ NOTABLE ☐ SOBRESALIENTE

(Nombre, apellidos y firma) Presidente/a		(Nombre, apellidos y firma) Secretario/a
(Nombre, apellidos y firma) Vocal	(Nombre, apellidos y firma) Vocal	(Nombre, apellidos y firma) Vocal

_____, _____ de _____ de _____

El resultado del escrutinio de los votos emitidos por los miembros titulares del tribunal, efectuado por la Escuela de Doctorado, a instancia de la Comisión de Doctorado de la UPC, otorga la MENCIÓN CUM LAUDE:

☐ SÍ ☐ NO

(Nombre, apellidos y firma) Presidente de la Comisión Permanente de la Escuela de Doctorado	(Nombre, apellidos y firma) Secretaria de la Comisión Permanente de la Escuela de Doctorado

Barcelona a _____ de _____ de _____

Abstract

There is an increasing demand for vehicles with less environmental impact and higher fuel efficiency. To meet these requirements, the transportation electrification has been introduced in both academia and industry during last years. Electric vehicle (EV) and hybrid Electric vehicle (HEV) are two practical examples in transportation systems.

The typical power train in the EVs consists of three main parts including energy source, power electronics and an electrical motor. Regarding the machine, permanent magnet (PM) motors are the dominant choice for light duty hybrid vehicles in industry due to their higher efficiency and power density.

In order to operate the power train, the electrical machine can be supplied and controlled by a voltage source inverter (VSI). The converter is subjected to various fault types. According to the statistics, 38% of faults in a motor drive are due to the power converter. On the other side, the electrical power train should meet a high level of reliability.

Multiphase PM machines can meet the reliability requirements due to their fault-tolerant characteristics. The machine can still be operational with faults in multiple phases. Consequently, to realize a multiphase fault-tolerant motor drive, three main concepts should be developed including fault detection (FD), fault isolation and fault-tolerant control. This PhD thesis is therefore focused on FD and fault-tolerant control of a multiphase VSI.

To achieve this research goal, the presented FD and control methods of the power converter are thoroughly investigated through literature review. Following that, the operational condition of the multiphase converter supplying the electrical machine is studied.

Regarding FD methods in multiphase, three new algorithms are presented in this thesis. These proposed FD methods are also embedded in new fault-tolerant control algorithms. At the first step, a novel model based FD method is proposed to detect multiple open switch faults. This FD method is included in the developed adaptive proportional resonant control algorithm of the power converter. At the second step, two signal based FD methods are proposed. Fault-tolerant control of the power converter with the conventional PI controller is discussed. Furthermore, the theory of SMC is developed. At the last step, finite control set (FCS) model predictive control (MPC) of the five-phase brushless direct current (BLDC) motor is discussed for the first time in this thesis. A simple FD method is derived from the control signals. Inputs to all developed methods are the five-phase currents of the motor.

The theory of each method is explained and compared with available methods. To validate the developed theory at each part, FD algorithm is embedded in the fault-tolerant control algorithm. Experimental results are conducted on a five-phase BLDC motor drive. The electrical motor used in the

experimental results has an in-wheel outer rotor structure. This motor is suitable for electric vehicles. At the end of each part, the remarkable points and conclusions are presented.

Acknowledgment

First of all, I would like to thank my supervisors, prof. Manuel Moreno-Eguilaz and Vicenc Sala, for their guidance, support, patience and trust during my studies in the Universitat Politècnica de Catalunya. I am forever grateful as this work has not been possible without their knowledge and experience.

Thanks to prof. Jose Luis Romeral, the head of MCIA group, since he believed in my capabilities and gave me the opportunity to pursue my PhD thesis in Spain. I also thank him for his discussions, comments, suggestions during this research. In addition, I appreciate his support for publishing the results in international conferences and journals.

To the members of MCIA research group, to all of them, many thanks for their friendship and support. You strongly supported me during those three years.

I also would like to thank my family for everything they have done for me. They have supported and encouraged me during my PhD. Thanks for teaching me the precious value of education.

To my friends in Spain, who have given me great moments and make me feel at home.

Contents

List of Figures

List of Tables

Acronyms

FD: Fault Diagnosis

VSI: Voltage Source Inverter

SMC: Sliding Mode Control

SMO: Sliding Mode Observer

SC: Short Circuit

FCS: Finite Control Set

MPC: Model Predictive Control

FC: Fault Code

BLDC: Brushless Direct Current

FOC: Field Oriented Control

PI: Proportional Integral

PR: Proportional Resonant

EMF: Electromotive Force

RLS: Recursive Least Squares

LMS: Least Mean Squares

CPWM: Carrier Based Pulse Width Modulation

SVM: Space Vector Modulation

PM: Permanent Magnet

PMSM: Permanent Magnet Synchronous Motor

EV: Electric Vehicle

HEV: Hybrid Electric Vehicle

MEA: More Electric Aircraft

MRAS: Model Reference Adaptive System

FPGA: Field Programmable Gate Array

FADI: Fault Alarm Detection Index

FS: Fault Signal

PLL: Phase Locked Loop

Symbols

i	phase current
v	terminal voltage of each phase
R	equivalent phase resistance
L	equivalent phase inductance
M_1	mutual inductance between two adjacent phases
M_2	mutual inductance between two nonadjacent phases
e	back EMF in each phase of the motor
v_x	neutral voltage of the motor
δ	difference between the estimated and real current
Sat	saturation function
S	sliding surface
ρ	cross correlation factor
N	number of samples
D	fault detection index
sign	sign function
ω	motor speed
Θ	rotor electrical angle
ω_e	electrical rotational velocity
V	Lyaponov function
K_p	proportional gain
K_r	resonant gain
λ	forgetting factor
ε	small positive value
T	period
τ	torque
v_{zs}	zero sequence voltage component
T_e	sampling period
f_{sw}	switching frequency

1.

Introduction

This chapter outlines the main lines of inquiry on which this thesis research is engaged. It takes the reader from an introduction of the research field to the thesis's contents, through the hypothesis statements and the exposition of the specific objectives.

CONTENTS:

1.1. Research topic

Since the invention of power electronics, in 1957, its application has been quickly expanded in different areas such as generation, transmission, distribution and end-user applications. Besides, intensive research on topologies, active and passive components, control methods, and digital signal processors have significantly improved its performance in terms of power density and efficiency [1].

Recently, in order to achieve certain level of safety in power electronics, a strict reliability concern has been established by automotive and aerospace industry. This trend has also been followed by other industries such as energy sector [1].

Motor drive is one of the most important application areas of power electronics among others. Recently, due to electrification of transportation, efficient motor drives applicable in automotive industry have gained a lot of attention. A typical power train of an EV is shown in Fig. 1. As it can be seen, it consists of an energy source, electrical motor and power electronics. Due to advantages of drive systems, this technology is increasingly used in other applications as well. There are some applications where a continuous operation of the drive is critical to ensure safety criteria. Aerospace, chemical industry, medical applications, power plants, automotive industry, railway locomotives and military area are among those application areas which need a drive system with high reliability level. The fault-tolerant design and redundancy are two solutions to meet this high level of reliability [3]. According to the fault-tolerant concept, regardless of a fault, continuous operation of the system can still be maintained. On the other side, the redundancy approach replaces the faulty system with similar healthy system. Although redundancy is a simple solution, its high implementation cost and required space outweigh its advantages. Consequently, developing of fault-tolerant drives has been presented in literature.

Multi-phase fault-tolerant PM motor drive is a reliable and efficient solution. This higher reliability is due to its fault-tolerant capability under single or multiple faults. Lower torque ripple than conventional three phase motors, less power per phase in comparison to conventional similar three-phase motor drive, and less operational noise are other advantages of this motor drive [4]. Another important aspect of this motor in comparison to conventional three-phase motor is the ability of fault-tolerant without adding extra hardware. This characteristic is very important in automotive industry due strict limits on space.

In order to implement a multiphase fault-tolerant drive, several subjects should be considered at the same time. The fault-tolerant control, fault detection, design and reconfiguration are among those interesting research topics to pursue. Therefore, each topic should be studied for application in power electronics converters and electrical machines used in the drive.

The aim of this dissertation is to study different alternatives for the FD and fault-tolerant control of multiphase converters supplying a multiphase electrical machine. Application area of this case study is mainly oriented to the automotive industry, such as EV and HEV.

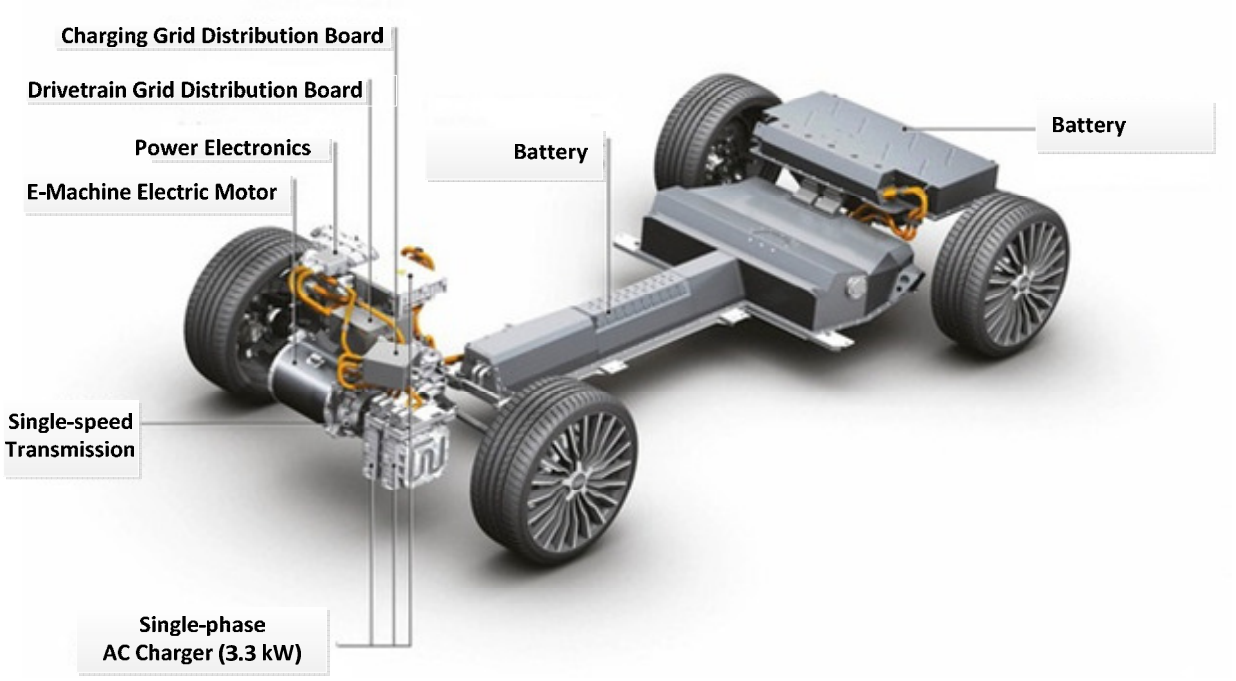

Fig. 1.1. Typical power train of an EV – Audi A3 e-tron [2]

1.2. Research problem

There is an increasing demand for higher reliability in power electronics. A fault-tolerant multiphase drive is a suitable choice to meet this requirement. In order to implement a fault-tolerant drive, three main subjects should be considered at the same time including: fault detection, fault isolation and fault-tolerant control [5].

Typically, the electrical motor is supplied by a two-level multiphase VSI. A power converter is subjected to different fault types during its operation life. A survey on reliability of power electronics converters has been presented in [6]. It has been concluded that power semiconductors and electrolytic capacitors are the most vulnerable components among others.

The possible fault types and protection methods in power converters have been thoroughly discussed in [7]. According to the presented literature review, two fault types are possible in a power switch. These faults are open switch and short circuit faults. The short circuit fault mainly happens due to high voltage and high temperature resulted from power losses. Failure in gate drive, wire bond lifts up or rapture are the main reasons for open circuit faults [8].

The short circuit fault is too serious; this fault should be detected and isolated very fast. Otherwise, the whole system should be shutdown. Detection and protection methods of this fault have been well established in research and industrial applications. Nowadays, hardware based solutions are used to detect and isolate the fault. Although there are new research lines for short circuit fault prognosis, this strategy can significantly reduce the maintenance costs due to unscheduled shutdown.

On the other side, open switch FD methods are less destructive. After the fault, system can be still operated with reduced performance. However, if the fault is not detected, the secondary faults may damage the whole system in long term. Both hardware and software based solutions can be used to detect the fault. Different FD methods have been well presented in literature for three-phase systems [7] such as motor drives, and grid connected converters.

Failure mechanism in power semiconductors can be classified as: wear-out failure and catastrophic failure. The former happens after long term operation of the device; this failure is predictable. On the other hand, the later is due to overstress in single events; it is difficult to predict this failure. The research trend is to predict the wear-out failures. This thesis investigates FD methods due to single event overstress. It should be noted that both failure types can have the same mechanism.

Due to the fault-tolerant capability of multiphase motor drives, simultaneous faults in more than one phase are possible. This case is not relevant for similar three-phase systems. On the other side, the drive can be operated by having non sinusoidal and unbalanced current in output phases of the power converter. The presented methods in literature show a low performance to detect the fault in

multiphase drives, since most of these methods have only considered single faults. It should be noted that state of the art three-phase fault-tolerant converters can tolerate only one fault, although this capability can be extended by adding complicated design and extra hardware. On the other side, due to the higher fault-tolerant capability in multiphase drives, a more complicated and flexible post fault control methods are necessary. There is a lack of knowledge and research on real time FD and control methods in multiphase converters.

1.3. Hypothesis

In order to address the presented research problems, the following hypotheses have been proposed as the starting point for this research work:

- **Due to its fault-tolerant feature, a multiphase drive can be operated under different faulty modes. Operational mode is different than in conventional three-phase system. Therefore, the classic FD methods may be used for this application.**

- **The low cost, fast FD speed, flexible, generality and robustness are the most important design criteria of the FD methods in industrial application.**

- **In order to implement real time continuous operation of a multiphase converter, a flexible fault-tolerant control should be developed. Due to higher phase number, implementation of the control method is more complicated than conventional three-phase motors. At the same time, a FD method with same reconfigurable characteristics should be included in the control method.**

- **Model based FD methods can be used to detect and localize different fault types such as open switch fault in voltage source inverter, and sensor faults.**

- **Information from the closed loop control algorithm can be used to diagnose the faults in VSI. This method is less expensive and requires lower computational cost.**

These exposed assumptions represent the basis of the resulting thesis research. The hypotheses are investigated by means of the research work reflected in this dissertation.

1.4. Aims and objectives

In order to solve the research problem and test the corresponding hypotheses, the aim of this thesis consists of the **investigation of novel, effective and systematic open switch FD methods with reconfigurable fault-tolerant control algorithms in multiphase power converters in order to realize continuous operation in multiphase drives**.

To achieve this aim, the following objectives are identified:

- **Review of the main FD methods in power converters.**
- **Evaluate the presented FD methods in literature for application in multiphase fault-tolerant drives.**
- **Evaluate the operational conditions of the multiphase machines and propose novel FD methods.**
- **Develop effective and simple fault-tolerant control methods with embedded FD algorithms in the power converter.**

1.5. Chapter descriptions

In order to cover the exposed objectives, this thesis has been divided into different stages, which are reflected in the chapters described below.

A literature review of previous works on FD in power converters is presented in **Chapter 2**. Each fault type is classified; advantages and disadvantages of each method are explained.

In **Chapter 3**, model based FDs method in a five-phase VSI supplying the BLDC motor are evaluated. A suitable model of five-phase BLDC motor is selected. A new model based FD method is proposed. Also, an adaptive fault-tolerant PR controller is proposed.

In **Chapter 4**, due to their simplicity and low implementation cost, the signal based FD methods are analyzed for application in fault-tolerant multiphase machine. According to the specific operational condition of this kind of machines, two novel cost effective FD methods are proposed. In order to control the drive, the detailed implementation of the conventional control methods are discussed and developed. Furthermore, theory of SMC is presented under healthy and faulty mode operation of the drive.

In **Chapter 5,** a simple, flexible and effective fault-tolerant FCS-MPC of the five phase converter is developed. Then, control signals available in the control method are used to develop a new FD method.

Although each chapter concludes with a partial conclusion focused on its respective topic, in **Chapter 6** the thesis work is analyzed from a general point of view, and the conclusions and contributions are clearly exposed.

Finally, the publications and collaborations resulting from the research work development are presented in **Chapter 7**.

2.

FD in Power Converters-Literature Review

State of the art fault types and FD methods in power converters are reviewed in this chapter. A comparison between these methods is presented as well.

CONTENTS

2.1. Introduction

To guarantee maximum level of safety, continuous operation is of paramount importance in applications such as EV, HEV, transportation, renewable energy sources, chemical industry MEA, and so on. Therefore, motor drives applicable in these areas should meet a high level of reliability. A fault-tolerant system is a high performance and cost effective solution to address this challenge.

In order to design a fault-tolerant system, FD, fault isolation and reconfiguration of the system should be considered at the same time.

Power electronics converters are used to supply the electrical machine used in a motor drive. These converters are subjected to various fault types during its operation life. Therefore, FD methods of the power converters have been investigated in literature.

Faulty types in power converters can be divided to open switch and short circuit faults. Open circuit faults are less destructive. Their primary effect of such faults is the reduction of the system performance. If the fault is not detected, secondary faults may happen [7]. Short circuit faults are really very destructive. Following these faults, the system should be shut down immediately. However, if the fault is detected fast enough, typically less than 10 µs in case of an IGBT, it is possible to avoid system shutdown. Such fast detection time is necessary to operate fault-tolerant converters with extra leg [9].

The FD methods for both aforementioned fault types have been presented in literature. These methods can be classified as shown in Fig. 2.1.

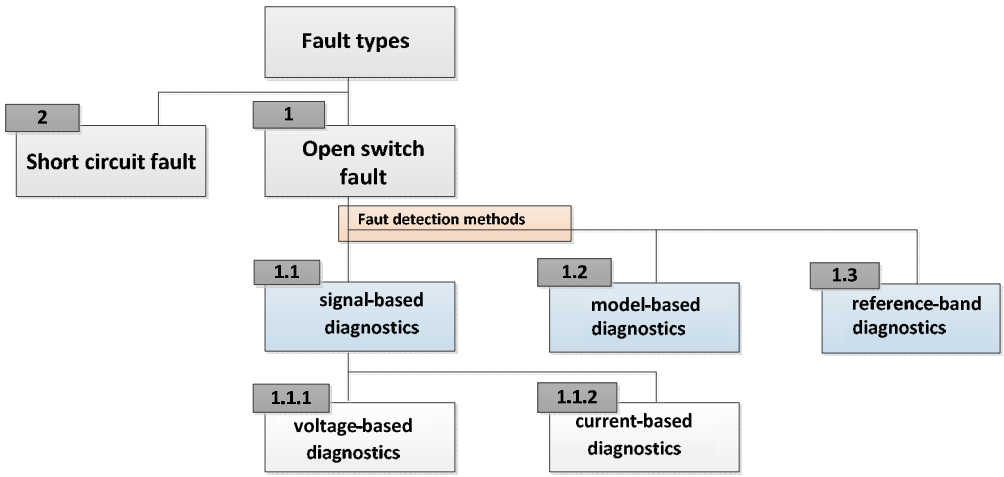

Fig. 2.1. Fault types and FD methods in power converters [9]

2.2 Short circuit FD and protection methods

According to statistics, 38 % of faults in a motor drive are related to power electronics devices [6], these faults are due to excessive thermal and electrical stresses.

The faults in the power switch can be categorized mainly to open switch and short circuit faults. In case of a short circuit fault in the power switch, in order to avoid fault propagation due to switching the complementary IGBT in the faulty leg of the power converter, a FD time below 10 µs is mandatory. Another reason for detection the fault too fast is the fault-tolerant converters equipped with an extra leg. In this application, it is necessary to detect the fault and isolate the faulty leg without doing shutdown the system; after that faulty leg is replaced with an extra leg. It should note that in contrast to open circuit faults, since time between short circuit fault initiation and failure is too short, it is much more difficult to detect and protect against this fault. So, a fast algorithm is needed to protect against this fault. In practice, to achieve a short FD time, hardware based methods are used.

It should be noted that, in practical designs, after short circuit FD and isolation, faulty leg operation is similar to the open switch fault.

In order to detect the short circuit fault, various FD methods have been addressed in literature. These methods are briefly discussed in the following.

Gate Voltage Monitoring:

The gate voltage of IGBT under healthy mode is different than faulty condition, as shown in Fig. 2.2. A method based on gate voltage monitoring for short circuit FD is proposed in [10], as shown in Fig. 2.3. After FD, gate voltage should be clamped to reduce the fault current. Also, IGBT should be softly turned off to reduce the overvoltage on switch due to stray inductance in the power converter.

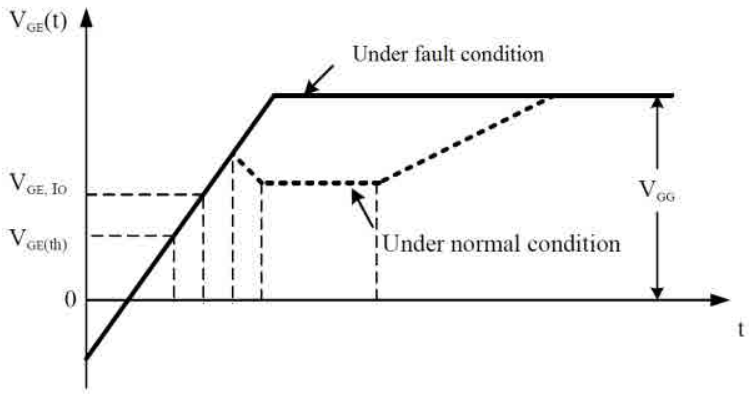

Fig. 2.2. IGBT turn on characteristics [10]

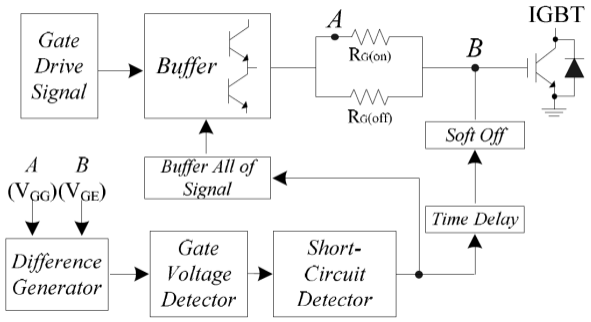

Fig. 2.3. Presented diagnosis method [10]

Voltage Monitoring of the Parasitic Inductance:

A short circuit and open circuit FD as shown in Fig. 2.4 - based on gate voltage monitoring in IGBT - is presented in [10]. FD time using this method is less than 3 µs. There are two disadvantages with this method. Firstly, it is not a general method; i.e. it is not possible to apply it to any kind of semiconductor switch. Secondly, extra voltage sensor is necessary. The fast FD time and ability to detect both open switch and short circuit faults are the important advantages of this method. Fig. 2.5 shows the voltage thresholds to distinguish the healthy from the faulty mode. Implementation of this method is complex, since accurate value of stray inductance is required.

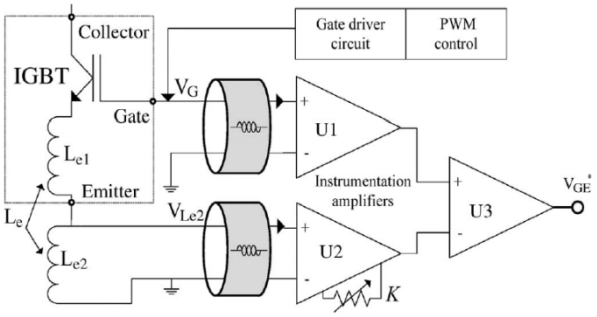

Fig. 2.4. Proposed measurement circuit [11]

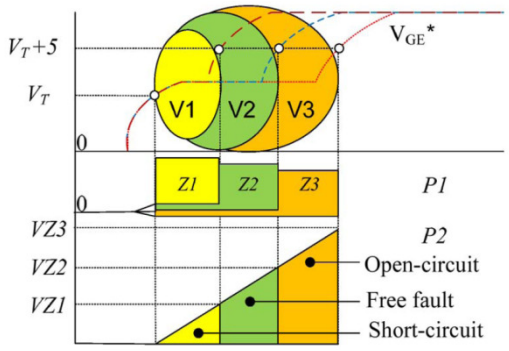

Fig. 2.5. Time diagram of condition monitoring [11]

Dc-link Current Measurement:

A single dc link current sensor as shown in Fig. 2.6 is presented in [12] in order to detect IGBT short circuit fault. Although this method is simple, it cannot locate the faulty switch.

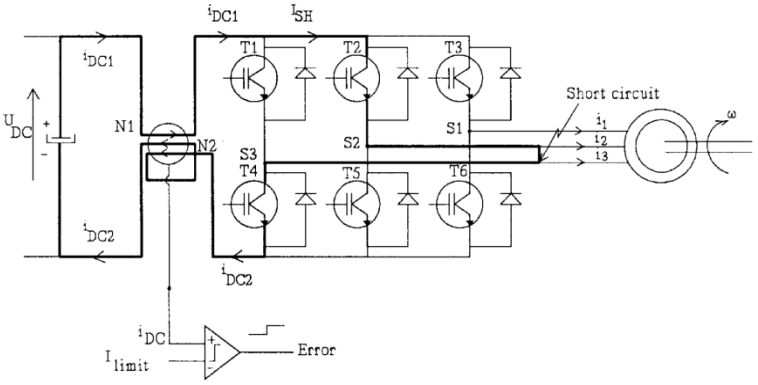

Fig. 2.6. Short circuit FD based on single dc link sensor [12]

De-Saturation Detection:

In case of short circuit fault; when gate signal is high, collector emitter voltage increases from saturation level to bus voltage value. Therefore, the short circuit fault can be detected by monitoring the collector emitter saturation voltage [13]. This detection method has been included in most commercial drivers. After FD, gate pulse is removed. Since collector emitter voltage is too noisy, a low pass filter is necessary to suppress the high frequency distortions. As a result, this detection method has a delay of FD between 1 to 5 µs typically. Protection method is shown in Fig. 2.7(a). This method is not effective for high switching frequencies.

Current Mirror Method:

In this method, a second IGBT is integrated in main IGBT [13]. Its current is reduced by a typical scale (i.e. 1:1000). Then, by sensing voltage drop across a resistor connected to auxiliary IGBT, FD is done. High cost is the main disadvantage of this method. This protection method is shown in Fig. 2.7(b).

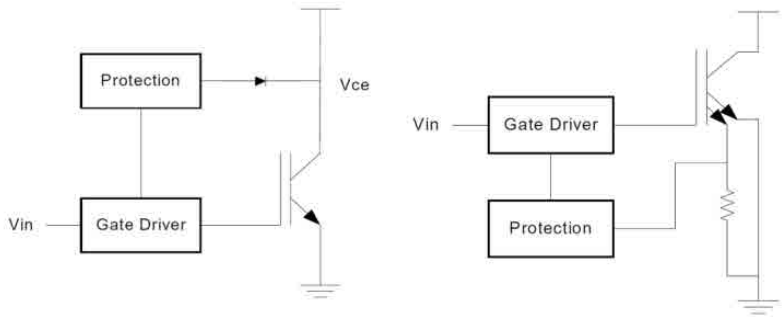

(a) (b)

Fig. 2.7. IGBT SC FD methods (a) de-saturation FD (b) current mirror method [13]

Average Current Park's Vector Approach:

In this method, average values of the phase currents in the power converter are calculated [14]. Then Park's vector transformation is utilized to extract current trajectory in a complex plane. Under normal operation, average current is zero and trajectory has a circle shape. Following the fault, trajectory has no longer a circle shape; its phase angle is utilized to localize the faulty switch. It should be noted that this method needs at least one fundamental cycle to detect the fault.

Vector Composition of Inverter Output Voltage:

After short circuit fault, a high component at switching frequency appears at converter output voltage. Filtered output voltage of converter is sampled by a rate more three times the switching frequency. By applying a linear transformation, voltage vector is obtained. If its magnitude is increased beyond a threshold value, FD is done [15]. The phase angle of the voltage vector is utilized to locate the faulty switch. Slow FD time is the main drawback of this method.

Gate Charge Sense:

A novel and high speed short circuit FD method based on gate charge measurement has been proposed in [16], with a FD time around 1 µs. The presented method is shown in Fig. 2.8. Protection circuit is connected to gate terminal. The FD method has been implemented in FPGA at [17]. Under short circuit fault, gate charge decreases, so difference between normal condition and faulty mode can be utilized to detect the short circuit fault.

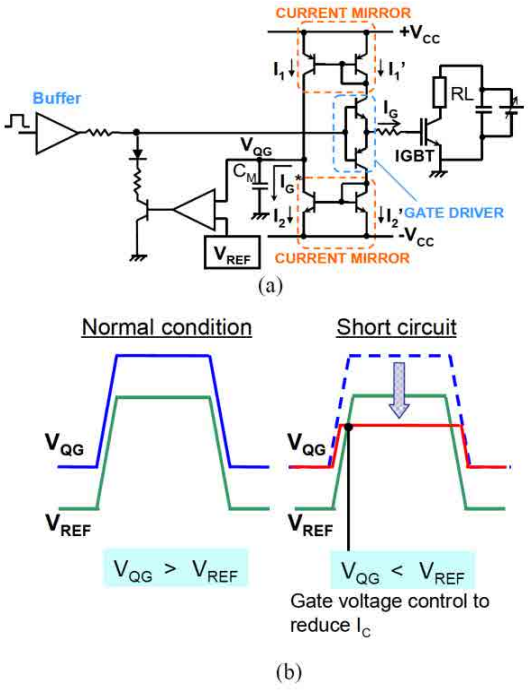

Fig. 2.8. FD scheme based on gate charge monitoring [16]

2.3. Open circuit FD and protection methods

The open switch FD methods can be classified in three groups as: signal based methods, model based methods, and reference based methods. The presented FD methods in each category are briefly discussed in the following.

2.3.1. Model based FD

According to model based FD methods shown in Fig. 2.9, the response of the system model to input *u* is predicted. After that, difference between the real output and estimated value (i.e. the residual value) is defined as the FD index. If the residual value is higher than a threshold value, fault is detected [18-20].

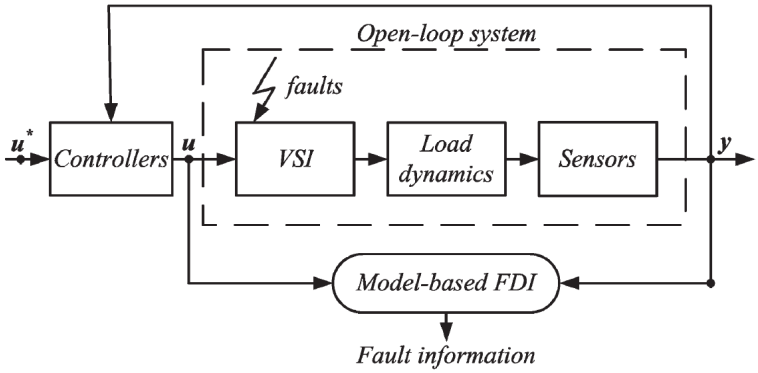

Fig. 2.9. Model based diagnosis [9]

Model Based FD Using Observer:

Campos et.al has proposed an observer based method to detect single and multiple open switch faults in the power converter [19]. FD method is independence of the load operating conditions; also, it does not need any additional sensors. The high computational cost and knowledge of machine parameters are the main drawbacks of this method.

Model Based ANN Diagnostic Method:

In order to detect single and multiple faults, a fault diagnostic neural network is developed [21-22]. Prediction rates of the single switch and open phase faults are 75% and 90%, respectively. This method does not need additional sensors; also, it is independent from load operational conditions. However it has a high computational cost; moreover, machine parameters should be known.

FD in a PMSM Drive Based on MRAS:

A simple open circuit FD method was presented in [23]. To detect and locate the faulty switch, two criteria are used: voltage distortion (difference between the estimated value from the model and the controller output) and time criteria. The proposed voltage distortion observer is shown in Fig. 2.10.

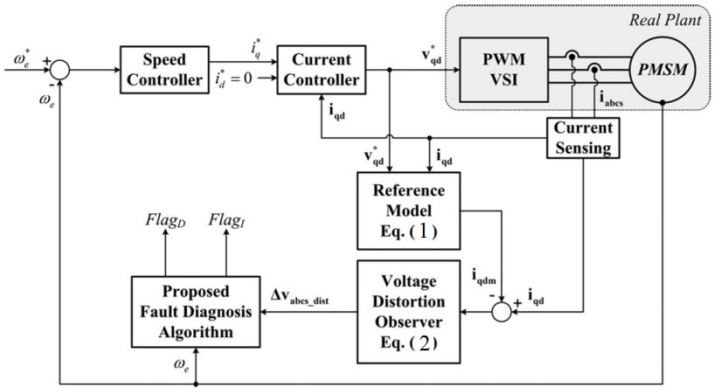

Fig. 2.10. Voltage distortion observer [23]

2.3.2. Reference based FD

In a closed loop system, reference value *u** is compared with system actual output *y*. The residue is defined as the FD index. This method is known as reference band FD method as shown in Fig. 2.11. A high residue value shows a fault in the system. It should be noted that this method can only be applied to a closed loop system.

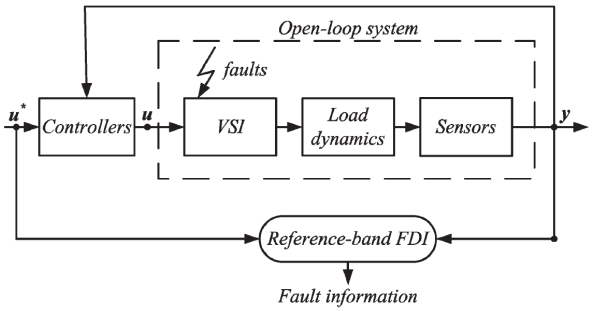

Fig. 2.11. Reference based diagnosis [9]

Reference Based FD Method:

A FD method based on reference current deviation from measured value of normalized inverter output current is proposed in [24], as follows:

$$\boldsymbol{c} = \boldsymbol{i}_{s,ref} - \boldsymbol{i}_{s,meas} \qquad (2.1)$$

By applying discrete fourier transform (DFT) to (2.1), its mean value c_0 and fundamental component c_1 are calculated. Then fault indicator is defined as follows.

$$f = \frac{c_1}{c_0} \qquad (2.2)$$

The FD index in (2.2) reduces the effect of load parameters. If parameter *f* is beyond the threshold value, FD is done. Using this method, the fault can be detected after two fundamental cycles. Under normal condition, *f* value is zero. In order to locate the faulty switch, phase angle of the *f* is utilized as shown in (2.3) and table II.I.

$$= \arg(f) \qquad (2.3)$$

Table II.I. Faulty switch localization [24]

Faulty switch	parameter
T1	| φ | <π/6
T2	-5π/6<φ< -π/2
T3	π/2<φ< 5π/6
T4	| φ |>5π/6
T5	π/6<φ< π/2
T6	π/6<φ< π/2

Improved Reference-band FD:

A novel open switch FD method is presented in [25], where motor phase currents and corresponding reference currents available by the control method are utilized to detect multiple open switch faults. This method is an improved version of the presented method in [24]. The FD is defined as the normalized residue value (i.e. the difference between the reference and real current) with respect to average absolute value of the phase currents as:

$$e_n = i_n^* - i_n$$
$$\langle e_n \rangle = \frac{1}{2\ /} \int_o^{2\ /} e_n dt \qquad (2.4)$$
$$d_n = \frac{\langle e_n \rangle}{\langle |i_n| \rangle}$$

In order to detect multiple open switch faults, a new auxiliary variable is defined as follows.

$$a_n = \frac{2\langle |i_n| \rangle}{\langle |i_l| \rangle + \langle |i_m| \rangle} \quad , \quad l \neq n \neq m \in (a,b,c) \qquad (2.5)$$

To detect multiple faults, two new fault variables are defined as (2.6),

$$D_n = \begin{cases} N & ,if\ d_n < -k_m \\ 0 & ,if\ |d_n| < k_m \\ P & ,if\ d_n \geq k_m \end{cases}$$

(2.6)

$$A_n = \begin{cases} L & ,if\ a_n \leq k_d \\ H & ,if\ a_n > k_d \end{cases}$$

In order to identify faulty switch, these values are applied to table II.II. It should note that threshold values k_f and k_d should be determined empirically by analyzing the motor current under different faulty conditions. Threshold values k_m and k_d can be determined analytically by analyzing motor load currents. The FD method is shown in Fig. 2.12.

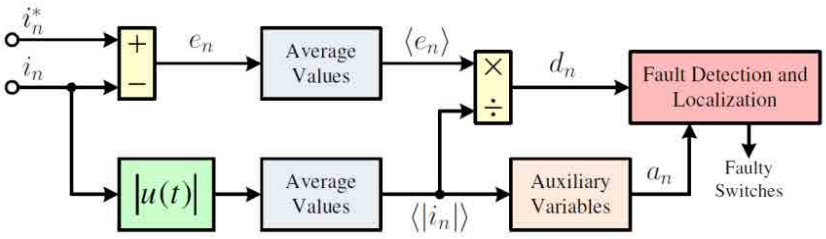

Fig. 2.12. Reference based FD method [25]

Table II.II. IGBT open circuit FD and localization [25]

Faulty Switches	D_a	D_b	D_c	A_a	A_b	Ac
T1	P	0	0	H	H	H
T2	N	0	0	H	H	H
T3	0	P	0	H	H	H
T4	0	N	0	H	H	H
T5	0	0	P	H	H	H
T6	0	0	N	H	H	H
T1, T2	–	0	0	L	H	H
T3, T4	0	–	0	H	L	H
T5, T6	0	0	–	H	H	L
T1, T4	P	N	0	H	H	H
T2, T3	N	P	0	H	H	H
T1, T6	P	0	N	H	H	H
T2, T5	N	0	P	H	H	H
T3, T6	0	P	N	H	H	H
T4, T5	0	N	P	H	H	H
T1, T3, [T6]	P	P	N	H	H	H
T2, T4, [T5]	N	N	P	H	H	H
T3, T5, [T2]	N	P	P	H	H	H
T4, T6, [T1]	P	N	N	H	H	H
T1, T5, [T4]	P	N	P	H	H	H
T2, T6, [T3]	N	P	N	H	H	H
T1, T2, (T3|T6)	–	P	N	L	H	H
T1, T2, (T4|T5)	–	N	P	L	H	H
T3, T4, (T1|T6)	P	–	N	H	L	H
T3, T4, (T2|T5)	N	–	P	H	L	H
T5, T6, (T1|T4)	P	N	–	H	H	L
T5, T6, (T2|T3)	N	P	–	H	H	L

Note: [ ] means that the switch may or may not be in open-circuit and (|) means that both or at least one switch is in open-circuit.

2.3.3. Signal based open switch FD

In case of signal-based FD methods, current or voltage waveforms of the power converter are used to define the FD index. Different signal based FD methods have been presented in literature. A brief review is presented in the following section. A general block diagram of signal based open switch FD methods is shown in Fig. 2.13.

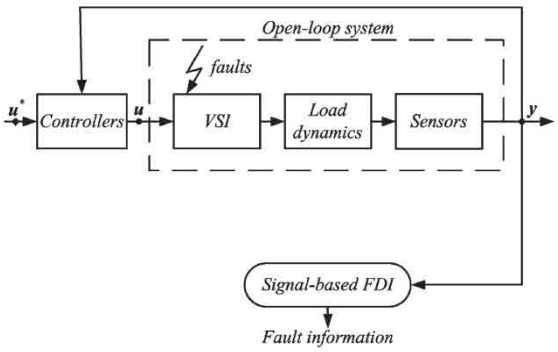

Fig. 2.13. Signal based FD method [9]

2.3.3.1. Voltage based techniques

By using voltage based techniques, it is possible to detect the fault too fast. Since this method needs an additional sensor, the implementation cost is high. Different voltage based techniques are reviewed in the following.

Gate Voltage Based Technique:

As it was aforementioned, both the short circuit and open circuit faults can be detected by monitoring the gate voltage in IGBT [26]. FD time (i.e. less than 3 µs) has been validated using this method. An important advantage of this method is detection of both open switch and short circuit faults. The FD circuit is same as shown in Fig. 2.4. This method is complex to implement.

FD by Measurement of the Lower Switch Voltage:

An open switch FD using a simple peripheral hardware is proposed in [27], the analog circuit measures the lower switch collector emitter voltage. According to the presented analysis, the voltage pattern under healthy mode is different than the faulty mode. This difference is utilized to detect the fault. Proposed circuit is shown in Fig. 2.14. Fast FD is the main advantage of this method. Since extra voltage sensors and electric circuit are necessary for FD; the implementation cost and complexity are high. According to this idea, two open switch FD methods have also been presented in [28] and [29].

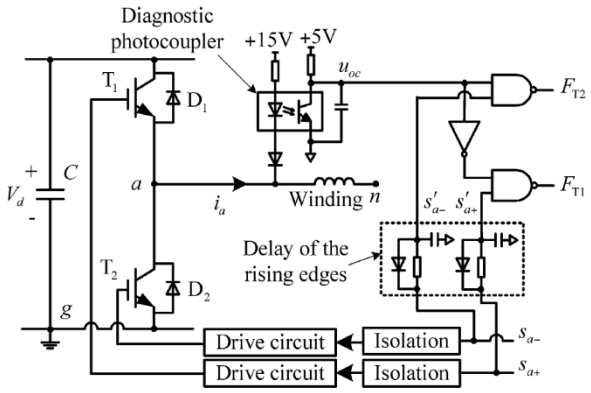

Fig. 2.14. Presented FD method based on lower switch monitoring [27]

Pole Voltage Measurement Using Analog Circuit:

FD using extra voltage sensors at different parts of a power converter is presented in [30]. Based on analytical model of the inverter, faulty switch is located. Different possible placements of the voltage sensor are shown in Fig. 2.15. Among the proposed methods, line to line voltage measurement is the easiest method for implementation. FD with a quadrant of a fundamental cycle is reported. Fig. 2.16 shows the detection scheme. Table II.III shows faulty switch localization.

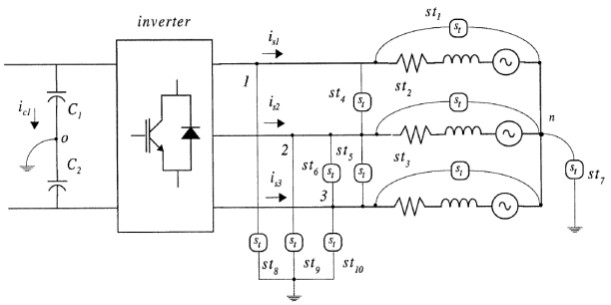

Fig. 2.15. Possible measurement strategies of the voltage [30]

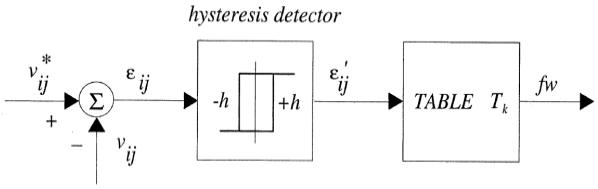

Fig. 2.16. FD block [30]

Table II.III. Faulty switch localization [30]

Faulty switch	ε12	ε23	ε31
Q1	Δv10	0	-Δv10
Q2	0	Δv20	-Δv20
Q3	-Δv30	0	Δv30
Q4	-Δv10	0	Δv10
Q5	0	-Δv20	Δv20
Q6	Δv30	0	-Δv30

FD by Using Pole Voltage Measurement and FPGA:

Karimi et al. [31] proposed a novel FD method in voltage source converters based on time and voltage criterion. The control algorithm and FD method in a shunt active filter have been implemented in an FPGA. Hardware configuration is shown in Fig. 2.17. Advantage of this method is fast detection speed; however additional voltage sensors are required. FD scheme is shown in Fig. 2.18. As it can be seen, estimated voltage and measured value are compared. In case of fault, counter starts, if its value reaches a threshold value, faulty mode is detected. The FD time less than 10 µs is achieved.

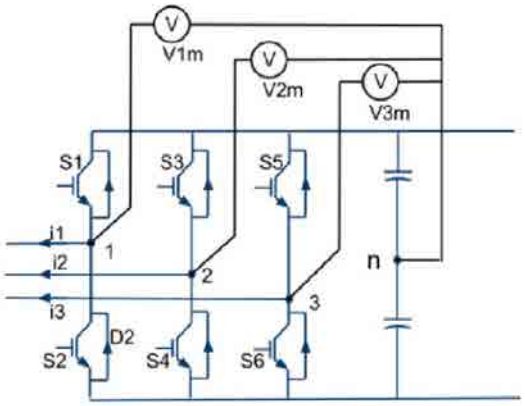

Fig. 2.17. Hardware configuration [31]

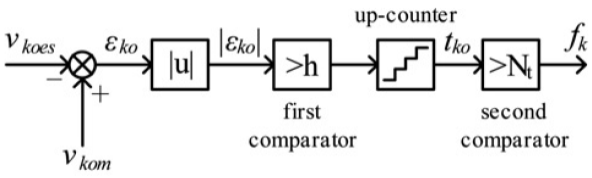

Fig. 2.18. The FD scheme [31]

Karimi et al. [32] demonstrated an open switch FD method for wind energy conversion systems. Basic idea is proposed in [31]. Detection time less than 10 µs is presented. Detection method is shown in Fig. 2.18. The time and voltage criterion are utilized to minimize the false alarms. Algorithm is implemented in an FPGA. Advantage of this method is fast detection speed; however it is complex and

expensive due to using additional voltage sensors. Authors investigated FD in shunt active filter [33], based on proposed approach in [32].

Improved FD by Using Voltage Measurement and FPGA:

A fast open switch FD method is proposed in [34] as shown in Fig. 2.19, the line to line voltage is measured and analyzed to determine the faulty component. This method is implemented in an FPGA. FD time around several ten microseconds is reported. Advantage of this method is the reduced number of sensors. On the other side, applying additional hardware to detect the fault increases system cost and complexity. Both voltage and time criterion are applied to minimize the false alarms.

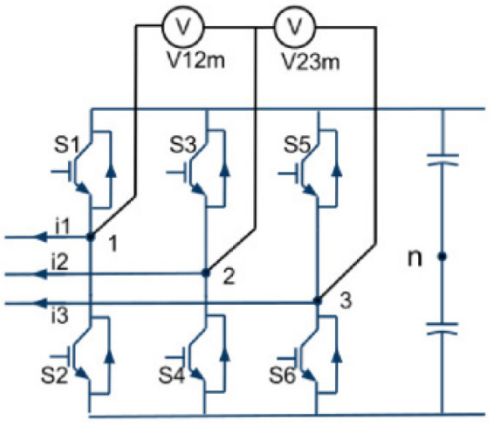

Fig. 2.19. Measurement circuit with reduced sensor count [34]

FD Based on Flying Capacitor Voltage Measurement:

A voltage based FD method in a three-level power factor converter is proposed in [35]. Considering this method, a simple voltage sensor is applied across the flying capacitors, if voltage value increases above or below a predetermined threshold value, fault alarm is activated. Detection method is shown in Fig. 2.20.

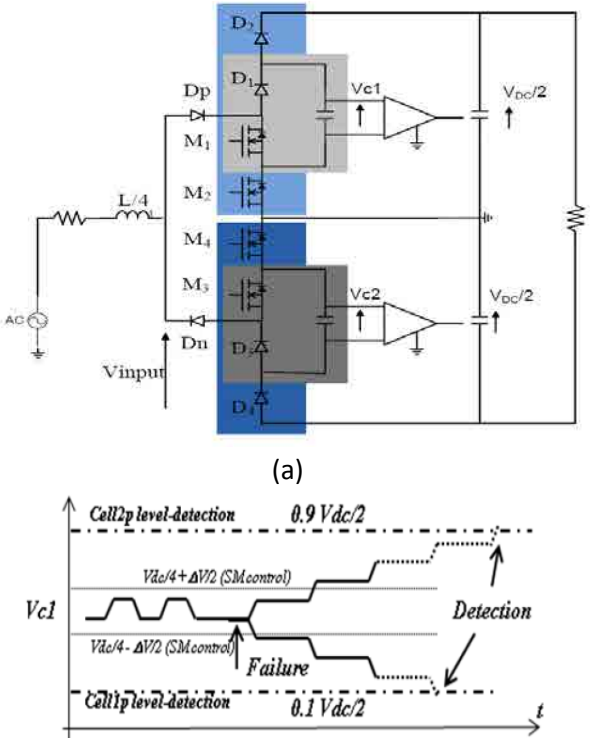

(a)

(b)

Fig. 2.20. (a) FD based on flying capacitor voltage measurement (b) FD method [35]

2.3.3.2. Current based open switch fault detection methods

Current signal of the power converters can be used to derive a FD index. A high percentage of the presented methods in literature use inverter output current instead of voltage, since current signal is often required for control purpose. Consequently extra hardware and costs are avoided. A brief review of the latest current based FD methods is presented in the following.

Park's Vector Approach:

After applying the Park transformation in (2.7) to motor three-phase currents shown in Fig. 2.21(a) under healthy condition, vector trajectory has a circle shape as shown in Fig. 2.21(b) [14].

$$\begin{bmatrix} i \\ i \\ i_o \end{bmatrix} = \frac{2}{3}\begin{bmatrix} 1 & \cos(2\ /3) & \cos(4\ /3) \\ 0 & \sin(2\ /3) & \sin(4\ /3) \\ 1 & 1 & 1 \end{bmatrix}\begin{bmatrix} i_a \\ i_b \\ i_c \end{bmatrix} \qquad (2.7)$$

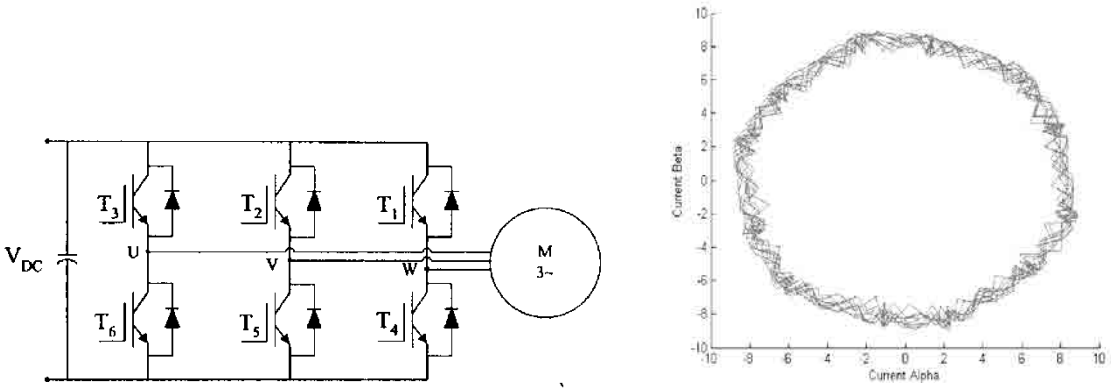

(a) (b)

Fig. 2.21. (a) Three phase motor drive (b) current vector trajectory [14]

However under faulty mode, current vector has no longer a circle shape, the trajectory depends on the faulty switch. According to the faulty switch in the three-phase power converter shown in Fig. 2.21(a), different trajectories of the phase current are shown in Fig. 2.22.

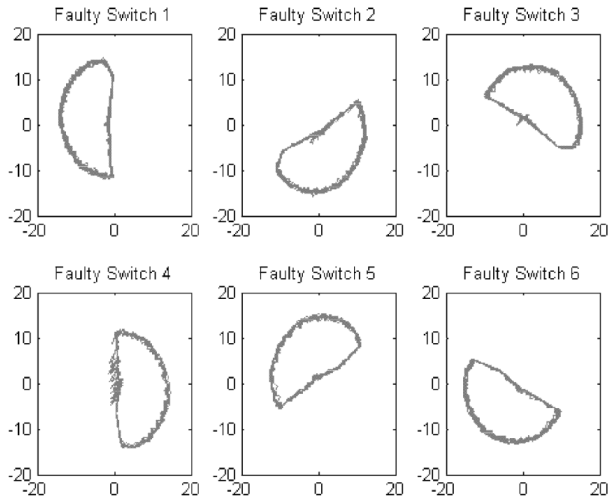

Fig. 2.22. Current vector trajectory under different faults [14]

This property can be utilized to detect and localize the faulty switch. According to this approach, by using current vector magnitude and phase angle, faulty switch can be detected and localized according to table II.IV.

Table II.IV. FD and localization [14]

Faulty Switch	Magnitude	Angle
T1	Exceeded Threshold	150 to 210
T2		210 to 270
T3		270 to 330
T4		330 to 30
T5		30 to 90
T6		90 to 150

Normalized DC Current Method:

A drawback of Park's vector approach is the load dependence. To overcome this problem, normalized DC current method is proposed [36]. According to this method, the average current of each phase is normalized with respect to the first fundamental component of the phase current as shown in (3.22). If the absolute average of the calculated index is higher than a threshold value, fault is detected. Its polarity is used to localize the faulty component.

Modified Normalized DC Current Method:

In case of closed loop control systems, the normalized DC current method has poor performance such as poor efficiency at low currents and satisfaction of multiple conditions. As a result, a modified normalized dc current method was proposed [37]. According to this method, same normalized dc current method is utilized to define the FD index. In order to avoid multiple satisfactory fault conditions, the largest absolute value of the FD index is compared to a threshold value.

Slope Method:

According to Park vector representation, trajectory of the current vector under faulty conditions has a linear shape for part of fundamental period; its slope depends on the faulty leg [36]. This slope can be calculated using (2.8).

$$= \frac{\boldsymbol{i}_{(\boldsymbol{k})} - \boldsymbol{i}_{(\boldsymbol{k}-1)}}{\boldsymbol{i}_{(\boldsymbol{k})} - \boldsymbol{i}_{(\boldsymbol{k}-1)}}$$

$$\textbf{\textit{Faulty Leg}} = \begin{cases} \boldsymbol{a} \;\; ; \;\; = 0 \\ \boldsymbol{b} \;\; ; \;\; = \sqrt{3} \\ \boldsymbol{c} \;\; ; \;\; = -\sqrt{3} \end{cases} \qquad (2.8)$$

where *k* and *k-1* are the present and previous sample values. From (2.8), the faulty leg is determined.

It should be noted that under healthy mode, the current vector trajectory is always sinusoidal; therefore σ value is always varying. The faulty switch can by localized by determining the polarity of the

phase current in the faulty leg. If the current polarity is positive then faulty switch is the lower switch otherwise the faulty switch is upper switch.

A modified version of slope method was presented in [38]. However it has still disadvantages such as long detection time, tuning problems, and detection issues under low current.

Simple DC Current Method:

According to this method, the average value of each phase current in one fundamental period is calculated using (2.9). After that the largest absolute value is used to detect the faulty phase [37]. Current polarity is also used to detect faulty switch in faulty leg according to table II.V.

$$i = \frac{1}{N}\sum_{k=1}^{N} i_i, \quad i \in (a,b,c) \qquad (2.9)$$

Table II.V. FD and localization [37]

Faulty Switch	μ_a	μ_b	μ_c
T1	> 0.45		
T2		> 0.45	
T3			> 0.45
T4	< -0.45		
T5		< -0.45	
T6			< -0.45

Frequency Method:

According to vector trajectory of the phase currents under faulty conditions as shown in Fig. 2.22, its instantaneous frequency at semicircle diameter is no longer a fixed value. This fact is utilized to detect open circuit fault in inverter [36]. Instantaneous frequency f_i is calculated using (2.10), calculated value is compared to a threshold value. If f_i is higher than the threshold value, FD is done.

$$f_i = \frac{1}{2T}\frac{1}{i_k i_{k-1}}(i_{(k)} i_{(k-1)} - i_{(k-1)} i_{(k)}) \qquad (2.10)$$

where T is the sampling period. Although this method is simple to implement, it is unable to localize the faulty switch.

FD Based on Load Current Analysis:

An improved version of normalized dc current method is presented in [9], here additional signals are used to improve the robustness of later method against the load transients also to detect multiple open switch faults. Additional signal shows percent of time that current is near zero. This signal is an effective indicator since current in faulty phase is near zero for a long interval. According to this method,

the average value of phase currents in the power converter is normalized with respect to average absolute value of phase currents as (2.11).

$$D_n = \frac{\langle i_n(k) \rangle}{\langle |i_n(k)| \rangle}, \; n \in (a,b,c) \qquad (2.11)$$

Then current samples are categorized as near zero using (2.12). The average value of $W_n(k)$ is calculated, this value is close to *0* under healthy leg, equal to *0.5* under single switch fault and close to 1 in case of double switch fault in the same leg.

$$_n(k) = \begin{cases} 1, & |i_n(k)| \le K_o \\ 0 & otherwise \end{cases}, \; n \in (a,b,c)$$

$$W_n(k) = \frac{1}{N} \sum_{j=k-N+1}^{k} {}_n(j) \qquad (2.12)$$

Then two new diagnostic variables are defined as (2.13)

$$R_n(k) = W_n(k).D_n(k)$$
$$S_n(k) = \frac{2\langle |i_n(k)| \rangle}{\langle |i_l(k)| \rangle + \langle |i_m(k)| \rangle}, \quad l \neq n \neq m \in (a,b,c) \qquad (2.13)$$

The variables $R_n(k)$ and $S_n(k)$ are fuzzified using the membership function given in Fig. 2.23. After that, by using fuzzified variables and from table II.VI, the faulty switches are localized. This method is able to detect single and multiple open switch faults with high resistivity against false alarms. Due to using additional diagnostic variables, high complexity and long detection time are the main drawbacks of this method.

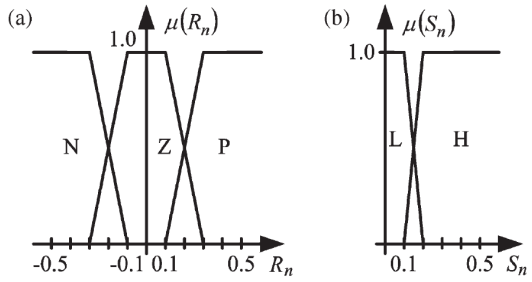

Fig. 2.23. Membership fuzzy function [9]

Table II.VI. Fault diagnostic table [9]

F	S_C	R_C	S_B	R_B	S_A	R_A	Faulty switches
0	H	Z	H	Z	H	Z	No fault
1	H	Z	H	Z	H	N	T1
2	H	Z	H	N	H	Z	T2
3	H	N	H	Z	H	Z	T3
4	H	Z	H	Z	H	P	T4
5	H	Z	H	P	H	Z	T5
6	H	P	H	Z	H	Z	T6
7	H	Z	H	Z	L	x	T1, T4
8	H	Z	L	x	H	Z	T2, T5
9	L	x	H	Z	H	Z	T3, T6
10	H	Z	H	P	H	N	T1, T5
11	H	P	H	Z	H	N	T1, T6
12	H	Z	H	N	H	P	T2, T4
13	H	P	H	N	H	Z	T2, T6
14	H	N	H	Z	H	P	T3, T4
15	H	N	H	P	H	Z	T3, T5
16	H	x	H	N	H	N	T1, T2, +T6
17	H	N	H	x	H	N	T1, T3, +T5
18	H	N	H	N	H	x	T2, T3, +T4
19	H	x	H	P	H	P	T4, T5, +T3
20	H	P	H	x	H	P	T4, T6, +T2
21	H	P	H	P	H	x	T5, T6, +T1
22	H	P	H	N	L	x	T1, T4, (T2|T6)
23	H	N	H	P	L	x	T1, T4, (T3|T5)
24	H	P	L	x	H	N	T2, T5, (T1|T6)
25	H	N	L	x	H	P	T2, T5, (T3|T4)
26	L	x	H	P	H	N	T3, T6, (T1|T5)
27	L	x	H	N	H	P	T3, T6, (T2|T4)

Note: x denotes a don't care condition

FD Based on Load Current Analysis Using Wavelet Transform:

In order to detect open switch faults, motor current analysis based on wavelet decomposition is proposed in [41]. This method detects and categorizes faults based on level 6 approximation and details. Using mean energy values of the phase currents, faulty phase is identified; after that, polarity of phase current is utilized to identify the faulty switch. The high computational cost is the main drawback of this method.

Improved FD Based on Average Absolute Values of Phase Current:

A new open switch FD method based on average absolute values of phase currents is presented in [39]. This method is capable of detecting multiple faults; also it is robust against false alarms. Proposed method is shown in Fig. 2.24, the Park's vector modulus is calculated as:

$$\begin{bmatrix} \boldsymbol{i} \\ \boldsymbol{i} \\ \boldsymbol{i_o} \end{bmatrix} = \frac{2}{3}\begin{bmatrix} 1 & \cos(2\ /3) & \cos(4\ /3) \\ 0 & \sin(2\ /3) & \sin(4\ /3) \\ 1 & 1 & 1 \end{bmatrix}\begin{bmatrix} \boldsymbol{i_a} \\ \boldsymbol{i_b} \\ \boldsymbol{i_c} \end{bmatrix} \tag{2.14}$$

$$\boldsymbol{i_s} = \sqrt{\boldsymbol{i}^2 + \boldsymbol{i}^2}$$

Considering a healthy machine, average absolute value of normalized three phase currents is calculated as:

$$\begin{cases} i_a = I_m \sin(\quad t + \quad) \\ i_b = I_m \sin(\quad t + \quad + 2 \quad /3) \\ i_c = I_m \sin(\quad t + \quad - 2 \quad /3) \end{cases} \tag{2.15}$$

$$i_s = \sqrt{i^2 + i^2} = I_m \sqrt{\frac{3}{2}}$$

Also, the ζ value is calculated as:

$$\begin{cases} i_{aN} = \sqrt{2/3} \sin(\quad t + \quad) \\ i_{bN} = \sqrt{2/3} \sin(\quad t + \quad + 2 \quad /3) \\ i_{cN} = \sqrt{2/3} \sin(\quad t + \quad - 2 \quad /3) \end{cases} \tag{2.16}$$

$$= \left\langle \left| i_{nN} \right| \right\rangle = \frac{1}{2 \quad / \quad s} \int_0^{2 \quad / \quad s} i_{nN} = \frac{1}{\sqrt{8/3}} = 0.5198$$

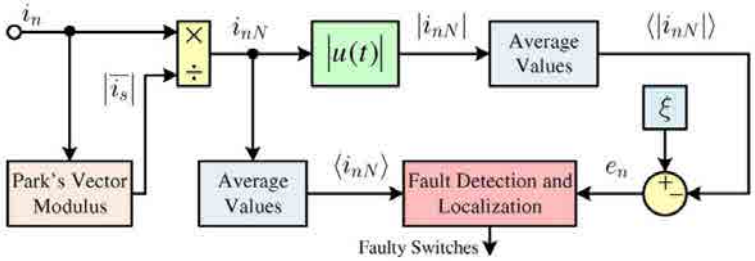

Fig. 2.24. Multiple open switch FD method [40]

FD Based on Derivation of Motor Current Phase Angle:

A novel open circuit FD method based on current signal is proposed in [43] as shown in Fig. 2.25. This method is robust against transients such as load and speed change. According to this method, after application of the Park's transformation to the motor phase currents, absolute derivative of the current phase angle in stationary reference frame is calculated. This value is fixed under healthy mode. In order to localize multiple faults, the polarity of the phase currents is determined.

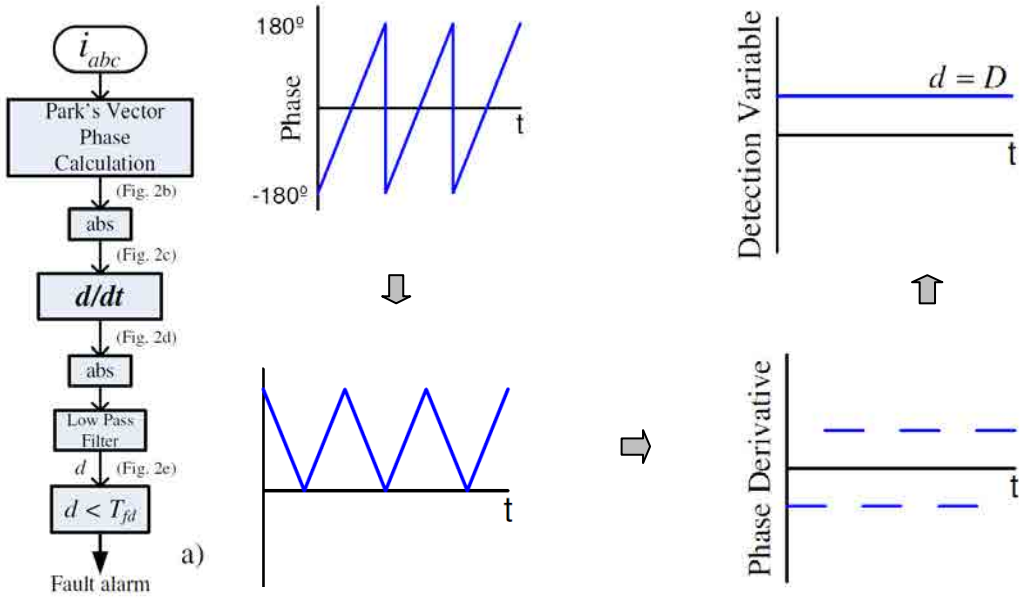

Fig. 2.25. FD based on phase angle estimation (a) FD method (b) park vector phase (c) absolute value of current vector phase (d) derivate of absolute current vector phase (e) absolute value for derivate of current vector phase [41]

Nuno et al. developed similar approach in [41] for open switch FD in PMSG Drives for wind turbine applications [42]. Where two back to back connected three phase power converters provide energy conversion approach.

FD in DC/DC Converter Based on Input Current Slope:

Shahbazi. et al. [43] has investigated FD in non-isolated dc-dc converters using FPGA. The sign of the input current slope and switch gate edge type are used to detect the fault. The power converter, waveforms and detection scheme are shown in Fig. 2.26. Under normal operation, detection law is as follows.

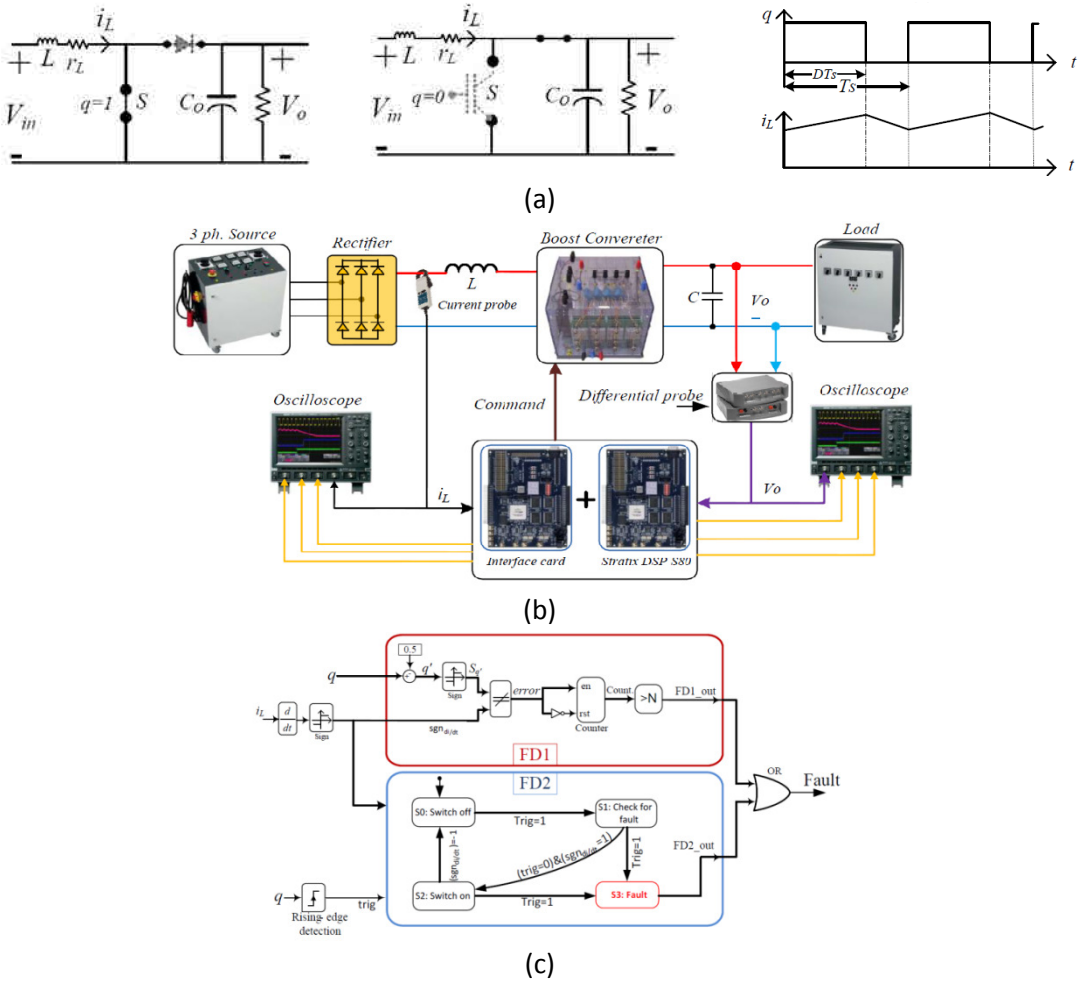

Fig. 2.26. FD in non-isolated dc-dc converters (a) dc-dc converter (b) detection scheme (b) experimental setup [43]

2.4. Discussion and conclusions

The fault types and fault protection methods presented in literature were briefly discussed in this chapter.

All presented FD methods have been studied for three-phase energy conversion systems such as motor drive applications, and renewable energy sources. Therefore, there is a lack of knowledge and research on faulty mode analysis and diagnosis of multiphase power converters.

Among the presented methods, hardware based solution by analyzing the voltage signal can achieve the shortest FD time. However, the implementation of such methods is expensive due to extra sensors.

Short circuit FD methods are usually implemented by hardware based solutions. The main reason is the too short time between failure detection and system shutdown. In case of an application with high reliability requirement, the system shutdown should be avoided.

Open switch faults can be detected and isolated after a short time. Therefore, cost effective, efficient and robust FD algorithms can be developed.

In case of multiphase system, multiple simultaneous faults can be still tolerated by traction motor drives. This characteristic makes multiphase drives distinguished from their counterpart three phase motor drives. Moreover, there is a lack of knowledge in literature to address efficient FD methods in multiphase drives. Consequently, new FD and fault-tolerant control algorithms should be developed for this application area.

For simplicity, all presented short circuit and open switch FD methods in literature are briefly compared in tables II.VII and II.VIII, respectively.

Table II.VII. Comparison between short circuit FD methods

Methods	Robustness	Detection Speed	Implementation Effort	Cost	Input
Gate voltage monitoring	medium	very fast	high	high	Gate voltage
Dc link current measurement	high	fast	medium	low	Dc link current
De-Saturation Detection	high	very fast	medium	medium	Collector-emitter voltage
Current Mirror Method	high	very fast	high	high	Switch current
Average Current Park's Vector Approach	poor	low	low	low	Phase current
Vector Composition of Inverter Output Voltage	high	medium	medium	medium	Load voltage
Gate Charge Sense	high	very fast	High	high	Gate charge

Table II.VIII. Comparison between open switch FD methods

Methods	Robustness	Detection Speed	Implementation Effort	cost	Input	Dependence on load?
Model based FD						
Model-based FD observer [18]	high	medium	medium	low	3ph-current	no
Model-Based ANN Diagnostic Method [21]-[22]	high	medium	high	low	3ph-current	yes
FD based on MRAS [23]	high	medium	low	low	3ph-current	-
Reference based FD method						
Reference-band FD [24]	medium	medium	low	low	3ph-current	no
Improved reference-band FD	high	medium	low	low	3ph-current	no
Signal based open switch FD						
- Voltage based techniques						
Gate voltage-based technique [26]	medium	very fast	high	high	Gate voltage	-
lower switch voltage measurement [27]	high	very fast	low	high	Collector emitter voltage	-
Pole voltage measurement [30]	high	very fast	low	high	Load or pole voltage	no
Pole voltage measurement and FPGA [31-34]	high	very fast	low	high	Load or pole voltage	no
Flying capacitor voltage measurement [35]	high	fast	low	high	Capacitor voltage	-
- Current based open switch FD methods						
Park's vector approach [14]	high	medium	low	low	3ph-current	yes
Normalized DC current method [36]	low	medium	low	low	3ph-current	no
Modified Normalized DC Current Method [39]	high	medium	low	low	3ph-current	no
Slope method [38]	medium	medium	low	low	3ph-current	no
Simple DC current method [37]	medium	medium	low	low	3ph-current	yes
Frequency method [36]	medium	medium	low	low	3ph-current	no
load current analysis [9]	high	medium	high	low	3ph-current	no
Improved FD - average absolute values of phase current [40]	high	high	low	low	3ph-current	no
FD based motor current phase angle	high	high	low	low	3ph-current	no
FD in DC/DC converter based on input current slope [42]	high	very fast	low	low	Inductor current	no

3.

Study and Contributions to Observer Based FD Methods

The model of a five phase power converter supplying a BLDC motor is studied in this chapter. The proposed model is used to develop a novel FD method capable of detecting open switch faults in the power converter. Real time fault-tolerant control methods with an embedded FD block are studied as well.

CONTENTS

3.1. Introduction

Nowadays, power converters are widely used in industrial applications. Along the rising applications, there is an increasing demand for higher reliability provided by the power electronic systems in applications such as transportation, electric and hybrid electric vehicle, space craft, and more electric aircraft. Fault-tolerant concept is an economic solution to meet this requirement [44]. To accomplish a fault-tolerant system, three main subjects should be considered at the same time in the final design including fault-tolerant design, control and fault diagnosis.

Multiphase fault-tolerant PM motor drive is a unique solution to achieve high reliability [47]. In the case of a five-phase motor, it is possible to maintain the operation with two faulty phases. Regarding this solution, it is necessary to supply the motor with a fault-tolerant converter. The fault-tolerant converter should be able to detect and isolate the faulty components.

According to a recent survey on reliability of power electronics converters [6], power switches are the most vulnerable components in a power converter among others. A complete review of the faulty modes and detection methods in a power converter was conducted in [7]. Open switch and short circuit faults are the most common faults in a power switch among others. The short circuit fault should be detected and removed quite fast; otherwise it can damage the whole system. Nowadays, hardware based methods are frequently included in commercial gate driver to protect against this fault. On the other side, a solution to detect and protect the open switch fault is not available in commercial products. If it is not detected, secondary faults may happen. Due to growing demand for higher reliability by industry, an extensive research has been conducted on open switch FD methods, recently. Regarding the presented open switch FD methods in literature, these methods can be considered in three different categories including signal based methods, reference based methods and model based methods. This classification is shown in Fig. 3.1; the focus of this chapter is on model based FD shown by red dash line.

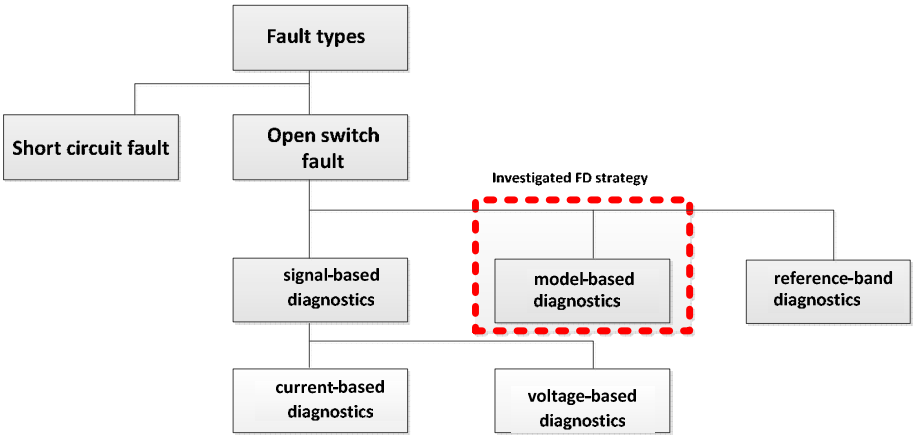

Fig. 3.1. FD methods and studied FD method in this chapter.

FD methods presented in literature are briefly discussed in the following. After that proposed novelties are explained.

The signal based FD schemes have been extensively studied in literature. To implement a signal based FD method, the current or voltage signal of the power converter can be used as an input to the FD block. The detection methods based on the voltage signal need extra hardware to detect the fault; as a result, implementation of these methods is expensive. However these methods are able to detect the fault very fast. Such schemes have been presented in [34], [47].

The FD methods based on the current signal have also been extensively addressed in literature. Different schemes using tools such as Park's vector modulus, wavelet transform, dc current method, normalized dc current method, Fourier transform and slope method have been presented to obtain a suitable FD index [7]. Low detection speed, complexity, inability to detect multiple faults, and sensitivity to fast load transients are the main drawbacks of FD methods based on the current signal. In this category, proposed methods in [42], [48-49] show the highest performance among others.

The second type of the open switch FD method is based on the reference current. According to this method, real current of the converter is measured and compared to the reference current in the control algorithm. After that, an FD index is defined based on the residue value. This method is cheap, fast and robust to the variations of load parameters. Estima et al. [25] presented an FD method based on the reference current. This method cannot be used in a system with open loop control.

The third type of the open switch FD method is based on the system model. According to this technique, the input signal to the plant is applied to an equivalent mathematical model of the plant, and its response is predicted. In the next step, difference between real output and the predicted signal is used to define the FD index [50], [25], [51-53]. This method is cheap, since extra hardware is not necessary for FD. An FD method based on observer has been presented in [52] to detect multiple open switch faults in a three-phase induction motor. A bank of observers has been proposed to detect the fault. Consequently, implementation of this method will be even more complicated in the case of a multiphase converter. Shao et al. [54] have presented an open switch FD method based on SMO for application in a modular multilevel converter. In order to detect the fault, the residue value (i.e. the difference between estimated and real signal) is compared with a fixed threshold value. This approach can lead to false alarms, since the FD index is not independent from load operational conditions.

Considering the model based FD methods, to overcome the limitations discussed above, a new model based FD method is introduced in this thesis. Based on this method, in the first step the phase currents are estimated by a full state SMO in a fault-tolerant five-phase BLDC motor drive. Comparing to conventional model based methods which use the residue value (i.e. the difference between measured and estimated state) to define FD index, here a cross correlation technique is proposed to define this

index. Inputs to the cross correlation technique are the measured and estimated current of the power converter. Proposed method still has the advantages of the conventional methods. At the same time, it can effectively detect multiple open switch or open phase faults. Furthermore, it is quite robust to transients and parameter uncertainties. An estimator is also designed to estimate the motor parameters. The estimated parameters are used for two purposes: the SMO design and the PR controller design.

3.2. Theoretical approach

The proposed FD technique intends to implement fault diagnosis in a five-phase VSI supplying a BLDC motor drive, as shown in Fig. 3.2. A FOC is used to control the motor; inputs to the control algorithm consist of the phase currents and rotor mechanical position. The same inputs are sent to the FD block. After FD, this block decides the operation mode (i.e. healthy or faulty) of the motor. In order to isolate the fault, it is necessary to remove the gate signal of the healthy switch in the faulty leg.

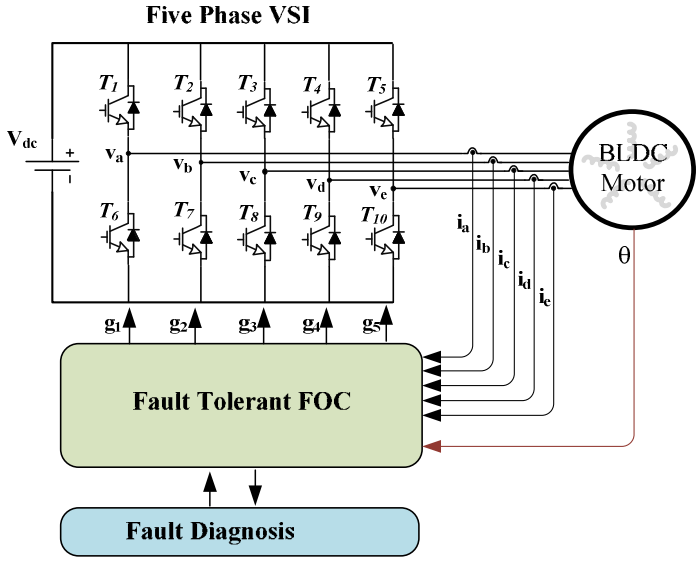

Fig. 3.2. Fault-Tolerant BLDC motor drive.

To implement the FD method, in the first step motor phase currents are estimated based on well-known models. The model in ABCDE reference frame is used due to its less computational requirements and simpler modeling, specially under faulty mode. The model of the five-phase BLDC motor with trapezoidal back EMF under healthy and faulty modes is:

$$\begin{bmatrix} v_a \\ v_b \\ v_c \\ v_d \\ v_e \end{bmatrix} = \begin{bmatrix} R_a & 0 & 0 & 0 & 0 \\ 0 & R_b & 0 & 0 & 0 \\ 0 & 0 & R_c & 0 & 0 \\ 0 & 0 & 0 & R_d & 0 \\ 0 & 0 & 0 & 0 & R_e \end{bmatrix} \begin{bmatrix} i_a \\ i_b \\ i_c \\ i_d \\ i_e \end{bmatrix} + \begin{bmatrix} L_a & M_1 & M_2 & M_2 & M_1 \\ M_1 & L_b & M_1 & M_2 & M_2 \\ M_2 & M_1 & L_c & M_1 & M_2 \\ M_2 & M_2 & M_1 & L_d & M_1 \\ M_1 & M_2 & M_2 & M_1 & L_e \end{bmatrix} \frac{d}{dt} \begin{bmatrix} i_a \\ i_b \\ i_c \\ i_d \\ i_e \end{bmatrix} \quad (3.1)$$
$$+ \begin{bmatrix} e_a \\ e_b \\ e_c \\ e_d \\ e_e \end{bmatrix} - v_x \begin{bmatrix} 1 \\ 1 \\ 1 \\ 1 \\ 1 \end{bmatrix}.$$

where *i* is the phase current, *v* is the terminal voltage of each phase, *R* is the equivalent phase resistance, *L* is the equivalent phase inductance, M_1 is mutual inductance between two adjacent phases, M_2 is mutual inductance between two nonadjacent phases, *e* is the back EMF in each phase of the motor, and v_x is the neutral voltage of the motor. The back EMF will be estimated as follows:

$$\begin{bmatrix} e_a \\ e_b \\ e_c \\ e_d \\ e_e \end{bmatrix} = \lambda_{m1}\, e \begin{bmatrix} \cos(\vartheta) \\ \cos(\vartheta - 2\pi/5) \\ \cos(\vartheta - 4\pi/5) \\ \cos(\vartheta - 6\pi/5) \\ \cos(\vartheta - 8\pi/5) \end{bmatrix} + \lambda_{m3}\, e \begin{bmatrix} \cos(3\vartheta) \\ \cos 3(\vartheta - 2\pi/5) \\ \cos 3(\vartheta - 4\pi/5) \\ \cos 3(\vartheta - 6\pi/5) \\ \cos 3(\vartheta - 8\pi/5) \end{bmatrix}. \quad (3.2)$$

where λ_{m1} and λ_{m3} are the first and third harmonic amplitudes of the rotor flux linkage; ω_e is the electrical rotational velocity, and Θ is the rotor electrical angle.

To simplify the model under healthy and faulty modes, the model in (3.1) is redefined in terms of voltage difference between machine terminals as follow:

$$\begin{bmatrix} v_{ab} \\ v_{bc} \\ v_{cd} \\ v_{de} \end{bmatrix} = \begin{bmatrix} R_a - R_b & 0 & 0 \\ 0 & R_b - R_c & 0 \\ 0 & 0 & R_c \\ R_e & R_e & R_e \end{bmatrix} \begin{bmatrix} -R_d \\ i_a \\ i_b \\ i_c \\ i_d \end{bmatrix} + \begin{bmatrix} e_{ab} \\ e_{bc} \\ e_{cd} \\ e_{de} \end{bmatrix} + \begin{bmatrix} R_d + R_e \\ L_a + M_2 - 2M_1 & M_2 - L_b & 2M_2 - 2M_1 & M_2 - M_1 \\ M_1 - M_2 & L_b - M_1 & M_1 - L_c & M_2 - M_1 \\ M_1 - M_2 & 2M_1 - 2M_2 & L_c - M_2 & 2M_1 - M_2 - L_d \\ L_e + M_2 - 2M_1 & L_e - M_1 & L_e - M_2 & L_e + L_d - 2M_1 \end{bmatrix} \frac{d}{dt} \begin{bmatrix} i_a \\ i_b \\ i_c \\ i_d \end{bmatrix}. \quad (3.3)$$

From the design point of view, in order to increase the reliability of a multiphase fault-tolerant machine, the mutual inductances should be minimized [55]. Due to this fact, and because of the small effect of mutual inductances given in (3.1) and (3.3), this parameter in the model is neglected in the rest of this thesis. It should be noted that under faulty mode, the corresponding row and column of the faulty phase are eliminated from (3.1). After that, the motor model can be simply redefined in terms of voltage difference between machine terminals similar to (3.3).

The model presented in (3.3) is utilized to estimate the phase currents and model parameters. The signal estimation methods, based on the load model, are quite sensitive to parameter uncertainties and non modeled dynamics [52]. Consequently, to estimate the phase currents accurately, a full state SMO is applied to the open loop model. Due to this observer, the error between real and estimated state variable converges to zero under healthy mode. Details of the designed observer are explained in the next section.

3.2.1. Accurate Current Estimation Using SMO

As discussed above, the motor phase currents are estimated based on the motor model. The current estimation is obtained using two separate observers. One observer is used to estimate model parameters in (3.3). The other observer (i.e. SMO) is used to estimate motor phase currents; the estimated motor parameters are used in the SMO. Therefore, the motor model used in the SMO is an ideal model.

If the motor parameters are known accurately, then estimated currents using the open loop model will be equal to the real current. However, these parameters are not easily accessible. On the other hand, parameter values can change with temperature and operational conditions of the motor. Furthermore, for condition monitoring and control purposes, it is desirable to calculate machine parameters online.

In order to diagnose the fault and design the *PR* controllers, the motor parameters are estimated in this thesis. The estimation method applied in this work is explained in the next section.

Stator's Parameter Estimation:

In a BLDC motor, the stator parameters (i.e. phase resistance and inductance) have a high effect on the accuracy of the open loop model. An estimator is designed to calculate these parameters. The basic equations of the machine model, given in (3.1), can be rewritten as:

$$\frac{d}{dt}\boldsymbol{i}_j = -\boldsymbol{A}_j\boldsymbol{i}_j + \boldsymbol{B}(\boldsymbol{v}_j - \boldsymbol{e}_j),\ \ \boldsymbol{j} = \boldsymbol{a},\boldsymbol{b},\boldsymbol{c},\boldsymbol{d},\boldsymbol{e}. \qquad (3.4)$$

where A=R/L and B=1/L. The goal is to estimate *A* and *B*.

In order to improve the estimation accuracy of the open loop model, a nonlinear model reference adaptive observer is designed to estimate the parameters. The estimated currents are as:

$$\frac{d}{dt}\hat{\boldsymbol{i}}_j = -\hat{\boldsymbol{A}}\hat{\boldsymbol{i}}_j + \hat{\boldsymbol{B}}(\boldsymbol{v}_j - \boldsymbol{e}_j), \qquad \boldsymbol{j} = \boldsymbol{a},\boldsymbol{b},\boldsymbol{c},\boldsymbol{d},\boldsymbol{e}. \qquad (3.5)$$

where ^ is used to denote the estimated components.

Stability Analysis:

In order to ensure the stability of the estimation algorithm and to design the corresponding observers, a stability analysis is done. Here a Lyapunov function is used to ensure stability of the system and measurement of parameters. This function is defined as:

$$\boldsymbol{V} = \frac{1}{2}\boldsymbol{S}^2 + \frac{1}{2}(\hat{\boldsymbol{A}} - \boldsymbol{A})^2 + \frac{1}{2}(\hat{\boldsymbol{B}} - \boldsymbol{B})^2. \qquad (3.6)$$

where *S* is an error function. There are different possibilities to choose the error function [56]. The error function used in this thesis is as follows:

$$S = \quad + \int dt. \qquad (3.7)$$

where δ is equal to difference between the estimated and real current in each phase of the power converter, and λ is a positive constant. If the error is equal to zero (i.e. S=0), then, the observer is no longer sensitive to parameter uncertainties. Taking into account (3.1) and (3.7), the derivative of S for the first element is calculated as:

$$\dot{S} = \dot{} + \quad . \qquad (3.8)$$

$$\dot{}_a = \dot{\hat{i}}_a - \dot{i}_a = (A - \hat{A})\dot{\hat{i}}_a - A \ _a + (v_a - e_a)(\hat{B} - B). \quad (3.9)$$

where $\dot{x}$ is equivalent to dx/dt. Similarly, other components are calculated.

According to Lyapunov stability theory, if derivative of V is less than zero for all positive V values, then the system is stable [56]. The derivative of (3.6) is as:

$$\dot{V} = S^T \dot{S} + (\hat{A} - A)\dot{\hat{A}} + (\hat{B} - B)\dot{\hat{B}}. \qquad (3.10)$$

From (3.9) and (3.10), the derivative of V function can be computed as:

$$\begin{aligned} \dot{V} &= (\ _a + \int \ _a) \times -(A - \ ) \ _a \\ &+ ((\ _a + \int \ _a) \times (A - \hat{A})\dot{\hat{i}}_a + (\hat{A} - A)\dot{\hat{A}}) \\ &+ ((\ _a + \int \ _a) \times (v_a - e_a)(\hat{B} - B) + (\hat{B} - B)\dot{\hat{B}}). \end{aligned} \qquad (3.11)$$

The first element in (3.11) is negative for λ values less than A. According to Lyapunov stability condition, the remaining components can be calculated as:

$$\dot{\hat{A}} = (\ _a + \int \ _a) \times \hat{i}_a \qquad (3.12)$$

$$\dot{\hat{B}} = -(\ _a + \int \ _a) \times (v_a - e_a) \qquad (3.13)$$

Under steady state condition, the error and its dynamic are zero. So, the resistance and inductance can be calculated from (3.12)-(3.13) as follows:

$$\frac{1}{\hat{L}} = \frac{1}{L} - \int (\ _a + \int \ _a) \times (v_a - e_a) dt. \qquad (3.14)$$

$$\hat{R} = R + \hat{L} \int (\ _a + \int \ _a) \times \hat{i}_a. \qquad (3.15)$$

From (3.14) and (3.15), instantaneous values of R and L can be calculated. In this thesis, the estimated parameters are used to design the *PR* controller and to estimate the phase currents using a SMO.

As aforementioned, the estimated parameters can be used for other purposes such as improving the controller of the motor. For example, in the case of using a predictive controller in a BLDC motor, it is possible to have both good transient and steady state performance; however the controller performance is sensitive to parameter uncertainties. Therefore, the parameter estimation can be used to design a robust predictive controller. Detection of high resistance connection in cables feeding the machine has been presented in [58], [59].

In order to detect a fault in VSI, the phase currents of the motor are predicted; a SMO is used for this purpose. The estimated parameters in (3.14)-(3.15) are used in the SMO. Details of SMO are presented in the following section.

Current Estimation

In order to estimate the phase currents, SMO is used in this thesis. It has many advantages, which make it a suitable option for the state variable estimation. Simple implementation, robustness to parameter uncertainty and measurement noise are the most important factors among others [54].

As it was shown above, a model reference adaptive observer was used to estimate motor parameters. Since real parameters are already known from the parameter estimator, response of the open loop model should be equal to real current. In the case of a healthy motor, error signal reduces to zero after few cycles. In presence of a fault, the model based estimator can no longer estimate the parameters accurately. Under this condition, the error signal increases remarkably.

To detect a fault, the error signal available in SMO is compared to a threshold above zero. If it increases beyond the threshold, a fault alarm is generated. Since the estimated parameters are no longer accurate in a faulty motor, the estimated values are always memorized during one cycle before the fault alarm. After the fault alarm, the controller and model parameters are updated with estimated values for one cycle before the fault.

To estimate the phase currents accurately, the SMO is designed as:

$$\begin{bmatrix} L_a & -L_b & 0 & 0 \\ 0 & L_b & -L_c & 0 \\ 0 & 0 & L_c & -L_d \\ L_e & L_e & L_e & L_e+L_d \end{bmatrix} \frac{d}{dt}\begin{bmatrix} \hat{i}_a \\ \hat{i}_b \\ \hat{i}_c \\ \hat{i}_d \end{bmatrix} = \begin{bmatrix} v_{ab}-e_{ab} \\ v_{bc}-e_{bc} \\ v_{cd}-e_{cd} \\ v_{de}-e_{de} \end{bmatrix} - \begin{bmatrix} R_a-R_b & 0 & 0 \\ 0 & R_b-R_c & 0 \\ 0 & 0 & R_c & -R_d \\ R_e & R_e & R_e & R_d+R_e \end{bmatrix}\begin{bmatrix} \hat{i}_a \\ \hat{i}_b \\ \hat{i}_c \\ \hat{i}_d \end{bmatrix} - K \times Sat\left(\begin{bmatrix} a \\ b \\ c \\ d \end{bmatrix}\right). \quad (3.16)$$

where *K* is the observer gain, and *Sat* is a saturation function defined as follows:

$$Sat(x)=\begin{cases} 1 & x \geq 1 \\ x & -1 < x < 1 \\ -1 & x \leq -1 \end{cases} \quad (3.17)$$

It is possible to use different functions instead of *Sat* such as Sigmoid and Sign function. The high frequency oscillations can be avoided in the estimated variables, if the saturation function in (3.17) is used. In order to obtain suitable values of *K*, a stability analysis is presented in the following section.

To evaluate stability of the SMO, the Lyapunov function is defined as:

$$V = \frac{1}{2}S^2. \qquad (3.18)$$

The Lyapunov function and its derivative given in (3.9)-(3.10) are similarly adapted here. Taking into account (1) and (18), the derivative of δ for the first element is calculated as:

$$\dot{\delta}_a = \dot{\hat{i}}_a - \dot{i}_a = -\frac{R_a}{L_a}(\hat{i}_a - i_a) - \frac{K}{L_a} \times Sat(\hat{i}_a - i_a). \qquad (3.19)$$

Similarly, other components are calculated. So, derivative of V function is as:

$$\dot{V} = [\delta_a \quad \delta_b \quad \delta_c \quad \delta_d \quad \delta_e]^T \times \begin{bmatrix} -\frac{R_a}{L_a}\delta_a - \frac{K}{L_a} \times Sat(\delta_a) \\ -\frac{R_b}{L_b}\delta_b - \frac{K}{L_b} \times Sat(\delta_b) \\ -\frac{R_c}{L_c}\delta_c - \frac{K}{L_c} \times Sat(\delta_c) \\ -\frac{R_d}{L_d}\delta_d - \frac{K}{L_d} \times Sat(\delta_d) \\ -\frac{R_e}{L_e}\delta_e - \frac{K}{L_e} \times Sat(\delta_e) \end{bmatrix}. \qquad (3.20)$$

Since *Sat* function is a linear function, sign of $\delta_a Sat(\delta_a)$ will be always positive. Consequently, the only condition to achieve sliding surface is for positive *K* values. According to (3.19), by choosing higher values of *K*, the dynamic behaviour of the resultant error will be even faster.

It should be noted that *K* value has a significant effect on the performance of the proposed FD method. If a very high value is chosen for *K*, the observed value will follow the real state too fast. Therefore, the residue value will be low. On the other hand, by choosing a small value for *K*, the estimated current will still follow the current pattern before the fault. In this case, it is easier to detect the fault, since the faulty current is significantly different from the healthy current. A low value of *K* is an optimal choice in this thesis. This assumption results in a robust SMO with slow dynamics. This claim will be later validated with experimental results.

3.2.2. Fault Diagnostic Method

In order to detect a fault, it is possible to define a simple FD index (i.e. the error between the estimated and real current values). Applying this approach for a multiphase machine can lead to false alarms. The main reasons are explained in details in the following.

When a fault occurs in one phase of the converter, closed loop control tries to minimize the error between the reference currents and real currents. As a result, in case that the healthy control method is still applied, output voltage of the control block for a faulty inverter will be changed. On the other hand, in the case of a single switch fault in one phase, a DC value is added to the remaining healthy phase currents. In the case of multiple open switch faults, this DC value can be very high.

Consequently, due to the effect of the control method, and faulty signals, the estimated currents in the remaining healthy phases can be different from the real values. In addition, simplifications in model can result in a small error. If estimated and real current values are different, this error can be interpreted as a false alarm based on the error value. As a result, FD block should be robust to these cases. These effects will be later validated by experimental results.

To overcome the drawbacks of a simple FD index based on the error function, an alternative solution is proposed in this thesis. Here the estimated and measured current signals are fed to a simple unique algorithm. The presented algorithm can detect both the single switch and open phase faults in a VSI. According to this algorithm, the similarity level between two input current signals is measured as a function of time; this measuring factor is based on a cross correlation function [60]. This factor is defined as:

$$\rho_{x_1-x_2} = \frac{\sum_{j=1}^{N}(x_{1j}-\bar{x}_1)(x_{2j}-\bar{x}_2)}{\sqrt{\sum_{j=1}^{N}(x_{1j}-\bar{x}_1)^2\sum_{j=1}^{N}(x_{2j}-\bar{x}_2)^2}}. \qquad (3.21)$$

where x_1 and x_2 are the estimated and measured current in each phase of the power converter, respectively; μ is the moving average value of the input variables and N is the number of samples. It is worth to note that N value determines the evaluation period in each sampling point. Choosing a small value for N makes the ρ value sensitive to noise. On the other side, a high N value increases the detection time. Moreover, the ρ value will be sensitive to frequency transients in a variable speed drive. It should be noted that the smallest value for N is one sample in one period; the highest value is the number of samples in one period of the fundamental frequency. So, a tradeoff should be reached between sensitivity to noise and FD speed.

The ρ value varies from -1 to 1. In the case of completely similar waveforms, its value approaches to 1. According to (21), under healthy condition in a motor drive, both the estimated and real currents are similar, so the correlation factor is near 1. However, under faulty mode, these waveforms are quite different, at least for the half of one fundamental cycle. Under faulty mode, the cross correlation factor reduces to zero. So, the ρ factor is a suitable index to distinguish a healthy condition from a faulty one.

In comparison to the conventional methods, this proposed method is robust to all false alarms due to fast load transients or unbalanced nonsinusoidal waveforms. Consequently, a FD index is defined as:

$$\boldsymbol{D} = \quad . \qquad (3.22)$$

The D value is equal to zero under faulty mode, while it is close to 1 under healthy mode. Therefore, D value equal to zero indicates a fault condition. To improve the robustness of the proposed

FD method against noise and fast transients, here FD is done with a small time delay denoted by t_d. If the D value is equal to zero during td, then the open switch or open phase fault is detected.

After FD, it is necessary to locate the faulty component in the power converter. The fault scenario in one leg of the VSI can be either a single switch fault or an open phase fault. Due to the single switch fault, average value of the phase current during one fundamental cycle is positive in the case of a lower switch fault or negative in the case of an upper switch fault. In the case of the open phase fault, the phase current and ρ factor are zero. Therefore, fault localization in the case of single switch fault is as:

$$\boldsymbol{sign}(\hat{\boldsymbol{i}}) = \begin{cases} > 0 & \boldsymbol{lower\ switch\ fault} \\ < 0 & \boldsymbol{upper\ switch\ fault} \end{cases} \qquad (3.23)$$

Here the estimated current is used to localize the faulty switch. In order to localize the open phase fault, average value of the ρ factor is calculated during one period as:

$$\boldsymbol{D}_{1\boldsymbol{j}} = \frac{1}{\boldsymbol{M}} \sum_{\boldsymbol{j}=1}^{\boldsymbol{M}} {}_{\boldsymbol{j}}, \quad \boldsymbol{j} \ \{\boldsymbol{a},\boldsymbol{b},\boldsymbol{c},\boldsymbol{d},\boldsymbol{e}\}. \qquad (3.24)$$

where *M* is number of samples in one period. If the average value is zero, then the fault type is an open phase fault. For the sake of simplicity, aforementioned fault types are codified. The fault codes are 1, -1 and 2 in the case of upper switch fault, lower switch fault and open phase fault, respectively. These codes are the same in the rest of this thesis. Block diagram of the FD method is shown in Fig. 3.3. In this figure, ε is a small positive value near to zero.

Based on the presented technique, fault localization in the case of a single switch fault is done during one sampling time after FD. Nonetheless, a time delay around one fundamental cycle is necessary to localize the open phase fault. As it can be seen from Fig. 3.3, once the fault is detected, fault localization block is enabled. It should be noted that the FD is done separately in each phase of the power converter. As a result, the presented FD technique can be applied to any two-level multiphase VSI.

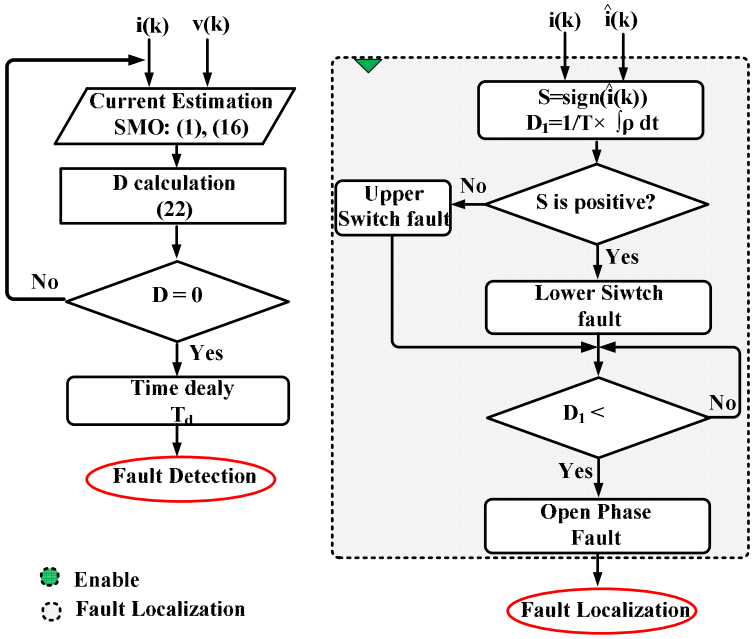

Fig. 3.3. FD and localization method.

3.2.3. Fault-Tolerant Control and Analysis of a Five-Phase BLDC Motor

Application area in this thesis is electric vehicles. High reliability is of paramount importance for this application. Five-phase fault-tolerant BLDC motors can meet this requirement. In this thesis, fault diagnosis and fault-tolerant control of a multiphase BLDC motor are studied. Block diagram of the proposed setup is shown in Fig. 3.4(a). This motor can be operated with one or two-faulty phases. For clarification, motor operational modes are shown with a code denoted by FC in Fig. 3.4(a). The operational control mode of the machine is determined by the FD block developed in section IV. Here, control modes of the machine are shown by codes 1, 2, 3, and 4 which correspond to healthy mode, one faulty phase mode, two-adjacent faulty phase mode and two-nonadjacent faulty phase mode, respectively. In the following part, the fundamentals of the fault-tolerant control are briefly reviewed.

In order to control the motor, a FOC technique is used. The control algorithm is implemented under healthy and each faulty mode, separately. The basic rules used to calculate the reference currents under different fault conditions are described in [61]. The calculated reference currents in [61] are shown in Table III.I. As it can be seen, both first and third harmonics are included in the reference currents. The reference currents are used in this thesis in order to realize the fault-tolerant FOC algorithm.

As it can be seen from Fig. 3.4(a), to implement the FOC algorithm, two controllers are used. An outer controller is used to set the motor reference speed shown by ω^*. A PI controller is typically used

to realize the speed controller. In addition, an inner controller is used to set the motor reference currents shown by *i**.

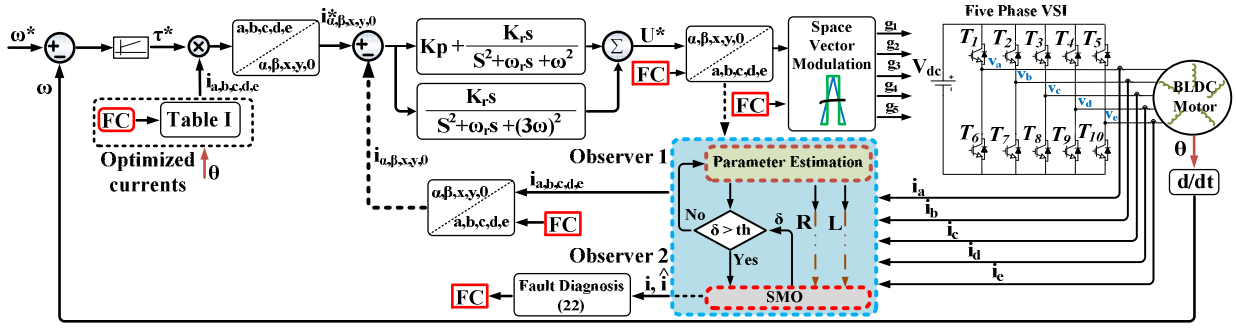

Fig. 3.4. (a) Fault detection, parameter identification and Fault-Tolerant FOC (b) Block diagram of the inner current controller under each operational mode of the motor.

TABLE III.I. Optimized phase currents with isolated neutral

Current	A	B	C	D	E
one faulty phase (FC=2)					
I_1(PU)	0	0.99	0.99	1	0.98
θ_1	-	51	137	232	-41
I_3(PU)	0	0.17	0.08	0.09	0.19
θ_3	-	23	52	186	-19
two adjacent faulty phases (FC=3)					
I_1(PU)	0	0	0.59	0.95	0.67
θ_1	-	-	82	218	0
I_3(PU)	0	0	0.12	0.29	0.16
θ_3	-	-	44	102	41
two nonadjacent faulty phases (FC=4)					
I_1(PU)	0	0.99	0	0.98	0.99
θ_1	-	77	-	2	-42
I_3(PU)	0	0.16	0	0.19	0.17
θ_3	-	15	-	55	-21

The output of the speed controller shown in Fig. 3.4(a) is the reference torque denoted by τ^*. One main assumption to calculate the optimized reference current values in [61] was no ripple in the generated torque. Therefore, authors here use the conventional PI control to set the reference speed.

Inner controller can be done in different ways. A comprehensive study has been done on different current controllers in [61]. One PI controller in synchronous reference frame and one PR controller in stationary reference frame are two possible control methods to set the reference currents. Regarding the optimized reference currents given in table I, under faulty mode, the phase currents are unbalanced and nonsinusoidal. In the case of using a simple PI controller, due to unbalanced nonsinusoidal phase currents, both DC component and oscillatory components appear in reference currents after transferring to synchronous reference frame. In order to have DC reference currents, PI controller should be designed separately for positive and negative sequence components. This implies high computational cost and complicated controller design. Furthermore, the PI controller should be able to track harmonic components as well. It is known in literature that PI controllers have a high performance to track DC components [62], [63]. In the case of sinusoidal components, there will be steady state error. Therefore, the second disadvantage of a PI control is poor tracking performance due to its limited bandwidth.

As it is shown in Fig. 3.4(a), in this thesis, a PR controller in stationary reference frame is used to implement the inner current controller. According to [62], this controller is able to set both positive and negative sequence components at the same time. On the other hand, resonant controllers can be set individually to track each desired harmonic component. In order to track the reference currents in a five-phase BLDC motor, PR controller should be able to control both the first and third harmonics.

Transfer function of PR controller is as:

$$G_c(s) = K_p + \frac{K_r s}{s^2 + \omega_r s + \omega_o^2} + \frac{K_r s}{s^2 + \omega_r s + (3\omega_o)^2} \qquad (3.25)$$

where $\omega_o=2\pi f_o$, and f_o is the resonance frequency of the controller, K_p is the proportional gain, K_r is the resonant gain, and ω_r is the bandwidth of the controller around the resonance frequency. It should be noted that ω_r is used to reduce the controller sensitivity at resonance frequency. This criterion should be considered in variable speed drives due to speed variations of the motor. Also, f_o is determined from the motor speed.

As aforementioned, a five-phase BLDC motor can be operated with two faulty phases. This means that inverter configuration under healthy mode, one faulty phase mode, and two faulty phase mode are the five-phase, four-phase, and three-phase, respectively. So, the inner current controller should be reconfigured under each operational mode of the machine. The inner current control scheme at each mode is shown in Fig. 3.4(b). It should be noted that the Park's transformation should also be updated for five-phase, four-phase or three-phase currents at each operational mode of the machine.

3.3. Experimental results

To validate the developed theory, experimental results are conducted on a five-phase BLDC motor. The experimental results are presented in three sections. In the first section, the motor model is tuned with estimated parameters. After that, the effect of *K* value on FD performance is discussed. Moreover, characteristics of FD method for application in a multiphase machine will be explained. In the second section, different faulty types are implemented in the inverter; FD method is used to detect and localize the faults. In the last section, the fault-tolerant control of a five-phase BLDC motor is presented; here the FD block is used to achieve the fault-tolerant operation.

Model Verification:

In order to tune the open loop model, in the first step, the presented algorithm in section III is implemented to estimate the stator resistance and inductance of the five-phase BLDC motor. The estimated parameters during four fundamental cycles are shown in Fig. 3.5(a). As it can be seen, the resistance and inductance value are 0.75 Ω and 490 µH, respectively. To validate effectiveness of the developed theory, a 0.25 Ω resistance was connected in series with phase a. After a short time, it is short circuited. Experimental result of the stator resistance estimation is shown in Fig. 3.5(b). As it can be seen, the presented parameter estimator can accurately measure the added value.

In the second step, after parameter estimation, the calculated values are used to design the PR controller. Details of the controller design are discussed in the following.

Different methods have been presented in literature to design the PR controllers. In comparison to PI controller, here by adding a resonance term in parallel to a proportional term, the frequency response is only affected around the resonance frequency. The bandwidth of the controller given in (3.25) at the resonance frequency is defined by the integrator term. The proportional gain can be designed similar to PI controllers. A similar gain can be chosen for both the first and third harmonics [64]. As a result, the controller design is only considered for the first harmonic.

In order to eliminate the high frequency noise, and at the same time to have a fast dynamic response, the cut off frequency shown by ω_c in this thesis is determined well above the resonance frequency [65]. Typical applications consider 1/5 of the switching frequency as the design specification. On the other side, to reduce the controller sensitivity around the resonance frequency, the ω_r value in (3.25) should be different from zero. In this thesis, the design specification is to set ω_r at 0.0628 rad/s, and ω_c at 600 Hz.

Using the estimated parameters, the PR controller is designed according the design method presented in [66]. A block diagram of the inner current controller is shown in Fig. 3.6(a). Regarding the

controller design specifications, the phase margin was considered higher than 45 degrees. Limited value of the motor operation speed for experimental setup is considered as 50 rpm; frequency of the motor phase current at this speed is 21.6 Hz. The designed values for K_p, K_r are 0.067, and 25.27, respectively. The frequency response of the designed PR controller is shown in Fig. 3.6(b). As it can be seen, the controller has a high gain at the resonance frequency. Therefore, the controller can effectively track both the first and third harmonic components of the motor phase current.

In the third step, the effect of *K* value on FD algorithm is evaluated. Two case studies are considered for different values of *K*. For the first case, single switch FD is studied for a low and a high *K* value. Experimental results are shown in Fig. 3.7(a). The estimated current, real current and error signal are shown. As it can be seen, for small *K* values, the error signal is significantly high. For the second case, open phase FD is evaluated. The final waveforms are shown in Fig. 3.7(b). As it can be seen, in case of small *K* value, the error signal is high. Consequently, a low value of *K* equal to 4 is considered in this thesis which is the same in the rest of this thesis.

As discussed before, faulty signals, inaccurate model, and control method performance can affect the estimated current in the remaining healthy phases. To validate this claim, two faulty scenarios are considered here. In the first case, an open switch fault in phase *a*, and an open phase fault in phase *b* are considered. The estimated current, real current and error value in phase *d* are shown in Fig. 3.7(c). As it can be seen, regardless of being a healthy phase, there is a DC value in phase *d* current. At the same time, the error value during half of one period is high. If the error is used as the FD index, false alarms can be generated in this phase. To further validate this claim, three lower switch faults are considered in phases *a*, *b*, and *c*. The phase *e* current and error value are shown in Fig. 3.7(d). Although there is no fault in this phase, the estimated and real current are different.

The presented analysis validates the necessity of a high performance FD method which is robust to these effects. As described above, the FD index presented in (3.22) in this thesis has this characteristic.

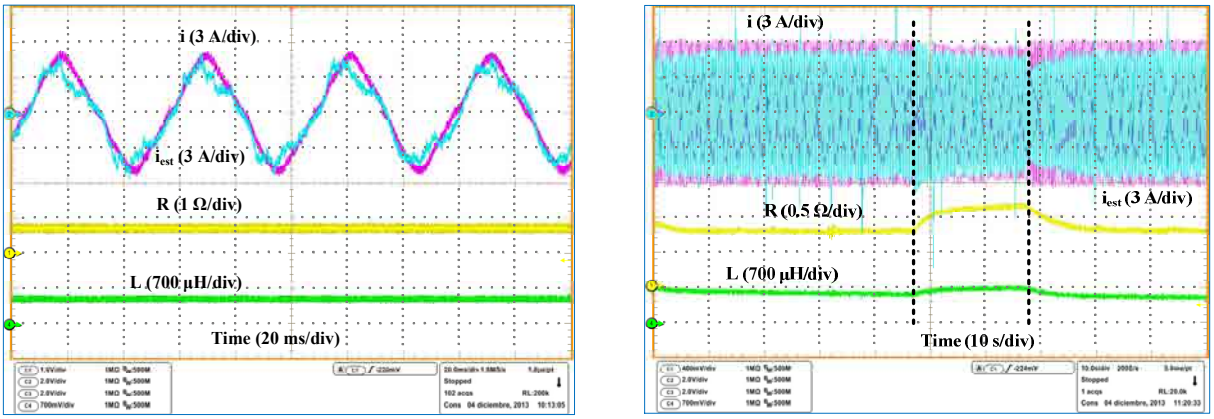

(a) (b)

Fig. 3.5. Estimated resistance of the stator. (a) Results during four cycles. (b) Results for long time.

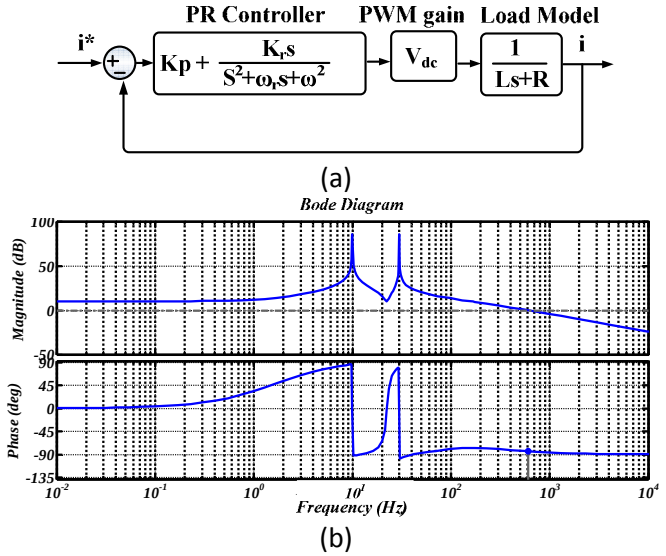

(a)

(b)

Fig. 3.6. Controller design (a) Block diagram of the current controller (b) frequency of the current controller and its frequency response at ω_c=3768 (rad/sec), ω_r=0.0628 (rad/sec) and ω_o=62.8 (rad/sec).

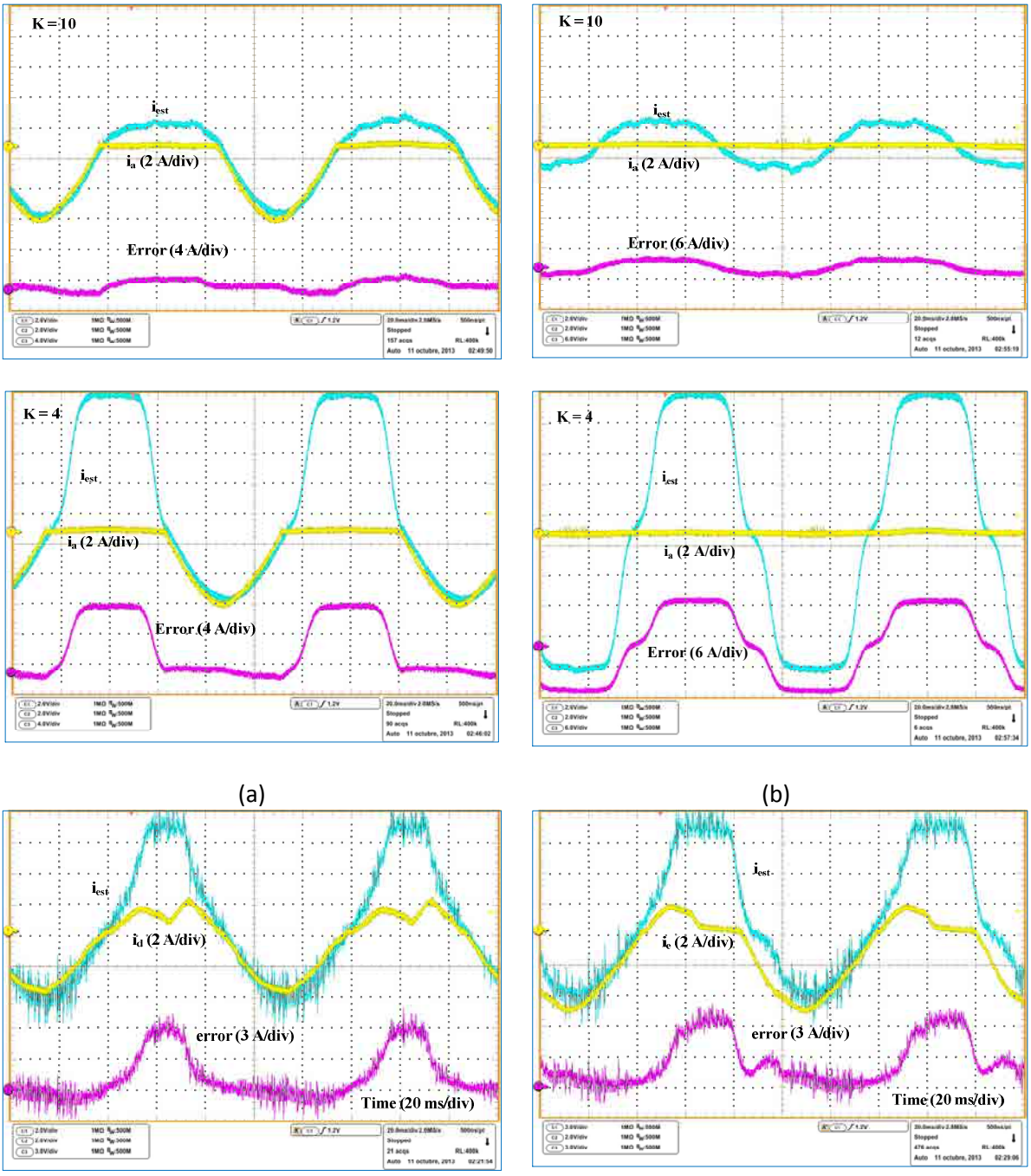

Fig. 3.7. Experimental waveforms of model verification - effect of *K* value on FD method (a) under open switch fault. (b) Under open phase fault. Effect of faulty mode and control on healthy phases (c) under single switch fault. (d) Under open phase fault.

Experimental Results of the FD:

In this section, different faulty modes are considered in the inverter. The proposed FD scheme is used to detect and localize the faulty component.

Robustness to the load transients is an important requirement for a high performance FD method. Considering this, a 75 % step was forced on the motor reference current; experimental results are shown in Fig. 3.8(a). As it can be seen, FD index *D* is equal to 1, and as a result, no false alarm was generated using the presented method. It should be noted that due to the limited number of the oscilloscope channels, here only estimated current, measured current, *D* value and fault signal in phase *a* are shown.

Open switch FD is considered as the second case study; an upper switch fault in phase *a* and a lower switch fault in phase *b* are triggered. The experimental results are shown in Fig. 3.8(b). As it can be seen, *D* value reduces to zero under faulty modes. In both cases, the fault is detected and localized during less than a quarter of one period.

It is possible to detect open phase faults without using any auxiliary variable. Experimental results of the open phase FD in phase *a* are shown in Fig. 3.8(c). As it can be seen, *D* value reduces to zero after fault. This fault is detected during less than a quarter of one period.

Since it is possible to operate a five-phase BLDC motor with two faulty phases, the proposed FD method should be able to detect a new fault in a motor with one faulty phase. In this section, the gate signals of phase *a* are removed and the motor is operated with the fault-tolerant control algorithm adapted for the one faulty phase mode. Subsequently, a new upper switch fault is forced in phase *b*. Experimental results are shown in Fig. 3.8(d). As it can be seen, the fault is detected and localized successfully.

As explained before, the presented FD method is not sensitive to the parameter uncertainty. To validate this capability, resistance value in all phases of the motor model has been decreased 20 %; at the same time, self inductance value has been increased 10 %. An open switch fault and an open phase fault were forced in phase *a*. Experimental results are shown in Figs. 3.8(e) and (f), respectively. As shown, the fault is detected successfully in both cases.

One remarkable advantage of the presented FD method is its robustness to speed transients. Similar to torque, the speed transients are usual in a variable speed drive for electric vehicles. Therefore, a FD method should also be robust to speed transients. Here, two experimental results are carried out to validate this capability; in the first case, motor speed is changed from 16 rpm to 23.8 rpm. After that, the motor speed is changed from -23 to 23 rpm. During transients, the parameters of the FD block are not changed. Experimental results are shown in Figs. 3.9(a) and (b), respectively. As it can be seen, the proposed FD technique is robust to speed transients.

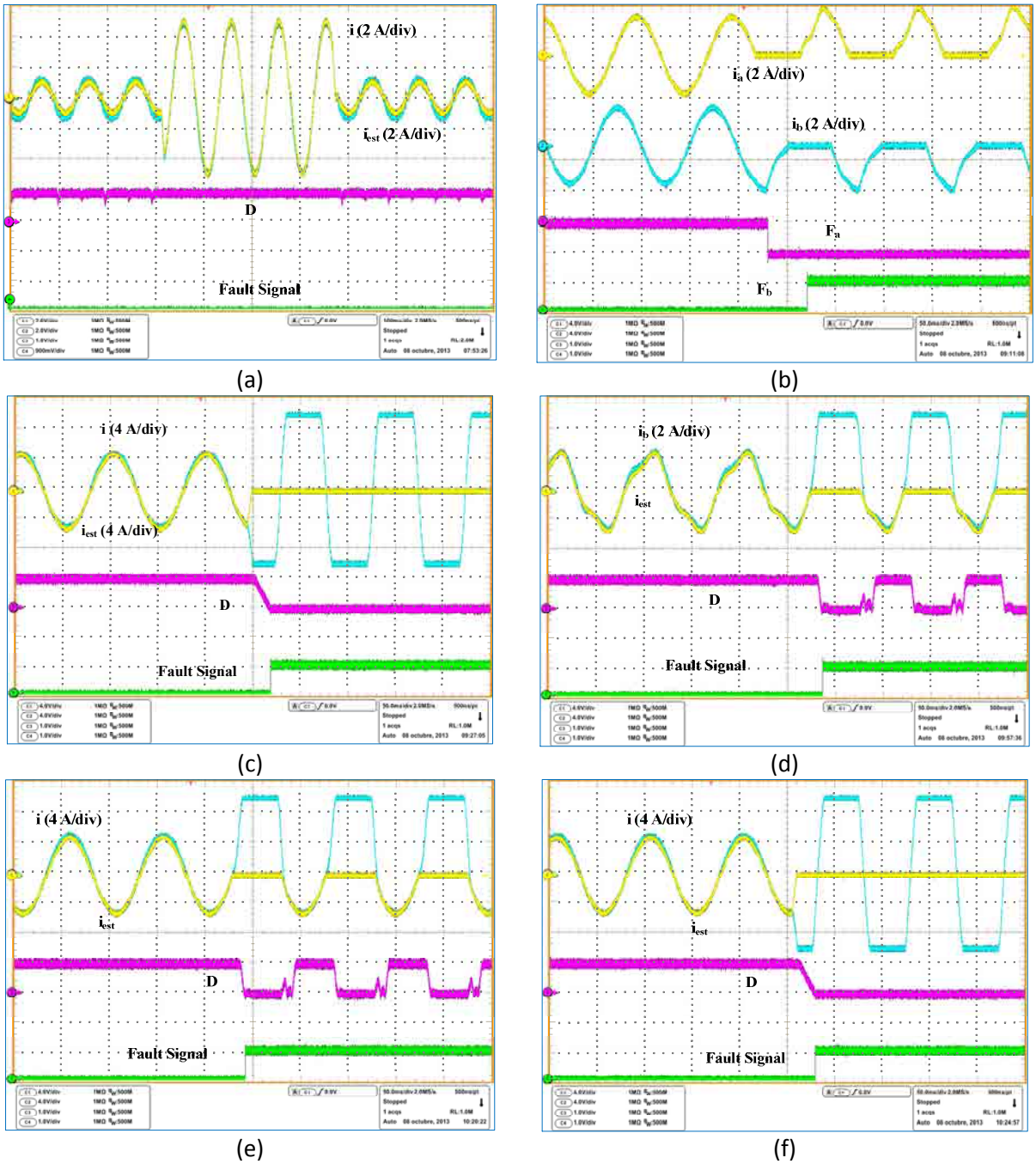

Fig. 3.8. Experimental waveforms of FD (a) Evaluation the effect of load transients. (b) Open switch FD. (c) Open phase FD. (d) FD under faulty mode operation. FD under parameter uncertainty and (e) open switch FD. (f) open phase FD.

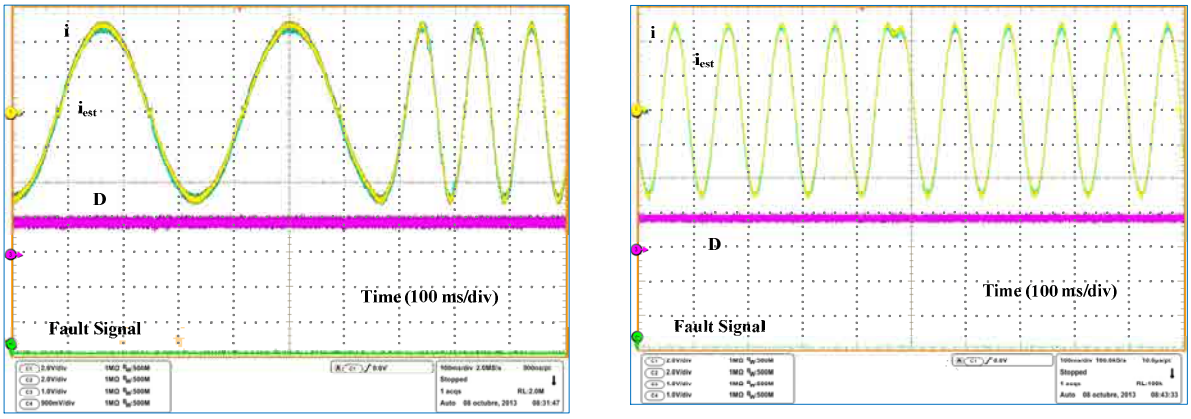

(g) (h)

Fig. 3.9. Experimental waveforms of FD under speed transients. (a) Results under speed variation. (b) Results under speed reverse condition.

Experimental Results of the Fault-Tolerant Operation:

A high performance FD method should be included in a fault-tolerant control algorithm. The FD block is used in the fault-tolerant control of the five-phase machine to detect the fault. After FD and isolation of the faulty leg, the control method is updated according to the new mode.

In the first step, a fault is started in phase *a*. After FD, the faulty leg is isolated by removing the gate signals in the corresponding leg. Healthy mode control is also replaced with faulty mode control. The motor is operated for 5 cycles with the control method for one faulty phase. After that, a new fault is forced in phase *b* which is adjacent to phase *a*. The FD time in phase *b* is less than a quarter of one fundamental cycle. After FD and isolation, control method of the two-adjacent faulty phase mode is used. Experimental results of this mode are shown in Fig. 3.10. The phase currents i_a, i_b, torque and fault-tolerant code are shown.

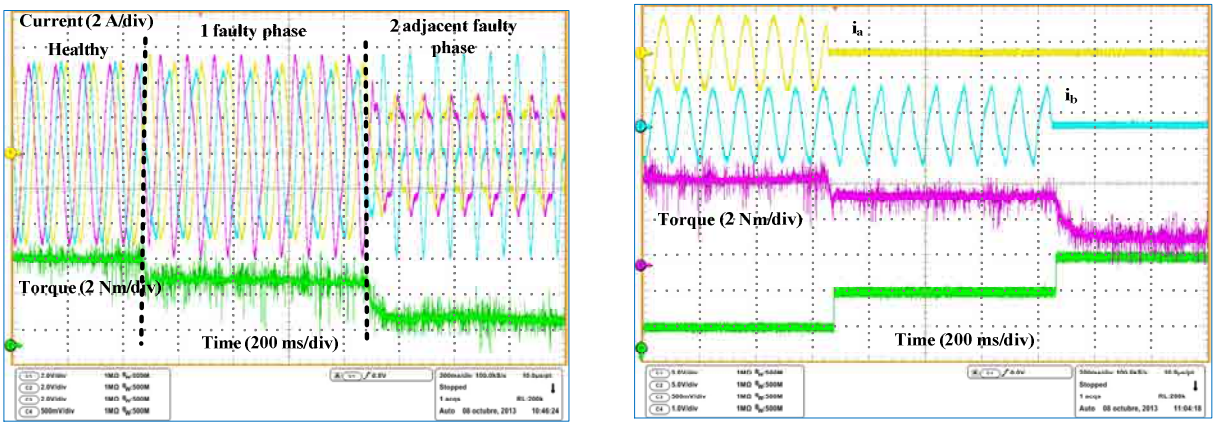

Fig. 3.10. Experimental waveforms of the fault-tolerant control in case of two adjacent faulty phases.

3.4. Discussion and conclusions

A novel model based open switch FD technique for two-level VSI-type power converters is presented in this chapter. The FD index is based on the cross correlation between the estimated phase currents using SMO and the real currents. By choosing a suitable evaluation period, a robust FD is achieved in less than a quarter of one period of the fundamental frequency. The detection speed is quite fast. Ability to detect multiple open switch and open phase faults without using auxiliary variables makes this method superior to the presented methods in literature. Moreover, the FD index is independent from the load parameters and it is robust against fast transients.

In order to design the SMO, an observer is used to estimate motor parameters. By using the estimated parameters, an ideal model was used in SMO. The estimated parameters are utilized to design the PR controller at the same time. These parameters can also be monitored as effective indicators of the machine connection such as high impedance connection. The proposed FD method was applied to a five-phase BLDC motor drive; both FD performance and fault-tolerant capability were evaluated. According to the results, it can detect all open switch faults successfully. Experimental results under fault-tolerant control validate the high efficiency of the proposed FD technique.

The effectiveness of parameter estimator was also validated by experimental results.

4.

Study and Contributions to Signal Based FD Methods

Industry is always demanding simple, robust, flexible and cost effective FD methods. This chapter investigates low cost signal based FD methods.

CONTENTS

4.1. Introduction

Higher reliability is a new challenge in power electronics especially in applications such as electric and hybrid electric vehicles, more electric aircrafts, chemical industries, transportation systems, renewable energy systems and spacecrafts [67-70]. Multi-phase fault-tolerant PM motor drive is a reliable and efficient solution for motor drive applications in electric and hybrid electric vehicles; this higher reliability is due to their fault-tolerant capability under single or two phase faults, lower torque ripple than conventional three phase motors, and less operational noise [68-70]. In such applications, power converters are principally used to feed the electrical motor. According to a recent survey, power switches are responsible for the main part of power converter failures [6]. In [7], Lu. et al. has presented a complete review on faulty modes and detection methods of power switches; in addition, a comparison is done between different detection schemes. The main focus of this chapter is to study and proposed open switch FD methods as shown with dash read line in Fig. 4.1.

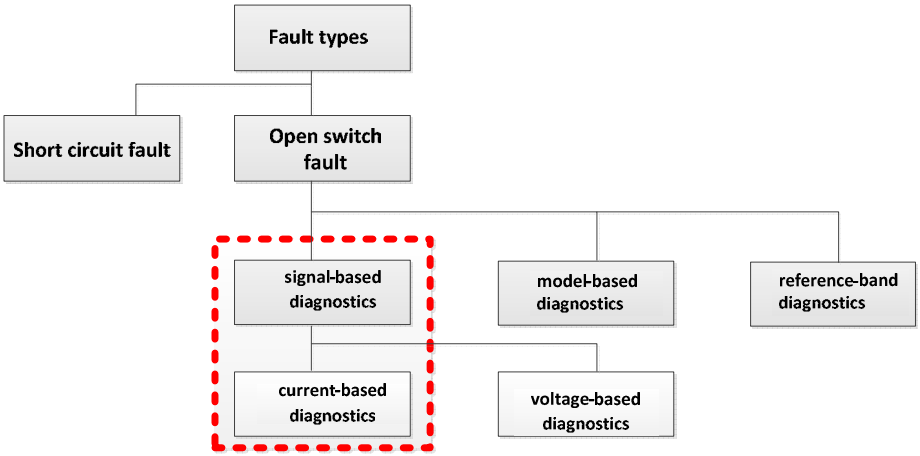

Fig. 4.1. Proposed FD method in this chapter.

Before discussing the proposed methods, a brief survey through literature is presented. Prone and cones of available methods are discussed.

On the other hand, open switch FD is not included in the commercial drivers, and should be added by the end user to the control algorithm. Three main solutions have been presented in literature to protect the system against open circuit fault [9]. These methods are based on reference signal, system model or measured signal (i.e. the output current or voltage of the power converter).

Considering reference based FD method, a residual value which is equal to the difference between the reference current and real current can be used as a detection index [25]. This method is fast, simple, cheap and robust under fast load transients. However, it can only be applied to a system with closed loop control.

Regarding the second method (i.e. model based open switch FD method), it is also possible to estimate system output using input signal and load model, and then subtract the estimated value from the real value. The residue values higher than zero are indications of the fault [19], [23], [71]. Although this method is simple and cheap, detection performance mainly depends on the load model. Obtaining an accurate model of the load under all operating conditions is quite difficult.

According to the third method (i.e. signal based open switch FD method), converter output voltage or current can be used to develop a detection method. Presented methods in [72-73] use an extra hardware to measure the voltage signal, this variable is not usually required in the controlling unit of most industrial applications. Although extra fast detection of both open switch and short circuit faults can be realized effectively by using the voltage signal based techniques, the higher implementation cost of these techniques can be considered as a serious issue for such methods.

Current signal based techniques have been addressed as well; Park's vector method, wavelet transform, slope method, and Fourier transform are the most well-known tools used in conventional methods among others [7]. Regardless from being simple and cheap, these methods suffer from some drawbacks such as complexity, false alarms, low flexibility, long detection time and not being able to detect multiple faults. Recently, several high performance FD methods using the current signal have been presented such as ideas in [40], [42], [48], [74]. All published methods can effectively detect the fault if the input currents are three phase, balanced, and sinusoidal. However if these methods are applied to a five-phase converter or a multiphase converter in a more general point of view with nonsinusoidal unbalanced phase currents, one or some of the following problems can reduce the FD performance. According to the presented methods in [9] and [74], in order to derive a FD index for a power converter, average value of the phase current is divided by the absolute average value of the phase current. This value is less than 0.5 under healthy mode. When a single switch fault occurs in one phase of the power converter, a dc component is added to the remaining healthy phase currents. If the dc value in the healthy phase current is high, a false alarm will be generated since the average value of the phase current is close to its absolute average value. Regarding the presented method in [15], after applying Park's transformation, the phase currents are normalized with respect to Park's vector modulus. After that absolute average value of the normalized phase current is calculated; this is a fixed value under healthy condition. In the case of five-phase machines, however, if this normalization factor is applied to the five-phase currents, absolute average value of the phase currents is no longer a fix value which is due to the unbalanced nonsinusoidal waveforms. Therefore, this method is not effective for application in a multiphase converter. Also, it is necessary to calculate a normalization factor (i.e. Park's vector modulus presented in [40]); this value is usually dependent on the converter configuration. As a result, with increased number of phases, it will be more complicated to calculate this value. A FD

method based on multiple fault indexes (i.e. current amplitude and angular frequency) has been presented in [48]. This method is computationally demanding. The main reason of higher computational load is the use of PLL for obtaining the angular frequency. Moreover, in the presence of third harmonic current, an additional block should be added to extract this component. As a result, development of this method for a multiphase machine will be complex.

To overcome the aforementioned drawbacks, a novel current signal based model identification method is presented in this chapter in order to detect the open switch or open phase faults in the power converter.

Although fault-tolerant control of the five-phase PM machines at steady state has been well treated in literature, but the implementation of all three main topics for a fault-tolerant motor drive including FD, fault isolation and fault-tolerant operation at the same time has not been discussed well. Therefore, fault-tolerant operation including FD, isolation and control of a five-phase converter is presented as a new approach for BLDC fault-tolerant motor drives.

In addition, two more contributions are shown in this chapter. Firstly, a new open transistor FD method in VSI is proposed; the proposed method is done by using a simple trigonometric function. Secondly, in order to evaluate the performance of the FD method in a closed loop system, SMC is developed to implement the inner controller of a five-phase PM motor drive; the proposed FD block is included in the control algorithm. The proposed FD algorithm is implemented on an FPGA due to its high processing power and number of input-outputs.

4.2. Theoretical approach

In this chapter, two novel signal based open switch FD methods are presented. These methods are based on model identification and phase angle estimation, respectively. Theory of each method is explained separately in the following sections.

4.2.1. Adaptive model identification method

This section presents a new simple adaptive model identification approach to detect an open switch or phase fault in two-level multiphase VSIs. This method is based on the current signal model, as described before. According to this method, in the first step, the current signal is identified by an adaptive approach. In order to identify the current, the first step is to model the converter current.

The current signals include fundamental frequency in the case of a three-phase motor drive, or combination of first and third harmonics in the case of a five-phase motor drive. It is important to note that in real applications, output current of the power converter can be distorted by high frequency switching harmonics, or even low order harmonics such as 7^{th} or 9^{th}. However, only the dominant components are considered in this dissertation. As a result, the purpose of the signal identification is to estimate dominant components in the current signal.

Usually first and third harmonics are utilized in five-phase BLDC motor drives to produce torque [69]. Therefore, the dominant components in the current signal are the first and third harmonics. Assuming that the input current signal *X* only consists of the first and third harmonics, a new variable X_{est} can be estimated as follows:

$$\boldsymbol{X_{est}(t) = I_1 \sin(\ \ t + \ _1) + I_3 \sin(3\ \ t + \ _3).} \qquad (4.1)$$

where ω is the angular frequency, φ is the phase, and *I* is the current amplitude. The signal X_{est} can be rewritten as follows:

$$\boldsymbol{X_{est}(t) = I_1 \cos(\ _1)\sin(\ \ t) + I_1 \sin(\ _1)\cos(\ \ t) + I_3 \cos(\ _3)\sin(3\ \ t) + I_3 \sin(\ _3)\cos(3\ \ t).} \qquad (4.2)$$

As a result, by considering (4.2), the converter current can be modeled as follows:

$$\boldsymbol{y = WU}. \qquad (4.3)$$

where *U* is the input matrix:

$$\boldsymbol{U = [\sin(\ \ t)\ \ \cos(\ \ t)\ \ \sin(3\ \ t)\ \ \sin(3\ \ t)]^T}. \qquad (4.4)$$

Here, *W* is a weight matrix which should be estimated in order to identify the current model:

$$\boldsymbol{W = [I_{d1}\ \ I_{q1}\ \ I_{d3}\ \ I_{q3}]}. \qquad (4.5)$$

Parameters given in (4.5) are defined from (4.2) as follows:

$$\begin{aligned} I_{d1} &= I_1 \cos(\ _1) \\ I_{q1} &= I_1 \sin(\ _1) \\ I_{d3} &= I_3 \cos(\ _3) \\ I_{q3} &= I_3 \sin(\ _3) \end{aligned} \qquad (4.6)$$

Adaptive model identification is an effective way to estimate the components of the weight matrix *W*. Consequently, it has been chosen in this thesis to estimate a new signal X_{est}. Details of the identification method are explained in the following section.

Adaptive Model Identification Method:

Adaptive filtering technique is an accurate method for system identification [75-76]. All adaptive techniques consist of the following parameters: input signal *x(n)*, desired signal *d(n)*, output signal *y(n)*, adaptive transfer function *ω(n)* and error signal *e(n)* which is equal to difference between the desired signal and the output signal. The adaptive system identification provides a discrete estimation of the transfer function for an unknown analog or digital input signal. Two algorithms can be used for the adaptation process: RLS and LMS adaptive filter [76]. RLS method has a fast convergence rate, although it has a high computational load. This algorithm is applied in this thesis. The general structure of this method for application in a five-phase motor drive is shown in Fig. 4.2, where Ts is the sampling frequency, $d_j(n)$ is the phase current of the power converter and, j= *A*, *B*, *C*, *D*, *E*.

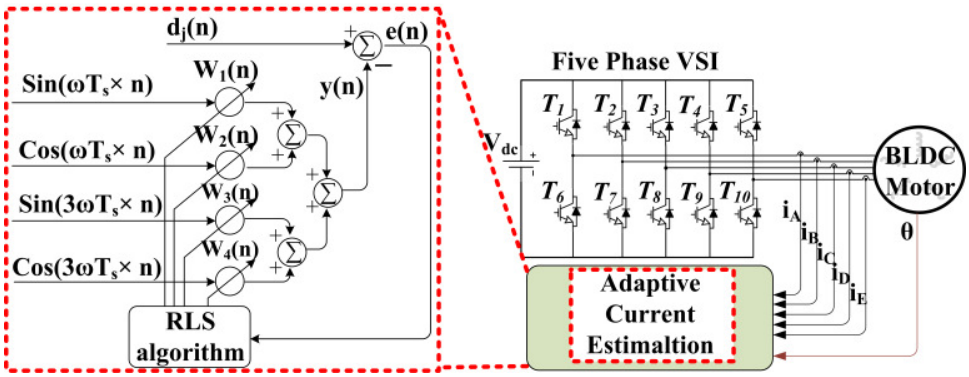

Fig. 4.2. Configuration of the adaptive system identification for application in a motor drive.

The RLS algorithm finds filter coefficients so that weighted linear square roots cost function is minimized. RLS filter parameters are: *p,* which is the filter order, *λ,* which is the forgetting factor and *δ*, which is the initial value of *P(0)* as autocorrelation matrix. Therefore, the algorithm steps are as follows:

Step 1- initialization:

ω(n)=0

x(k)=0 where k=-p,…,-1

P(0)=δ^{-1}I, where *I* is an identity matrix with *p* order.

Step 2-gain calculation:

$$\boldsymbol{g}(\boldsymbol{n}) = \frac{\boldsymbol{P}(\boldsymbol{n}-1)\boldsymbol{x}(\boldsymbol{n})}{+\boldsymbol{x}^{T}(\boldsymbol{n})\boldsymbol{P}(\boldsymbol{n}-1)\boldsymbol{x}(\boldsymbol{n})}. \qquad (4.7)$$

Step 3-calculation of the error between output signal and desired input signal:

$$\boldsymbol{e}(\boldsymbol{n}) = \boldsymbol{d}(\boldsymbol{n}) - \boldsymbol{W}(\boldsymbol{n}-1)\boldsymbol{U}(\boldsymbol{n}). \qquad (4.8)$$

Step 4-update of the coefficient matrix as:

$$\boldsymbol{W}(\boldsymbol{n}) = \boldsymbol{W}(\boldsymbol{n}-1) + \boldsymbol{e}(\boldsymbol{n})\boldsymbol{g}(\boldsymbol{n}). \qquad (4.9)$$

Step 5-computation of the autocorrelation coefficient:

$$\boldsymbol{P}(\boldsymbol{n}) = {}^{-1}\boldsymbol{P}(\boldsymbol{n}-1)(\boldsymbol{I}-\boldsymbol{g}(\boldsymbol{n})\boldsymbol{x}^{T}(\boldsymbol{n})). \qquad (4.10)$$

After initialization, the weight matrix *W*, shown in (4.5), is always updated by repeating steps 2 to 5. In order to initialize the algorithm, the values of δ and λ should be known in advance. Both of these parameters are independent from load operation conditions. The δ value can be easily chosen as a small positive value. However, the λ value has a significant effect on the performance of the detection method. This parameter will be discussed with more details in the following.

It is worth to note that the speed of the estimation using RLS algorithm depends on λ. Its value can be changed between 0 and 1. The choice of λ<1 gives more weight to the most recent samples. The estimated signal will be close to the real signal if λ value is chosen a high value close to 1 at steady state. In addition, noise rejection capability of the algorithm is high. However, tracking performance in transients is not fast. To minimize the difference between the estimated and real input signal, a low value can be chosen for λ in the transients. In the case of latter choice, there will be an error in steady state [19].

Under open switch and open phase fault in a power converter, the phase current will be zero for half of a period or one period, respectively. If a low value is chosen for λ, the estimated current tracks the faulty current excessively fast. As aforementioned, this is due to the more weight given to the recent values for λ<1. Since difference between the estimated and real current under faulty mode will be a small value for λ<1, it will be more difficult to distinguish the faulty current from the healthy current. On the other side, if λ is chosen close to 1, it takes more time for the estimated current to track the real current. It means that although the real current is zero, the estimated current is still following the current pattern before the fault. As a result, it will be more effective to distinguish the healthy mode from the faulty mode.

Regarding implementation of this algorithm for the FD purpose in this thesis, the filter order will be considered as 1, the forgetting factor λ is equal to 0.99, and δ value is set to 0.5. These values are

constant in the rest of this dissertation. At each execution of the algorithm, steps 2 to 5 are executed to update separately each component of matrix *W* given in (4.2). The estimated output *y* will be equal to the sum of the estimated components as shown in Fig. 4.2. FD scheme using the model identification is explained in the next section.

Fault Detection Algorithm:

As discussed above, the model identification block calculates the first and third harmonic components of the input current signal. As it is shown in (4.8), an error value e(n) is obtained, which is equal to the difference between the estimated and the input signal. Under the healthy condition, the error value is small while in case of a fault, it has a significant value. This fact is used to detect the faulty switch.

After the model identification, a residue value, which is equal to the difference between the original signal *X* and new estimated signal in (4.1), is defined as follows:

$$\boldsymbol{r} = \boldsymbol{X}_{\boldsymbol{est}} - \boldsymbol{X}. \qquad (4.11)$$

It is important to note that the value of *r* is equal to the calculated error in (4.8). Theoretically, this value is zero under ideal healthy condition. As a result, if a threshold equal to zero is considered to detect the fault, an *r* value different than zero can be considered as an indication of the fault in the power converter. However, in practical application, the *r* value could be never exactly equal to zero. Its value depends on the order of the adaptation process, harmonic distortions in the input signal, sampling frequency, etc. Besides, measurement errors, inaccurate modeling and noise can affect the *r* value. It should be mentioned that the *r* value also changes with the amplitude of the input current signal. It means that at high current amplitudes, the *r* value is higher. To detect the fault, a threshold value should be chosen which is not sensitive to aforementioned effects. So, a dynamic threshold value is proposed in this thesis. To obtain this value, first the amplitude of the estimated signal X_{est} is calculated from (4.5) as:

$$\boldsymbol{N}_f = \sqrt{\boldsymbol{I}_{\boldsymbol{d}1}^2 + \boldsymbol{I}_{\boldsymbol{q}1}^2 + \boldsymbol{I}_{\boldsymbol{d}3}^2 + \boldsymbol{I}_{\boldsymbol{q}3}^2}. \qquad (4.12)$$

Under ideal faulty conditions, the *r* value is equal to X_{est}. It means that absolute value of *r* changes between zero and N_f. In order to compensate inaccuracy of the estimation algorithm, it is proposed to define the threshold value as a small portion of N_f. If the absolute value of the residue is more than this threshold, one fault is detected. The definition of the dynamic threshold is an advantage since the detection process becomes totally independent from the load operation conditions.

Consequently, a diagnostic variable *D* is defined as the difference between residue and threshold values:

$$\boldsymbol{D} = 0.1 \times \boldsymbol{N_f} - |\boldsymbol{r}|. \qquad (4.13)$$

As it is shown in (4.13), here the threshold value is chosen as 10 % of N_f. The threshold value was chosen empirically based on extensive simulation and experimental observations. The ideal value of D signal in (4.13) is equal to or less than $0.1 \times N_f$ and more than zero under healthy condition, since the residue value is close to zero. On the other side, under faulty conditions, its value is between $0.1 \times N_f$ and $-0.9 \times N_f$. Regarding the D value in (4.13), in order to avoid false alarms, the detection signal D is compared with a small threshold value close to zero as follows:

$$\boldsymbol{Fault\ \ Detection} = \begin{cases} \boldsymbol{Fault} & \boldsymbol{D} < - \\ \boldsymbol{Normal} & \boldsymbol{otherwise} \end{cases}. \qquad (4.14)$$

where ε is a small positive value which can be chosen close to zero. It should note that since absolute zero is on border between the healthy and faulty mode, in order to distinguish the healthy mode from faulty mode, a small ε value was used instead of zero.

There are two possibilities for the false alarms using the proposed detection method. The first case happens during a load transition, and the other one occurs while a high DC average value is included in the converter current. The latter case is due to a fault with the same polarity in more than one phase of the power converter such as three upper or three lower switch faults. Both of these false alarms can be avoided by a simple method. In both cases, the current value is different from zero. Consequently, if the fault alarm is activated while the current amplitude is different from zero, the residue value is changed to a small ε value. This means that there is a false alarm.

Regarding the presented FD method, in the first step, the phase current is estimated based on a model. This model only considers the dominant frequency components. Here, it has been assumed that only the first and third harmonics are included in the output current of a five-phase machine. However, in a practical implementation, depending on the back EMF waveform, other harmonics can also appear in the current signal under normal and faulty mode operation. Since amplitude of the remaining harmonics is low in comparison to the dominant components (i.e. the first and third harmonics in case of a five-phase machine) [70], these components have not been considered in the current model. This simplification significantly reduces the computational cost of the algorithm.

As explained before, in order to detect a fault, it is not necessary to estimate the phase currents accurately. In this case, the residue value will not be exactly equal to zero due to inaccurate modeling. To avoid false alarms, the FD scheme should be robust to non-zero residue due to inaccurate modeling. Here, an anti-false alarm method has been included in the FD algorithm which successfully distinguishes the error due to the inaccurate modeling from the faulty mode. This method is implemented in two steps.

In the first step, as shown in (4.13) in order to detect a fault, the residue value is compared to a threshold value. As discussed before, the theoretical value of the threshold is zero; however here the *r* value is compared to 10 % of N_f. Therefore, choosing a threshold value higher than its theoretical value is the first solution to compensate the effects of the inaccurate model.

Secondly, the phase current under faulty mode has a unique feature. It means that the phase current is equal to zero for some time. As explained earlier, if the *r* value is high due to inaccurate model, while the current amplitude is different than zero, the *r* value will be changed to ε. As a result, false alarms can be effectively avoided. This capability of the algorithm will be validated later with the obtained experiments results.

Fault Localization Method:

In order to have a high performance fault-tolerant system, the faulty components are localized after FD. The single switch and open phase fault are the most possible fault types in a leg of the power converter. Moreover, in the case of single switch fault, the fault may be located in the upper switch or in the lower switch.

Considering the single switch fault, a sub block is enabled to determine the polarity of the residual value. If the polarity is positive then the upper switch is the faulty component. Otherwise, the lower switch is the faulty component. This block can be written as follows:

$$\boldsymbol{Sign}(\boldsymbol{r}) = \begin{cases} > 0 & \boldsymbol{upper\ switch\ fault} \\ < 0 & \boldsymbol{lower\ switch\ fault} \end{cases} \qquad (4.15)$$

In order to localize the open phase fault, absolute average value of the input signal *X* is calculated at one period *T*. The phase current is equal to zero at steady state under the open phase fault. Therefore, if the average value is equal to zero during one period, the fault type is the open phase.

The block diagram of the proposed FD and localization method is shown in Fig. 4.3. As it can be seen, the fault is detected in the first step. In the next step, the faulty switch or phase is localized.

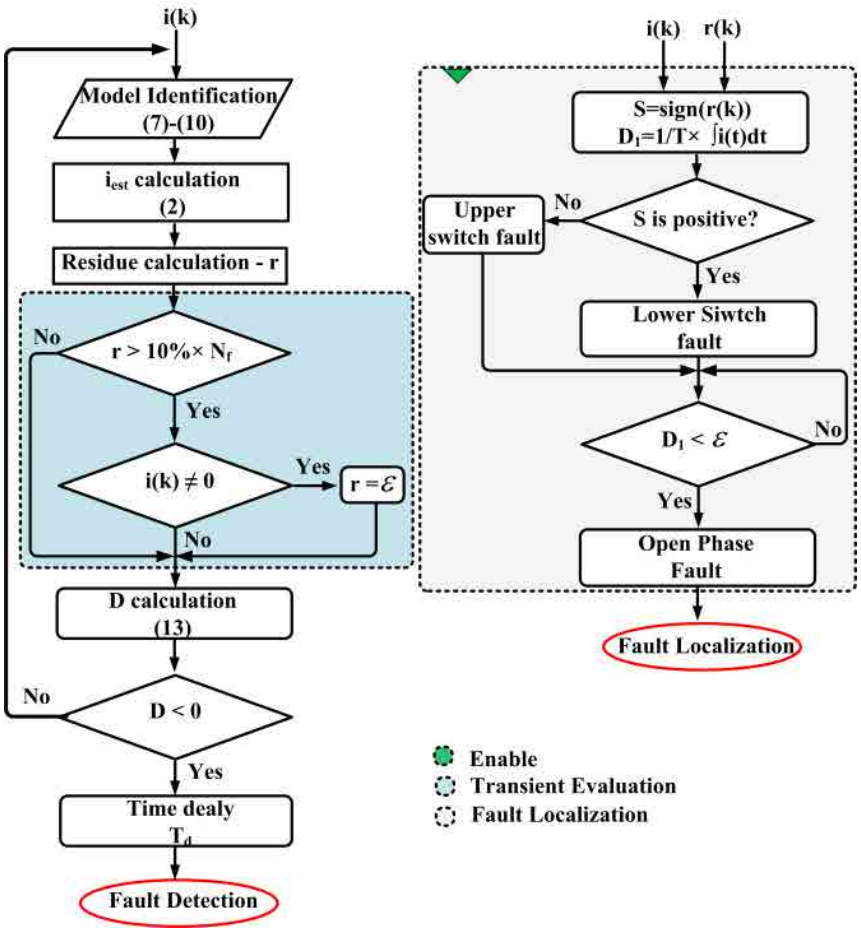

Fig. 4.3. FD and localization block.

Since the FD and localization is done for each phase of the converter separately, the presented method is general and flexible. It should be noted that according to the proposed method, fault localization in the case of a single switch fault is done immediately after the FD. Nevertheless, one fundamental period is required to locate the open phase fault. Moreover, after FD, the fault signals are shown by a simple code. The upper switch fault is codified by 1, the lower switch fault by -1 and the open phase fault by 2.

According to the FD algorithm, a time delay (T_d) has been considered to detect the fault. This delay increases the robustness of the FD method to noise and transients. In this thesis, this value is considered as 12.5% of one period. A higher time delay increases the detection time while making the algorithm even more robust to the transients. On the other hand, a lower time delay makes the detection method vulnerable to false alarms.

In order to validate the effectiveness of the proposed method, two different signals were applied to the detection block. In the first step, a nonsinusoidal signal was simulated with two transients. Furthermore, to show the effect of the λ value on the performance of the FD method, the same signal is simulated for two different λ values. A single switch fault was initiated at time 0.22 s. Original signal, estimated signal, N_f value, residue value and threshold value are shown in Fig. 4.4. As it can be seen, the residue value is less than the threshold value, shown by *TH*, in transients. Moreover, after the fault, it exceeds from the threshold value immediately. Also, it can be seen from Figs. 4.4(a) and (b) that the faulty mode can be easily distinguished from the healthy mode for higher values of λ.

An additional simulation was considered to detect the open phase fault; simulation waveforms are shown in Fig. 4.5. As it can be seen, in both Figs. 4.5(a) and 4.5(b), for higher values of λ, it is easier to detect the fault. However, the tracking speed in transients is not fast.

As it is shown, the presented FD method is not sensitive to the load transients. As a result, tracking speed in transients is not a priority. Considering this fact and easier detection of the fault, a high λ value is always preferred in the proposed method of this thesis.

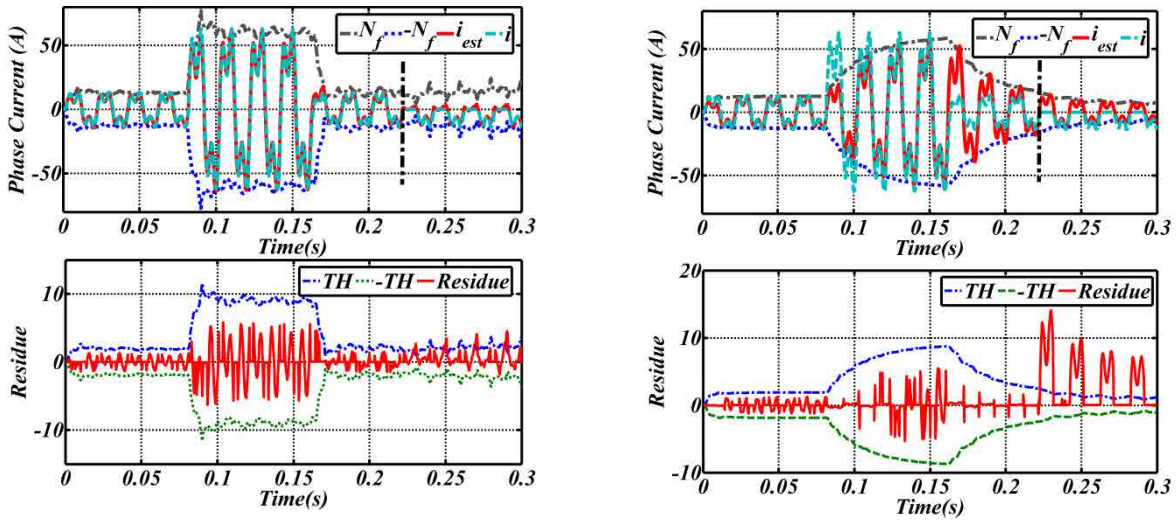

(a) (b)

Fig. 4.4. Adaptive signal identification in case of single switch fault (a) λ is 0.7 (b) λ is 0.99

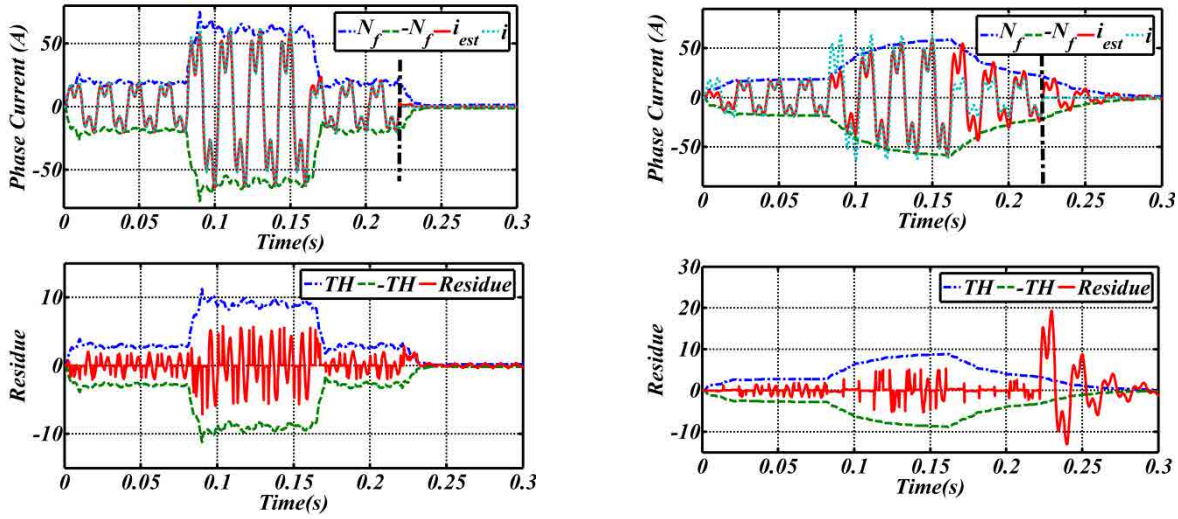

(a) (b)

Fig. 4.5. Adaptive signal identification in case of open phase fault (a) λ is 0.7 (b) λ is 0.99

Fault-Tolerant Control and Analysis of a Five-Phase BLDC Motor:

Application area in this thesis is a five-phase fault-tolerant BLDC motor drive with an isolated neutral point. Different parts of the considered system are shown in Fig. 4.6. A two-level five-phase inverter is used to supply the motor. The drive configuration and control method are shown in Fig. 4.6(a); Park transformation and rotor mechanical speed are shown by *T* and ω_r, respectively. Since the motor neutral is isolated, it can be operated up to two faulty phases [78].

As it is shown in Fig. 4.6(a), a fast fuse has been connected in series with each phase of the power converter. It is assumed that in the case of the short circuit fault in one leg of the power converter, the faulty leg is isolated by the fast fuses. After isolation, the corresponding phase will be open circuit. As it can be seen, *TRIAC* switches denoted by *TR* are used to isolate the faulty leg in the case of short circuit faults. It is important to note that the focus of this study is only on the open switch and open phase FD. To isolate the faulty leg in the case of open circuit or open switch fault, the gate signal for healthy IGBT in the faulty leg should be removed.

To achieve the fault-tolerant concept, a fault-tolerant control algorithm is proposed as shown in Fig. 6(b). According to this scheme, first of all, the fault must be detected; the detection block produces a fault code (*FC*). After that, according to *FC*, the gate signal for the remaining healthy switch in the faulty leg is removed. To control the new configuration of the motor, both modulation method and control algorithm are changed at the next step. The FD algorithm is continuously running. If the number of faulty phases is higher than 2, all switches will be turned off to shut down the converter. Details of the control algorithm and modulation method are presented in the following parts.

Fault Tolerant Field Oriented Control:

As it can be seen in Fig. 4.6, a FOC method was used to control the drive. Based on this method, it is necessary to calculate separately the reference current values under each operational mode of the power converter. The motor can continue the operation with one faulty phase, two adjacent faulty phases and two nonadjacent faulty phases. In the following, general basics of reference current calculation under different faulty conditions are briefly reviewed.

Trapezoidal back-EMF waveform of a five-phase BLDC machine can be approximated by its first and third harmonic components:

$$\boldsymbol{E} = \boldsymbol{e}_1 \cos\left(\ -\frac{2\ \boldsymbol{n}}{5}\right) + \boldsymbol{e}_3 \cos\left(3\left(\ -\frac{2\ \boldsymbol{n}}{5}\right)\right),\ \boldsymbol{n} = 0,1,2,3,4. \qquad (4.16)$$

where n=0, 1, 2, 3, 4 and respectively represents phase *A*, *B*, *C*, *D*, *E*.

Considering fundamental and third harmonic component of the stator currents, instantaneous active power of each phase can be computed as:

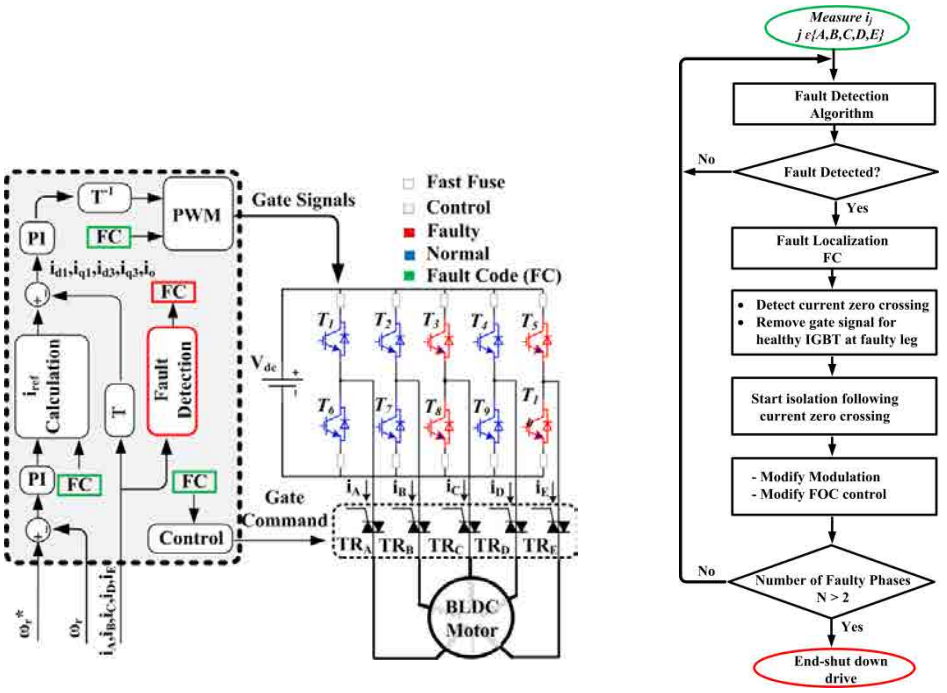

(a) (b)

Fig. 4.6. Fault-tolerant system (a) drive configuration and control method. (b) fault-tolerant control strategy of the power converter

$$\begin{aligned} \boldsymbol{i}(\boldsymbol{t}) &= \boldsymbol{I}_1 \cos(\ \boldsymbol{t} - \ _{\boldsymbol{i}1}) + \boldsymbol{I}_3 \cos(3\ \boldsymbol{t} - \ _{\boldsymbol{i}3}) \\ \boldsymbol{e}(\boldsymbol{t}) &= \boldsymbol{E}_1 \cos(\ \boldsymbol{t} - \ _{\boldsymbol{e}1}) + \boldsymbol{E}_3 \cos(3\ \boldsymbol{t} - \ _{\boldsymbol{e}3}) \\ \boldsymbol{p}(\boldsymbol{t}) &= \boldsymbol{e}(\boldsymbol{t}).\boldsymbol{i}(\boldsymbol{t}) \end{aligned} \qquad (4.17)$$

The non-oscillating component of p(t) given in (4.17) can be computed as:

$$\boldsymbol{P_o} = 0.5\boldsymbol{I}_1\boldsymbol{E}_1 \cos(\ _{\boldsymbol{i}1} - \ _{\boldsymbol{e}1}) + 0.5\boldsymbol{I}_3\boldsymbol{E}_3 \cos(\ _{\boldsymbol{i}3} - \ _{\boldsymbol{e}3}) \quad (4.18)$$

The oscillating components of p(t) are responsible for torque ripples. The control objective is determined so that P_o is maximized while the torque ripples due to the oscillating elements of p(t) are minimized.

To avoid high operational temperatures along the stator, maximum RMS value of the stator phase currents is limited to its rated value under healthy conditions (i.e. 1 p.u.). It is worth noting that this constraint will be the main limitation of produced electrical torque under faulty conditions. Moreover, in the case of having an isolated neutral point, total sum of the stator currents in the remaining healthy phases must be zero:

$$\sum_{\boldsymbol{j}=\boldsymbol{A},\boldsymbol{B},\boldsymbol{C},\boldsymbol{D},\boldsymbol{E}} \boldsymbol{i}_{\boldsymbol{j}} = 0. \qquad (4.19)$$

An optimization algorithm was used to calculate the reference currents [78]. The optimized phase current values under different faulty conditions with an isolated neutral point are presented in table III.I. These values are used in the FOC algorithm to drive the motor under healthy and faulty modes.

Fault Tolerant Modulation:

To produce a voltage waveform with a five-phase converter, different modulation methods have been addressed in literature. These methods can be considered in two main groups including SVM and CPWM [79], [80]. Although SVM methods have higher performance due to better utilization of DC link voltage and higher waveform quality, these methods are too complex. On the other hand, carrier based methods equivalent to SVM have also been presented which are easier to implement for a five-phase converter. So in this thesis, latter strategy is considered. A non-sinusoidal CPWM law can be written as:

$$v_j^* = v_j + v_{zs} \; ; \quad j = A, B, C, D, E. \qquad (4.20)$$

where v_{zs} is the zero sequence component, and can be used as a degree of freedom to improve the modulation performance.

To achieve a modulation method equivalent to SVM, the zero sequence component is calculated as [80]:

$$v_{zs} = -\frac{\max(v_A, v_B, v_C, v_D, v_E) + \min(v_A, v_B, v_C, v_D, v_E)}{2}. \qquad (4.21)$$

SVM is equivalent to injection of all odd multiples of the zero sequence components. The block diagram of the modulation strategy for a five-phase converter is shown in Fig. 4.7. Under one and two faulty phases, the modulation law should be recalculated for four-phase and three-phase converter using (4.20) and (4.21), respectively. It is important to note that under faulty mode, the zero sequence components impose distortion on the output waveforms. These distortions can be minimized by detection and isolation of the fault within minimum possible time. It is suitable to apply a soft transition from previous to new modulation scheme. This concept will be further explained in the experimental section.

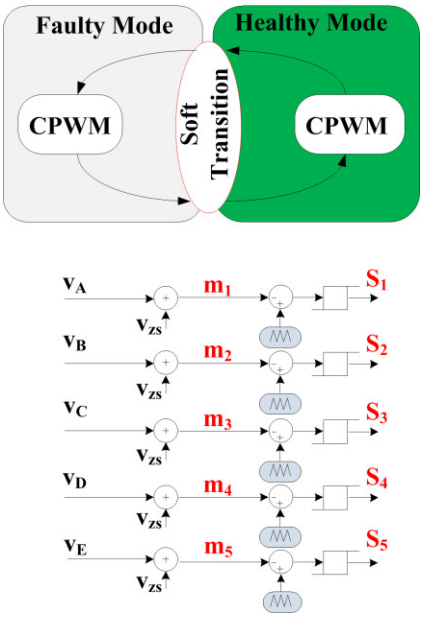

Fig. 4.7. Fault-tolerant modulation method

4.2.2. Phase angle estimation method

Due to their fault tolerant capabilities, five-phase PM motors can maintain a high level of safety and reliability [45]. To implement the fault-tolerant algorithm, such systems should detect and isolate the fault and continue operation with minimal derating. To achieve these goals, a multiphase fault-tolerant converter with FD and isolation ability is considered here, as shown in Fig. 4.8. It should be noted that the converter output current in this specific application can be non-sinusoidal, and unbalanced under different operational modes.

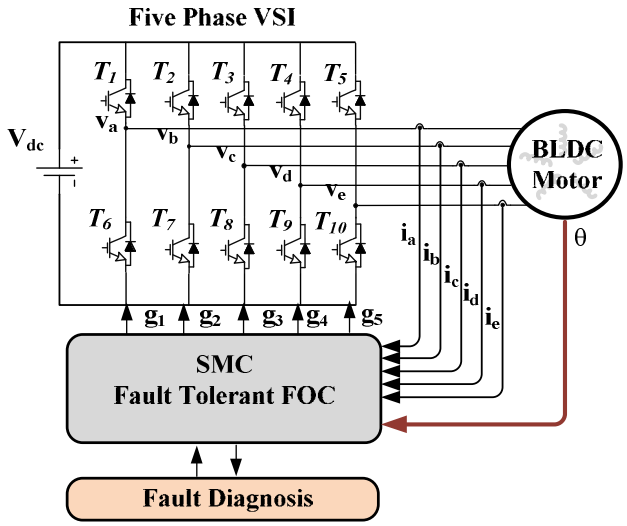

Fig. 4.8. Configuration of the fault-tolerant power converter

Considering a multiphase converter, the following faulty modes can occur: single switch open circuit, single phase open circuit, multiple open switch and open phase faults. It should be noted that the number of faulty modes in a multiphase converter can be much more than in a three-phase converter. Considering practical cases, a five-phase BLDC motor drive can tolerate until two faulty phases.

To evaluate a FD method, some performance criteria should be considered. Firstly, it should be fast, which it means that the FD method should detect the fault with minimum time after fault. After FD, to realize fault-tolerant operation, it is necessary to localize and isolate faulty switch. So, fault localization is another performance criterion. Thirdly, FD method should be robust to transients; it means that FD method should avoid false alarm during load transients. It should be noted that transient type in a motor drive may occur due to speed or torque reference variations. Fourthly, FD method should be general; this means that the FD strategy can be used in any converter configuration such as three-phase, four-phase, five-phase or any multiphase converter. Finally, simple implementation is an

important advantage for the FD strategy. Regarding all of the aforementioned criteria, a novel FD method is proposed as follows.

To detect a fault, it is important to define a FD index. In practical application, the converter output current is usually a noisy signal. Prior to do a signal processing, it is necessary to apply a low pass filter to eliminate non-desirable components in current spectrum. It is recommended to set the cut off frequency of the filter at least 10 times of the fundamental frequency. If the cut off frequency is chosen too high, it cannot eliminate distorting components effectively. On the other side, if a low value is selected, filter imposes a high delay on the filtered signal. This delay can slow down detection speed, which is a critical criterion in a FD method.

To define the FD index, phase angle of the converter output current is estimated in this thesis. Being independent from the load operational conditions makes phase angle a unique variable to define the FD index. Its value varies between $-\pi$ and π under normal operational condition.

After filtering the signal, the current signal and its delayed current sample during a quarter of one fundamental cycle T are divided. The FD index is calculated from inverse tangent of the calculated signal as:

$$\boldsymbol{D} = \tan^{-1}\left(\frac{\boldsymbol{i(t)}}{\boldsymbol{i(t-T/4)}}\right). \qquad (4.22)$$

where i is the current signal of the power converter, and D is the FD index. Under healthy condition, the value of D varies between -π and π. Under faulty mode, the phase current is zero during half of a period in case of a single switch fault. Under open phase fault, the phase current is zero. Regarding single switch fault and from (4.21), D value is as:

$$\boldsymbol{D} = \begin{cases} -\ ,-\frac{}{2},0,\frac{}{2}, & \text{single switch fault} \\ 0 & \text{open phase fault} \end{cases} \qquad (4.23)$$

Once D value is equal to faulty mode, FD is done after a delay. To realize this purpose, a new function is defined as:

$$\boldsymbol{y} = \begin{cases} 1 & \left|\boldsymbol{D}\right| = 0,\frac{}{2}, \\ 0 & \boldsymbol{otherwise} \end{cases} \qquad (4.24)$$

After that, the average value of y is calculated during one cycle as:

$$\boldsymbol{x} = \frac{1}{\boldsymbol{T}}\int_0^{\boldsymbol{T}} \boldsymbol{y}\boldsymbol{dt}. \qquad (4.25)$$

The x value is zero under healthy condition. Its value increases to one in case of the fault. This value is compared with a threshold value to detect the fault. If x value is higher than the threshold value, then fault is detected. It should be noted that the theoretical value of the threshold value is zero. However, in practice and due to noise and calculation accuracy, a higher value is chosen.

In order to maintain fault-tolerant concept in a multiphase power converter, it is necessary to localize the faulty switch. After that, the faulty component can be replaced with an extra leg or isolated totally from the converter. Here a simple approach is applied to localize the component which is based on the current polarity. According to this method, input phase current is passed through a weight function. This function estimates input current *i* to values between -1 and 1 as follow:

$$\boldsymbol{S}(\boldsymbol{i}(\boldsymbol{t}))=\begin{cases}1 & \boldsymbol{i}(\boldsymbol{t})\geq 0.1\\ 0 & -0.1<\boldsymbol{i}(\boldsymbol{t})<0.1\\ -1 & \boldsymbol{i}(\boldsymbol{t})\leq -0.1\end{cases} \qquad (4.26)$$

Where current values less than 0.1 A (i.e. a typical threshold value) are considered equal to zero. However, in practice, a different value can be chosen for this threshold. The fault localization block samples and calculates the average value of the converter output current, simplified by equation (4.26) during one fundamental cycle as follows:

$$\bar{\boldsymbol{I}}=\frac{1}{\boldsymbol{T}}\int_{\boldsymbol{o}}^{\boldsymbol{T}}\boldsymbol{S}(\boldsymbol{t})\boldsymbol{dt}. \qquad (4.27)$$

where $\bar{I}$ is the average value of the phase current in one fundamental period. The $\bar{I}$ value is compared with a positive and a negative threshold value. If the average value is higher than the positive threshold, then lower switch is the faulty component at corresponding phase. Similarly, if the average value is lower than the negative threshold, then upper switch is the faulty component. The absolute threshold value chosen in this thesis is 0.5.

Under open phase fault, *D* value approaches to zero; this advantage is utilized to localize the open phase faults in this dissertation. The average value of *D* is calculated during one fundamental cycle. If this value is equal to zero, the fault type will be an open phase.

For clarification, each faulty mode in one leg of the power converter is shown by a numerical code. Codes -1, 1, and 2 correspond to the upper switch fault, lower switch fault and open phase fault, respectively.

The FD block, fault localization block and diagnostic variable waveforms at different faulty modes are shown in Fig. 4.9. Considering the proposed FD method, its main advantage is the simplicity of implementation. Since the FD index is calculated from the phase angle, it is a robust method to high load transients. On the other side, this method is general, since no special transformation related to the converter topology is used. This method can be used in a two-level converter with any number of phases. Moreover, this method only needs the measurement of the converter output current, therefore it can be used in a system with open loop or closed loop control. Finally, it is possible to detect an open phase fault without using an auxiliary variable, in contrast to the presented methods in literature.

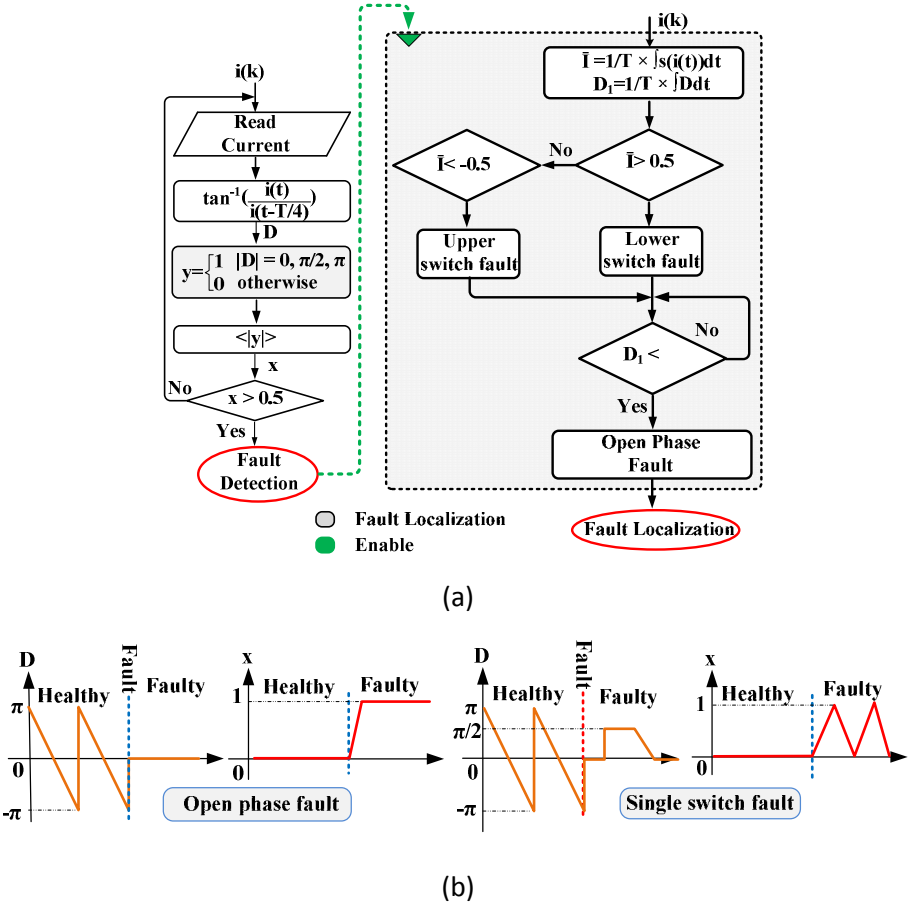

Fig. 4.9. Proposed FD method (a) FD block diagram. (b) FD index.

Fault-Tolerant SMC of a Five-Phase BLDC motor Using Proposed FD Method:

In this part, the presented FD method is used to maintain fault-tolerant concept in a five-phase BLDC motor with a closed loop control.

A five-phase PM motor drive can be operational with two faulty phases [45]. To achieve desired torque and speed control, it is necessary to calculate the reference currents of the motor under healthy and faulty modes. Recently, a considerable research has been conducted in this subject. Salehi et al. presented an optimization algorithm to calculate the reference currents under healthy and faulty mode [18]. According to this method [19], a fault-tolerant control with torque ripple free is achieved. Here, final results of the optimized reference currents are summarized in table III.I.

Fault-Tolerant SMC:

In order to set the reference torque and speed in a five-phase PM motor drive, a closed loop control can be used. The FOC is used to control the drive. To implement this FOC, an inner controller is used to track the reference currents. According to the analysis presented in [82], a torque ripple free using the optimized reference currents in table I can be achieved. The SMC is used in this thesis to set the current references. Block diagram of the fault-tolerant control method is shown in Fig. 4.10. As seen, SMC provides the reference voltage for space vector modulator; therefore the switching frequency is constant.

Theory of the SMC method is presented in the following. It should be noted that focus of this thesis is on the inner controller of the motor. Its effect on performance of the FD method is evaluated in the rest of this thesis.

Due to its robustness to parameter uncertainties, external disturbances, simple implementation, and fast convergence rate [83], [84], [85], here nonlinear SMC is used to implement the inner controller of the fault-tolerant FOC algorithm. SMC can be done in two steps. First, the sliding surface is chosen. After that, a control law is calculated so that the sliding surface is achieved. The control law is designed to enforce system states on sliding surface and remain on the surface. In the following section, basic equations of a five-phase BLDC motor are reviewed

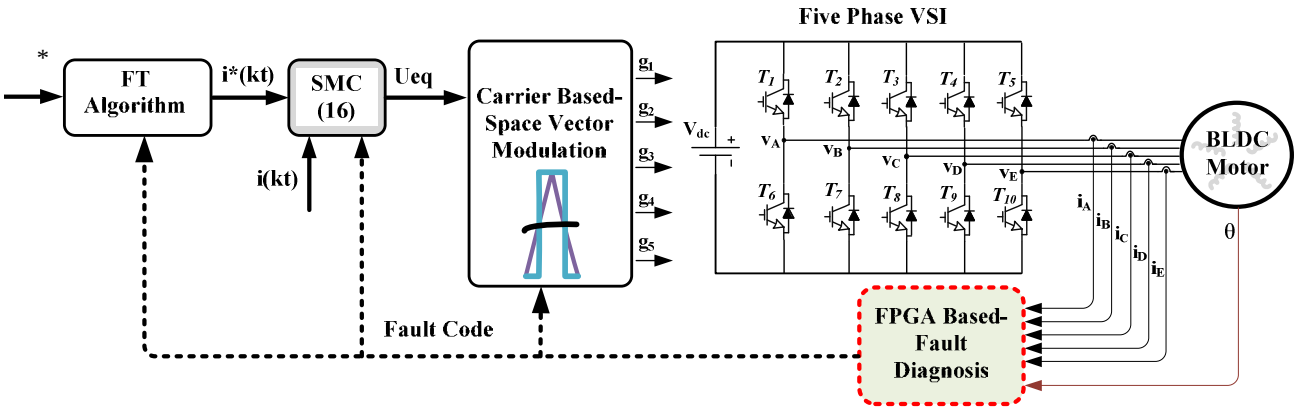

Fig. 4.10. FD and the fault-tolerant control.

The model of a BLDC motor with trapezoidal back EMF under healthy and faulty mode is as:

$$\begin{bmatrix} v_a - e_a - v_x \\ v_b - e_b - v_x \\ v_c - e_c - v_x \\ v_d - e_d - v_x \\ v_e - e_e - v_x \end{bmatrix} = \left(\begin{bmatrix} r_a & 0 & 0 & 0 & 0 \\ 0 & r_b & 0 & 0 & 0 \\ 0 & 0 & r_c & 0 & 0 \\ 0 & 0 & 0 & r_d & 0 \\ 0 & 0 & 0 & 0 & r_e \end{bmatrix} + \begin{bmatrix} l_a & m_1 & m_2 & m_2 & m_1 \\ m_1 & l_b & m_1 & m_2 & m_2 \\ m_2 & m_1 & l_c & m_1 & m_2 \\ m_2 & m_2 & m_1 & l_d & m_1 \\ m_1 & m_2 & m_2 & m_1 & l_e \end{bmatrix} \frac{d}{dt} \right) \begin{bmatrix} i_a \\ i_b \\ i_c \\ i_d \\ i_e \end{bmatrix} \quad (4.28)$$

where i is the phase current, v is the voltage of each phase, r is the phase equivalent resistance, l is the phase equivalent inductance, m_1 is mutual inductance between two adjacent phases, m_2 is mutual inductance between two nonadjacent phases, e is the back EMF in each phase of the motor, and v_x is the neutral voltage. The back EMF will be estimated as follows:

$$e = \lambda_{m1}\,\omega_e \cos\left(\theta - \frac{2n}{5}\right) + \lambda_{m3}\,\omega_e \cos\left(3\left(\theta - \frac{2n}{5}\right)\right),\ n = 0,1,2,3,4. \quad (4.29)$$

where λ_{m1} and λ_{m3} are the first and third harmonic amplitudes of the rotor flux linkage; ω_e is the electrical rotational velocity, Θ is the rotor electrical angle, and n=0, 1, 2, 3, 4 and respectively represents phase a, b, c, d, e.

To design the controller, the sliding surface is defined as the error between the reference and actual phase currents as follows:

$$\delta = [i_a^* - i_a \;\; i_b^* - i_b \;\; i_c^* - i_c \;\; i_d^* - i_d \;\; i_e^* - i_e]^T. \quad (4.30)$$

$$s = \delta + \lambda \int \delta. \quad (4.31)$$

where s is the sliding surface, δ is the error function and λ is a positive constant. Due to integrator term in (4.31), zero steady state error can be achieved.

To achieve the sliding surface, the exponential approach law is used as:

$$\frac{ds(t)}{dt} = -\eta \times Sat(s(t)) - Ks(t). \quad (4.32)$$

where K>0, 0<ε<1 and *Sat* is a saturation function defined as:

$$Sat(x)=\begin{cases}1 & x\geq 1\\ x & -1<x<1\\ -1 & x\leq -1\end{cases} \qquad (4.33)$$

Dynamic of the control law is affected by *K* and *ε* [86]. For higher *K* values, the control law will be less sensitive to uncertainties. On the other hand, by increasing *ε* value, the controller will be faster. However chattering level on the controller output will be higher. To design these parameters, a tradeoff should be done to ensure the desirable dynamics and low chattering level on the control signal.

The SMC produces the reference voltages for space vector modulator. The SMC law in (4.32) can be rewritten in discrete form as:

$$s(k+1)-s(k)=-T_e Sat(s(k))-KT_e s(k). \qquad (4.34)$$

where T_e is the sampling period. By substituting (4.30) into (4.34), control law in phase *a* is as:

$$-T_e Sat(s(k))-KT_e s(k)=(i_a^*(k+1)-i_a(k+1)) -(i_a^*(k)-i_a(k)). \qquad (4.35)$$

The discrete form of the machine model in (4.28) can be written in matrix form as:

$$v(k)=Ri(k)+L\frac{i(k+1)-i(k)}{T_e}+e(k). \qquad (4.36)$$

By substituting (4.35) into (4.36), equivalent control law is obtained as:

$$U_{eq}=LT_e^{-1}(T_e Sat(s(k))+KT_e s(k)+(i_a^*(k+1)-i_a^*(k))) +Ri(k)+e(k). \qquad (4.37)$$

where U_{eq} is the reference voltage; this voltage should be produced by the inverter.

By integrating both sides of (4.34), the time to reach the sliding surface is as:

$$t=\frac{1}{-}(s(0)+\frac{K}{2}s^2(0)). \qquad (4.38)$$

From (4.38), it can be concluded that by increasing *ε* and decreasing *K*, reaching time is reduced. At the same time, robustness increases. However, chattering level on control state increases.

When control state is driven on sliding surface, s(k) is a small positive or a small negative value. So, (4.34) can be rewritten as:

$$s(k+1)=\pm T_e. \qquad (4.39)$$

According to (4.39), sliding band (i.e. chattering level) is a fixed value equal to εT_e. The chattering level can be decreased by decreasing *ε* and T_e.

The necessary condition to reach the sliding surface is [85]:

$$\boldsymbol{s(t).\dot{s}(t)} < 0 \qquad (4.40)$$

It should be noted that under healthy condition, sliding surface approaches to a small value. This value depends on the controller design. Under faulty condition, its value is increased significantly. On the other side, controller performance under faulty condition may reduce significantly. This can affect the performance of the FD block. Once motor phase currents are equal to the reference currents, FD index in (4.22) can be calculated accurately. In case of SMC, it can still maintain a good tracking performance even under faulty mode. So, it was used in conjunction with the proposed FD block in this thesis.

4.3. Experimental results

The experimental results are provided separately for each of the developed FD and fault-tolerant control methods. Details and discussions corresponding to each method are as following.

4.3.1. Experimental results of the model identification method

The experimental results are presented on a laboratory setup based on a five-phase BLDC motor fed by a fault-tolerant converter. Results are presented in two parts. First, the FD is evaluated, and after that, the fault-tolerant algorithm is discussed.

Experimental Results of FD:

In order to validate the theory, the proposed FD method is applied to the five-phase motor drive former described. The detection performance is evaluated under four different faulty modes; these cases include the most common possible faults in the power converter. The phase currents, diagnostic variable *D* and fault code are shown with sub indexes *A*, *B*, *C*, *D*, and *E*. Moreover, the threshold value is denoted by *Th*.

As the first case, the effect of load transient on fault detection performance is evaluated. The motor current is changed from a low to high value and vice versa at times 0.231 s and 0.71 s, respectively. The current waveforms and diagnostic variable are shown in Fig. 4.11(a). The phase currents are measured by Hall Effect sensors and converted to a voltage signal. Furthermore, due to limited number of oscilloscope channels, only the current waveforms of four phases of the converter were shown. The current of phase *E* is not included in the experimental results. According to the results shown in Fig. 4.10(a), the detection block is robust against the load transients.

As the second case study, an upper switch fault in phase *A* was initiated at time 0.242 s. The results are shown in Fig. 4.11(b). The fault was detected at 0.267 s with a fault code equal to 1, which means an upper switch fault. The detection time is less than one fourth of a fundamental cycle (i.e. 25 ms).

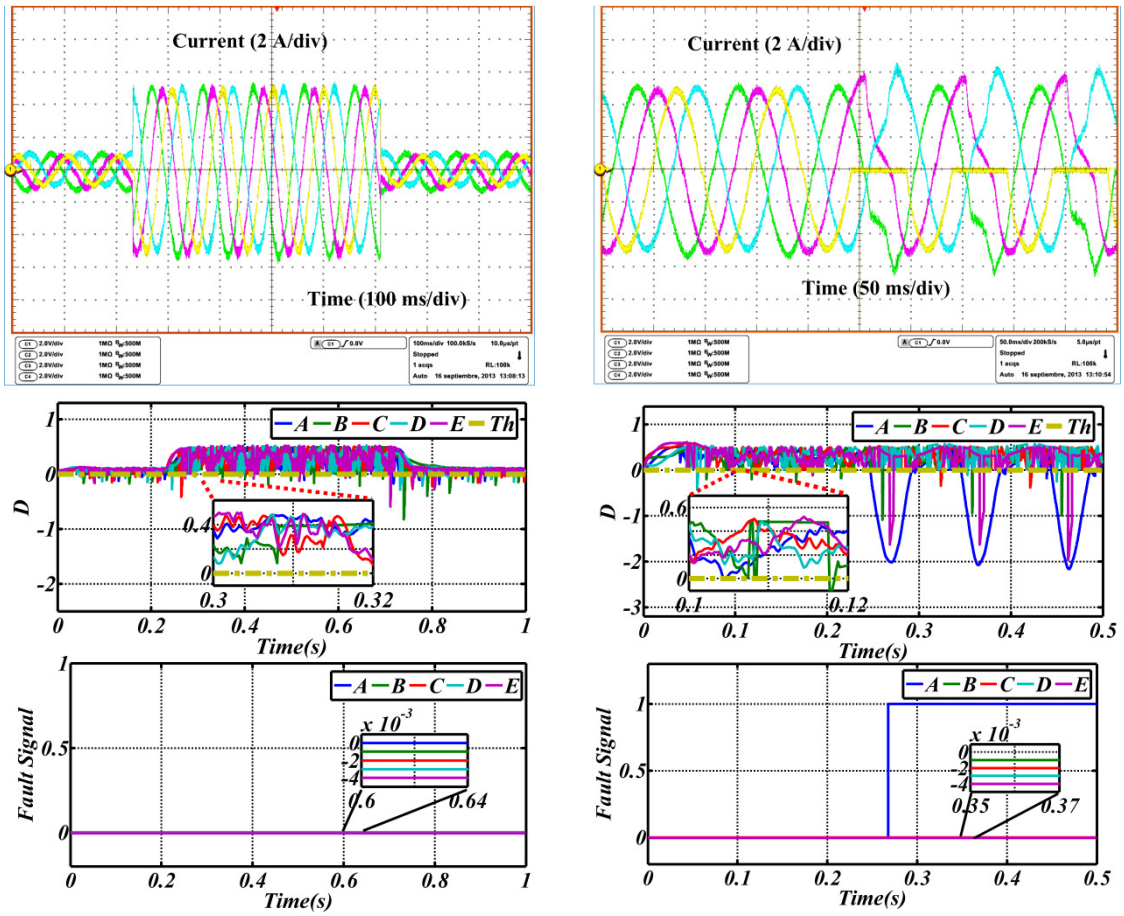

Fig. 4.11. Experimental waveforms (a) transient performance evaluation (b) single switch fault detection.

In the next case study, an open phase fault is considered. An upper switch fault in phase *A* and an open phase fault at phase *B* were implemented at time 0.247 s. The experimental waveforms are shown in Fig. 4.12(a). The fault in phase *B* was detected at 0.273 s. As a result, the detection time is a quarter of one period. However, fault localization is completed at 0.347 s with a resultant fault code equal to 2 in phase *B*. As shown, around one fundamental cycle (i.e. 100 ms) is necessary to localize the open phase fault.

Finally, a combination of three upper switch faults was analyzed. Under this fault, a high DC value is available in the remaining healthy phases. Moreover, closed loop control of the five-phase drive is more difficult. According to the results shown in Fig. 4.12(b), the detection performance was the same as previous cases. It was observed that in all faulty phases, the current signal was zero after FD. In all cases, the FD time was under 25 % of the fundamental period.

According to the experimental results of the FD, multiple faults were detected without any false alarm, demonstrating the FD algorithm is robust and efficient.

It is worth noting that after a fault in one or more phases of the power converter, the current in the remaining healthy phases is no longer a combination of the first and third harmonics. Subharmonics and higher order harmonics are also included in the waveforms. This can be seen in the experimental results of the current waveforms for the single switch FD (i.e. Fig. 4.11(b)), combination of single switch and open phase FD (i.e. Fig. 4.12(a)) and three upper switch faults (i.e. Fig. 4.12(b)). As seen in Fig. 12(a), after a fault in phases *A* and *B*, the current in other phases is not sinusoidal. The spectrum of phase *C* current is shown in Fig. 4.12(a); as it can be seen, there are DC component and second harmonics in the phase current. These components are not included in the model. As it is shown in Fig. 4.12(a), the FD scheme is robust to non modeled harmonics.

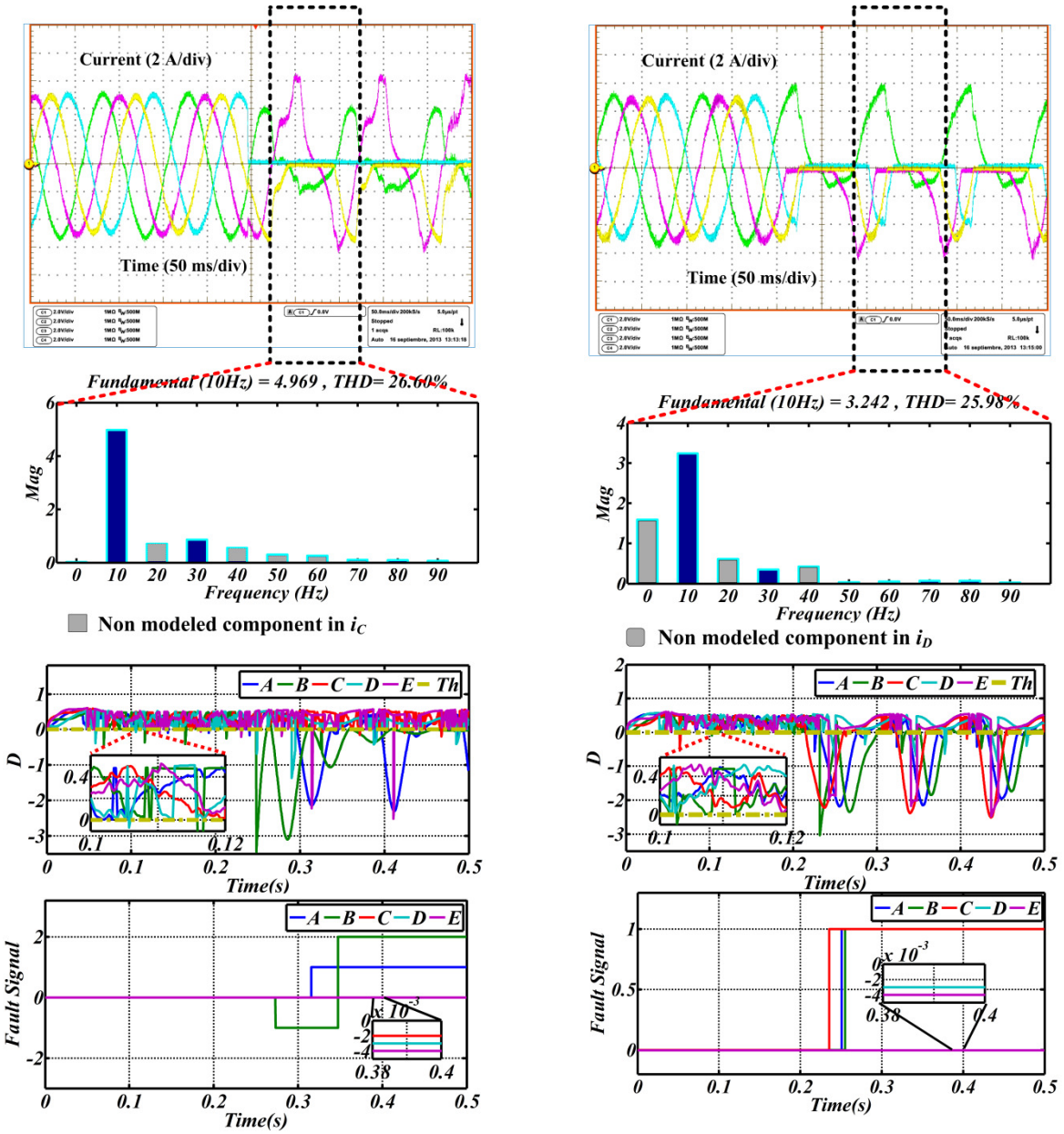

(a) (b)

Fig. 4.12. Experimental waveforms (a) single switch and open phase FD (b) three upper switch FD.

Regarding the experimental waveforms in the case of three upper switch faults shown in Fig. 4.12(b), the spectrum of the phase *D* current is calculated. Similar to the previous case, there are harmonics in the remaining healthy phases after fault occurrence in phases *A*, *B*, and *C*; these harmonic components have not been considered in the current model. As it can be seen, regardless of non modeled harmonics in the remaining healthy phases, false alarms are avoided in phases *C* and *D*. Therefore, the presented method is robust to non modeled harmonics and subharmonics.

A high performance FD method should also be robust to the frequency transients for application in a variable speed drive. In order to show robustness of the presented method to the speed transients, two case studies were considered. In the first case study, the speed value was changed from 7 to 23 rpm. The current waveform in phase *A*, the estimated current in same phase using RLS algorithm, the detection index *D*, and the fault signal are all shown in Fig. 4.13(a). As it can be seen, the estimated current follows the real current with fast dynamics. This is due to high convergence rate of the RLS algorithm. As a result, no false alarm was observed in this case. As second case study, a fast speed reversal was considered. The speed value was changed from -23 rpm to 23 rpm. The final experimental results in phase *A* are shown in Fig. 4.13(b). As expected, the detection scheme is robust to the speed transients.

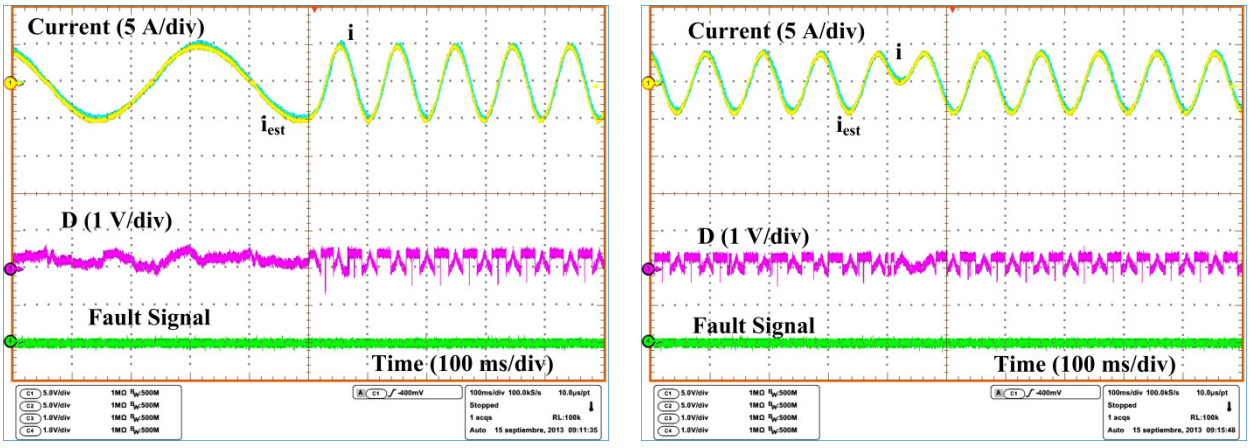

(a) (b)

Fig. 4.13. Experimental results under the frequency transients (a) first case study (b) second case study.

Experimental Results of Fault Tolerant Control:

In the previous section, detection performance of the proposed method was validated by the experimental results. In this section, the proposed method is included in a fault-tolerant control algorithm of the five-phase BLDC motor. For simplicity, operational modes of the motor drive were shown by a simple code. The healthy mode, one faulty phase mode, two-adjacent faulty phase mode,

and two-nonadjacent faulty phase mode are codified with 1, 2, 3, and 4, respectively. Two scenarios were studied. In the first scenario, an open phase fault was initiated in phase *A*. In the next step, the operational condition was changed to two adjacent faults. The second fault was created in phase *B*. The experimental waveforms of the phase currents, motor torque, and fault code are shown in Fig. 4.14. As it can be seen, the fault-tolerance was realized by using the presented FD method. It should be noted that due to high number of the signals, the torque waveform was captured once with three remaining healthy phase currents. Also, its waveform was demonstrated only with faulty phase currents, and fault code.

As discussed before, the current value was equal to zero after FD. Therefore, this time was considered as zero crossing point (i.e. soft transition point) for the phase current in control algorithm. After FD, the gate signal for the remaining healthy IGBT in the faulty phase was removed immediately. The modulation law and FOC were updated with respect to the new configuration of the converter.

It should be noted that according to the experimental results, the ratio of torque value under one faulty phase to healthy mode is 73 %. This value is reduced to 27 % and 54 % in the case of two-adjacent and two-nonadjacent faulty modes, respectively. Therefore, by implementing the proposed detection method, the fault-tolerant concept can be achieved in a motor drive with a closed loop control.

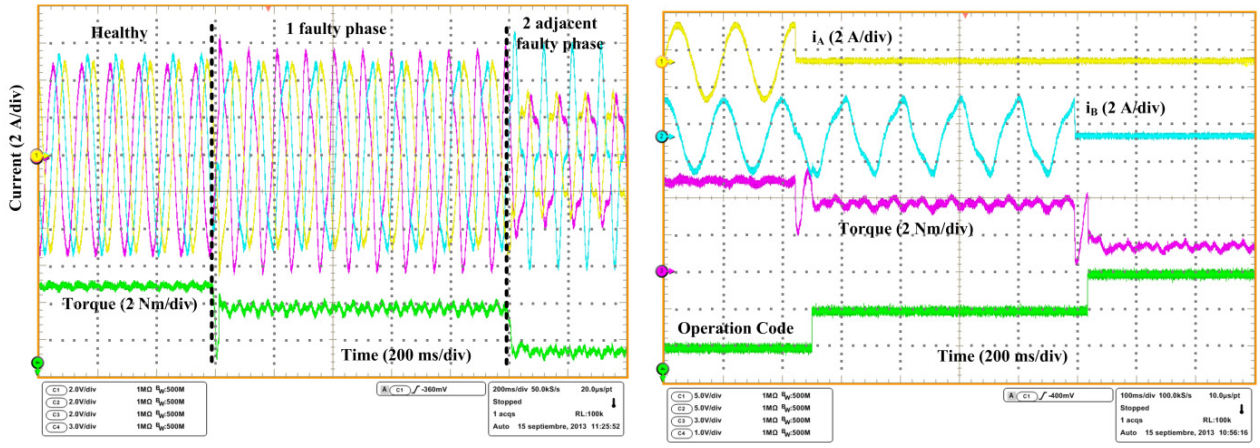

(a) (b)

Fig. 4.14. Experimental waveforms of fault-tolerant results under two-adjacent faulty phase (a) torque and healthy phase currents (b) faulty phase currents, torque and fault code.

4.3.2. Experimental results of the phase angle estimation method

In order to validate theory, experimental results are carried out. Results are presented in three sections. In the first one, implementation of the FD algorithm on FPGA is discussed. In the second one, performance of the FD method is evaluated under different faulty conditions. In the third one, FD method is used to implement the fault-tolerant control algorithm in real time. Here, firstly, the fault is detected; after that, according to the faulty mode, appropriate remedial strategies are taken to maintain continuous operation of the motor.

Implementation of the FD Algorithm on FPGA:

Nowadays, FPGAs are getting more industrial applications due to decreasing cost and increasing logic resources [87], [88]. On the other side, due to high processing power and number of digital I/O, FPGA is chosen to implement the FD algorithm in this dissertation.

It should be noted that FPGA is a powerful candidate for FD in power electronics and motor drives. Due to its high processing power, algorithms of FD either in power converter or motor can be implemented on FPGA. On the other side, it can sample a signal with a very high frequency. This is very important to detect and protect short circuit faults in the power converters. Moreover, due to its high number of input-outputs, a lot of signals can be measured to implement the FD algorithm. Regarding a highly reliable motor drive (e.g. a fault tolerant motor drive applicable in electric vehicles), in practice, there are a lot of feedbacks from the fault detectors already embedded in the hardware (e.g. over current sensor, short circuit signal from switch gate driver, over voltage sensor, temperature sensors, and etc). In a fault tolerant system, a very fast and powerful processor is necessary to manage and protect these faults. A low cost FPGA is a high performance candidate to implement the FD algorithm. Therefore, the author was motivated to use a FPGA for implementing FD algorithm in this thesis.

In fact, the FD algorithm was implemented on an EP4CE22F17C5N FPGA Cyclone IV from Altera Company available on DE0_Nano board. Hardware implementation of the FD algorithm on the FPGA is shown in Fig. 4.15. Motor phase currents are sampled at 15 kHz. The sampled signals are stored in a 12 bit register. According to the FD index in (4.22), phase currents are delayed during one-quarter of the fundamental cycle. This block is denoted by *Delay* in Fig. 4.15.

After that, phase angle of the current signal is estimated by *Inverse Tangent* function; this function was implemented on FPGA based on the *Cordic* algorithm. The inputs to the FD method are the real and the delayed current in each phase of the motor. All the codes were written in Verilog HDL. In order to optimize the resources, only one block was used to implement the Cordic algorithm. The phase currents are sent to this block by a multiplexer. After estimation of the phase angle, phase angle of each phase is extracted by a demultiplexer.

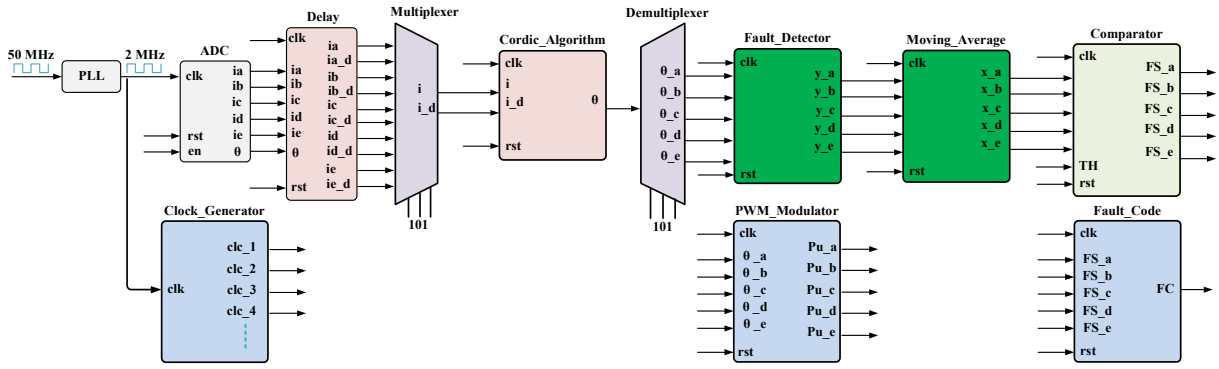

Fig. 4.15. Hardware implementation of the FD block on FPGA

After this phase angle estimation, the Fault_Detector block already described in (4.24) is used to determine if there is a faulty sample. Average value of the fault signal is calculated during one fundamental cycle by a *Moving_Average* block; the output of this block was described in (4.25). Finally, to generate the fault signal (FS), an *x* value is compared with a threshold value. The threshold value can be set by a 12 bit register *TH*.

In order to simplify the evaluation of the developed algorithm, a simple PWM block shown by PWM_Modulator in Fig. 4.15 was developed in the FPGA. Here, any signal can be modulated by this block. Digital outputs are filtered by a simple LC filter on developed FPGA board. This method is quite suitable to evaluate the efficiency of the developed algorithm step by step.

To further improve the hardware implementation of the FD algorithm, a simple counter shown by *Clock_Generator* block in Fig. 4.15 was used to generate the custom clocks for each block of the algorithm. Moreover, fault signals in all phases were sent to a Fault_Code block. This block produces a simple numerical code for each operational mode of the motor drive. By using this code, reconfiguration of the whole system can be done quickly.

To validate the performance of the implemented algorithm, two case studies are considered. In the first case, the healthy mode control of the motor is implemented, after five cycles, a lower switch fault is forced in phase *a*. To show the effectiveness of the developed algorithm on the FPGA, the FD index and fault signal are converted to the analog signals. A summary of resource utilization is shown in table IV.III. Experimental results of this case are shown in Fig. 4.16(a). As it can be seen, fault is detected during a quarter of one cycle. The estimated phase angle value is constant after the fault. In the second case study, open phase fault is forced in the inverter, resultant waveforms are shown in Fig. 4.16(b). As it can be seen, the fault is detected during less than a quarter of one fundamental cycle. The phase angle value after fault is equal to 45 degrees. According to the presented experimental results, open switch and open phase faults were detected effectively. Besides, phase angle of the motor current was estimated successfully.

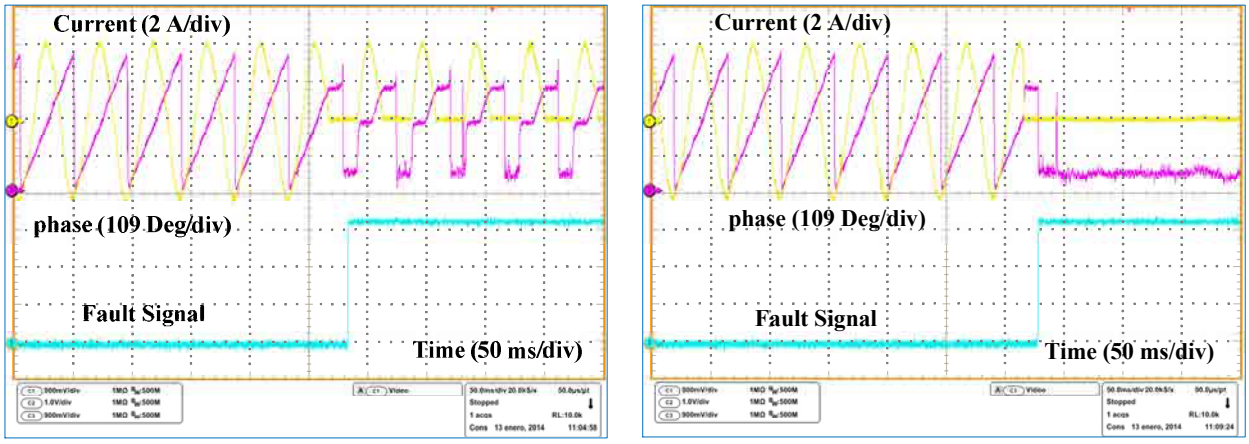

(a) (b)

Fig. 4.16. Experimental results of FD with FPGA. (a) Results of the FD under lower open switch fault. (b) Results of the FD under open phase fault.

Table IV.III. Utilization of resources in FPGA.

Logic utilization	Used	Available	Utilization (%)
Combinational functions	1673	22320	7
Total registers	1139	22320	5
Pins	19	154	12
Memory bits	4896	608256	1
PLL	1	4	25

As it was earlier discussed in section II, the estimated phase angle under faulty mode is a constant value equal to 0, π/2, and π. However, in the experimental results, it was approached to π/4. The main reason is due to a specific implementation of the Cordic algorithm. As it can be seen from Fig. 4.15, FD is separately done by FPGA; the FS in each phase is sent to dSPACE control board.

Experimental Results of the FD:

To evaluate the performance of the FD method, experimental results are conducted under different operational modes. In the first step, the robustness to the load transients is evaluated. Two 50 % step response are imposed on the phase current. Experimental waveforms are shown in Fig. 4.17(a). According to these results, FD block is robust to the transients.

In the second step, a single lower switch fault and an upper switch fault are forced in phases *a* and *b*, respectively. This case study is a common fault type in VSIs. Experimental results of this case are shown in Fig. 4.17(b). As it can be seen from the fault signal waveform, fault code in phase *a* is equal to 1 which corresponds to the lower switch fault. At the same time, fault code in phase b is -1. From these results, it can be seen that FD time is less than a quarter of one period.

In the third experiment, an open phase fault is forced in the inverter. This case was implemented in phase *a*. The corresponding experimental waveforms are shown in Fig. 4.17(a).

According to the results, the fault is detected during less than a quarter of one fundamental cycle. However, the fault is localized during one fundamental cycle.

In the last experiment, FD under faulty mode is considered. To emulate this mode, phase *a* of the motor is disconnected. Control method is updated for one faulty phase mode. A new open switch fault is forced in phase *b*. The results are shown in Fig. 4.18(b). As it can be seen, the fault is effectively detected under faulty mode.

As it was shown by the experimental results, the proposed FD method is robust to the load transients. Besides, it can detect multiple open switch and open phase faults. The FS sent by the FPGA block is included in the fault-tolerant SMC algorithm to maintain the continuous operation of the motor. Details are discussed in the next section.

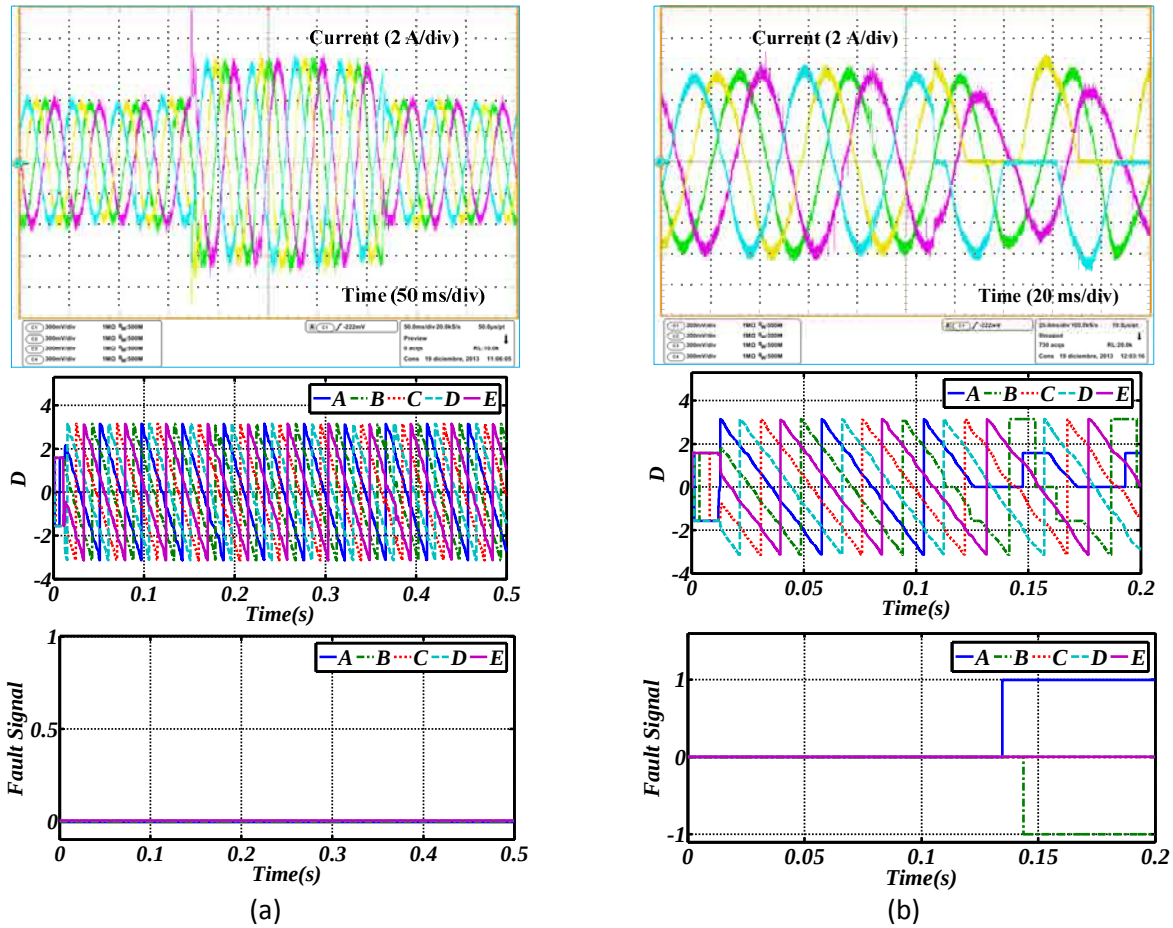

(a) (b)

Fig. 4.17. Experimental results of FD. (a) Performance evaluation of FD method under load transients. (b) Single switch FD under healthy mode.

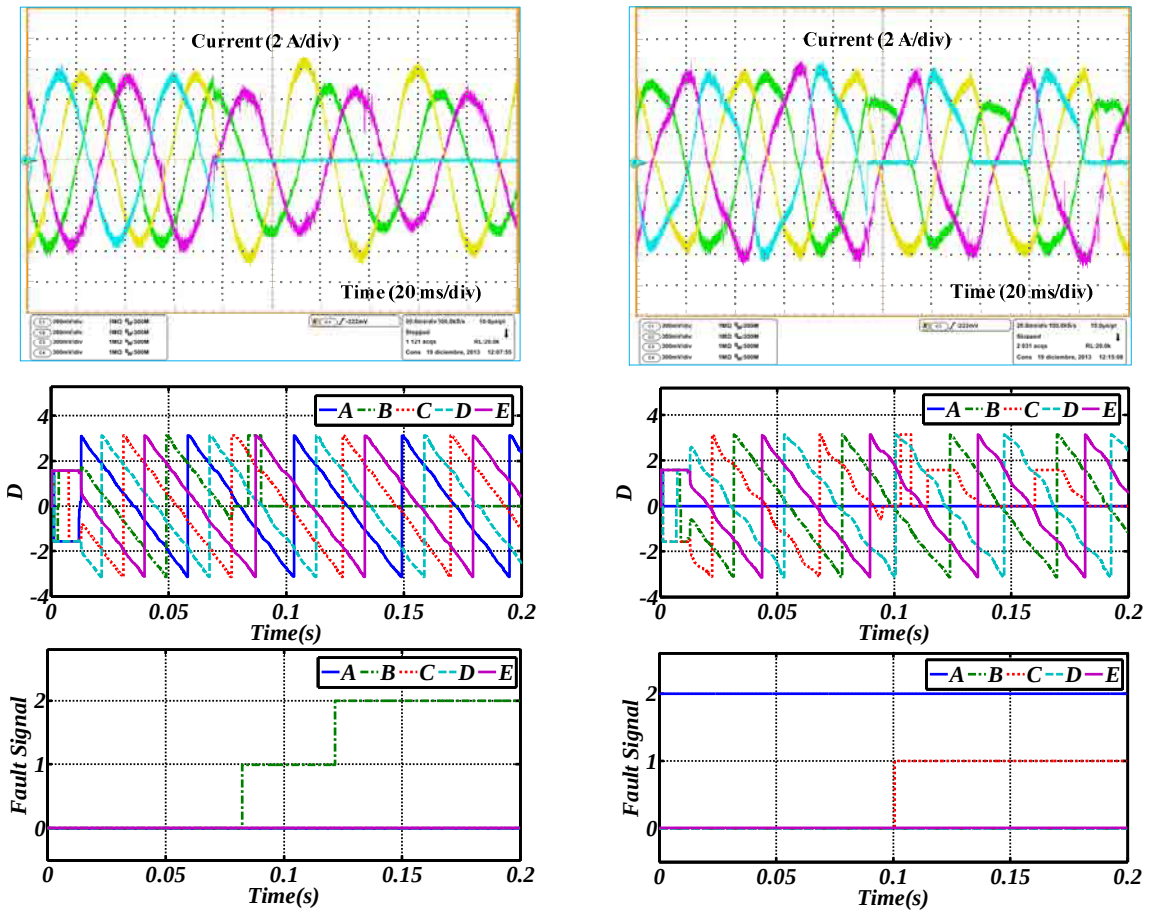

Fig. 4.18. Experimental results of FD. (a) Open phase FD. (b) Single switch FD under faulty mode.

Experimental Results of the Fault-Tolerant Control Algorithm:

In order to implement the fault-tolerant control of the five-phase PM motor, the provided FS is included in SMC algorithm. Under each operational mode, a simple code is produced by the FD block implemented on FPGA. Operation code of the healthy mode, one faulty phase mode, two-adjacent faulty phase mode and two-nonadjacent faulty phase mode are 1, 2, 3, and 4, respectively. Algorithm of the space vector modulation, the reference currents and SMC are updated according to this code.

In the first step, the motor was operated under healthy mode. Then, a fault was forced in phase *a*. After that, another fault was started in phase *b*, which is adjacent to phase *a*. Experimental waveforms of this case are shown in Fig. 4.19.

As it can be seen, fault-tolerant algorithm is done effectively. Healthy phase currents are shown with torque waveforms. Faulty phase currents are also shown with the torque waveform and the operational code of the motor drive. According to these results, the proposed FD method can be effectively applied in a system with a fault-tolerant capability.

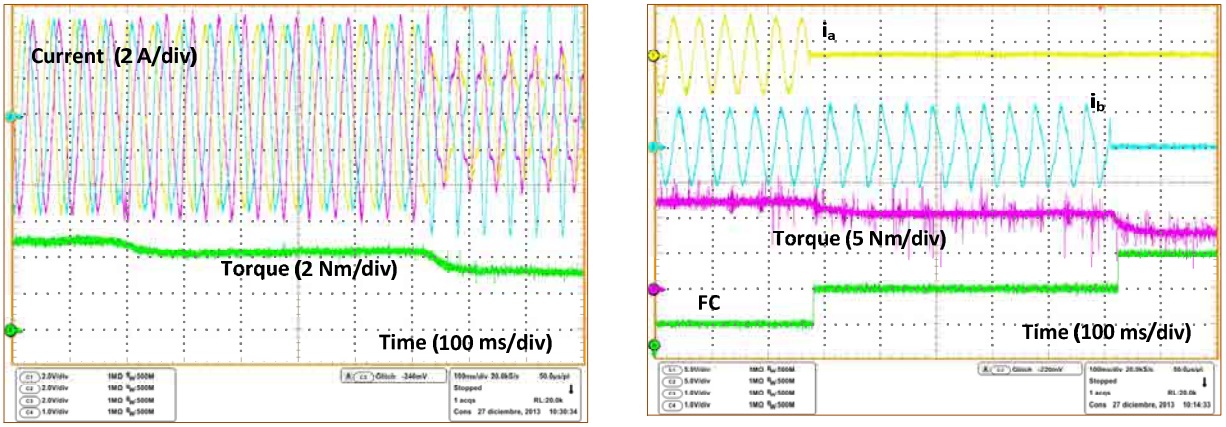

(a) (b)

Fig. 4.19. Experimental results of the fault-tolerant control. (a) Healthy phase currents and torque. (b) Faulty phase currents, torque and fault code.

4.4. Comparison between proposed FD method and other methods in literature

In order to further validate the characteristics of the proposed FD, a comparison is conducted between two high performance FD methods already presented in literature and proposed method. The performance of each method is evaluated under eight operation mode including acceleration, deceleration, braking, reverse mode, load transient, multiple switch fault, open phase fault, and faulty mode operation. It should be noted that all considered tests are normal to happen in traction drives.

Regarding the presented FD methods in this thesis, proposed method in section 4.2.2 of the thesis is chosen. The main reasons are due to high robustness to false alarms, simple implementation, being capable of detecting single switch and open phase faults, and flexibility. According to this method, a single trigonometric function is defined to extract the FD index as follows:

$$\boldsymbol{D} = \tan^{-1}\left(\frac{\boldsymbol{i}(\boldsymbol{t})}{\boldsymbol{i}(\boldsymbol{t}-\boldsymbol{T}/4)}\right). \qquad (4.41)$$

As the first presented method in literature for comparison, the idea presented in [9] is calculated as shown in (4.42) without using auxiliary variable; average current is normalized with respect to its absolute average value as:

$$\boldsymbol{m} = \frac{\langle \boldsymbol{i} \rangle}{\langle |\boldsymbol{i}| \rangle} \qquad (4.42)$$

where <> is signal average value at fundamental frequency and || is absolute value. Main advantage of this diagnostic variable is simplicity. However there are two major problems using this method. To avoid its disadvantages, some auxiliary signals have been proposed in [9]. However, using these signals, detection circuit complexity increases. Here, simple formula shown in (4.42) is used for comparison.

Third case study is utilization of Park's vector modulus as presented in [40]. Here, later idea is developed for a five-phase converter as follows. In the first step, current signals are transformed to space vector using Park's transformation shown in (4.43) and (4.44).

$$\boldsymbol{T} = \frac{2}{5}\begin{bmatrix} 1 & \cos(2\ /5) & \cos(4\ /5) & \cos(6\ /5) & \cos(8\ /5) \\ 0 & \sin(2\ /3) & \sin(4\ /3) & \sin(6\ /5) & \sin(8\ /5) \\ 1 & \cos(4\ /5) & \cos(8\ /5) & \cos(12\ /5) & \cos(16\ /5) \\ 0 & \sin(4\ /3) & \sin(8\ /3) & \sin(12\ /3) & \sin(16\ /3) \\ \frac{1}{\sqrt{2}} & \frac{1}{\sqrt{2}} & \frac{1}{\sqrt{2}} & \frac{1}{\sqrt{2}} & \frac{1}{\sqrt{2}} \end{bmatrix} \qquad (4.43)$$

$$\begin{bmatrix} \boldsymbol{i} \\ \boldsymbol{i} \\ \boldsymbol{i_x} \\ \boldsymbol{i_y} \\ \boldsymbol{i_0} \end{bmatrix} = \boldsymbol{T} \begin{bmatrix} \boldsymbol{i_a} \\ \boldsymbol{i_b} \\ \boldsymbol{i_c} \\ \boldsymbol{i_d} \\ \boldsymbol{i_e} \end{bmatrix} \tag{4.44}$$

After that, input current is normalized with respect to magnitude of Park's vector modulus. The calculated value is subtracted from absolute value of normalized motor phase currents (i.e. ζ) under balanced sinusoidal waveforms as shown in (4.45):

$$\boldsymbol{D} = \left\langle \left| \frac{\boldsymbol{i}}{\sqrt{\boldsymbol{i}^2 + \boldsymbol{i}^2 + \boldsymbol{i_x^2} + \boldsymbol{i_y^2}}} \right| \right\rangle - \tag{4.45}$$

It should note that ζ value for balanced sinusoidal current waveforms is equal to 0.4.

Acceleration:

Acceleration is a common operational mode in variable speed drives applicable in traction drive; therefore the performance of FD methods is studied under this case. The motor speed is increased from 20 rpm to 50 rpm; experimental results under acceleration mode are shown in Fig. 4.20(a). As it can be seen in Fig. 4.20(a), in contrast to the methods in [9] and [40], the proposed method is robust to acceleration condition. Moreover proposed method in [40] can still be used by increasing the FD threshold slightly (i.e. TH equal to 0.1). Method in [9] shows a poor performance in this case.

Deceleration:

The deceleration is another common operational mode in motor drives. Results under deceleration mode are shown in Fig. 4.20(b); under this case, motor speed is decreased from 50 rpm to 20 rpm while torque reference is still constant. As it can be seen, all methods are robust to deceleration test as shown in Fig. 4.20(b).

Braking:

In the third step, a comparison is done under braking operational mode; results are shown in Fig. 4.21(a). Under braking mode, the torque reference value is changed from -4 to 4 Nm; motor speed is fixed at 23.8 rpm. According to Fig. 4.21(a), the method in [9] is not robust to the braking test.

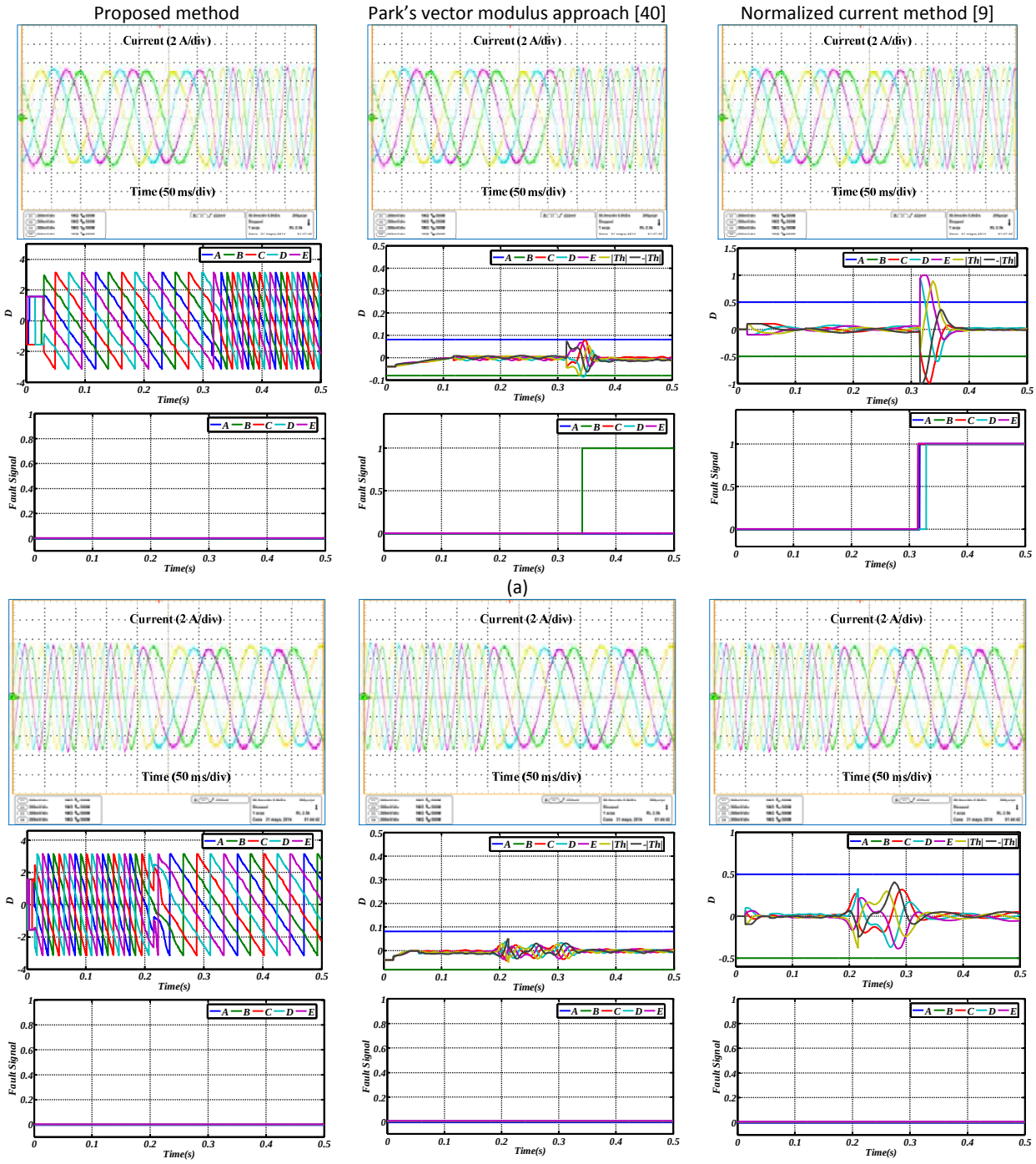

Fig. 4.20. Comparison of FD methods under (a) acceleration mode. (b) deceleration mode.

Reverse Operation:

In case of reverse test, motor speed is changed from -23.8 rpm to 23.8 rpm instantaneously; torque reference value is fixed at 4 Nm. Experimental results are shown in Fig. 4.21(a). Under reverse operational mode, all methods produce false alarm except the proposed method.

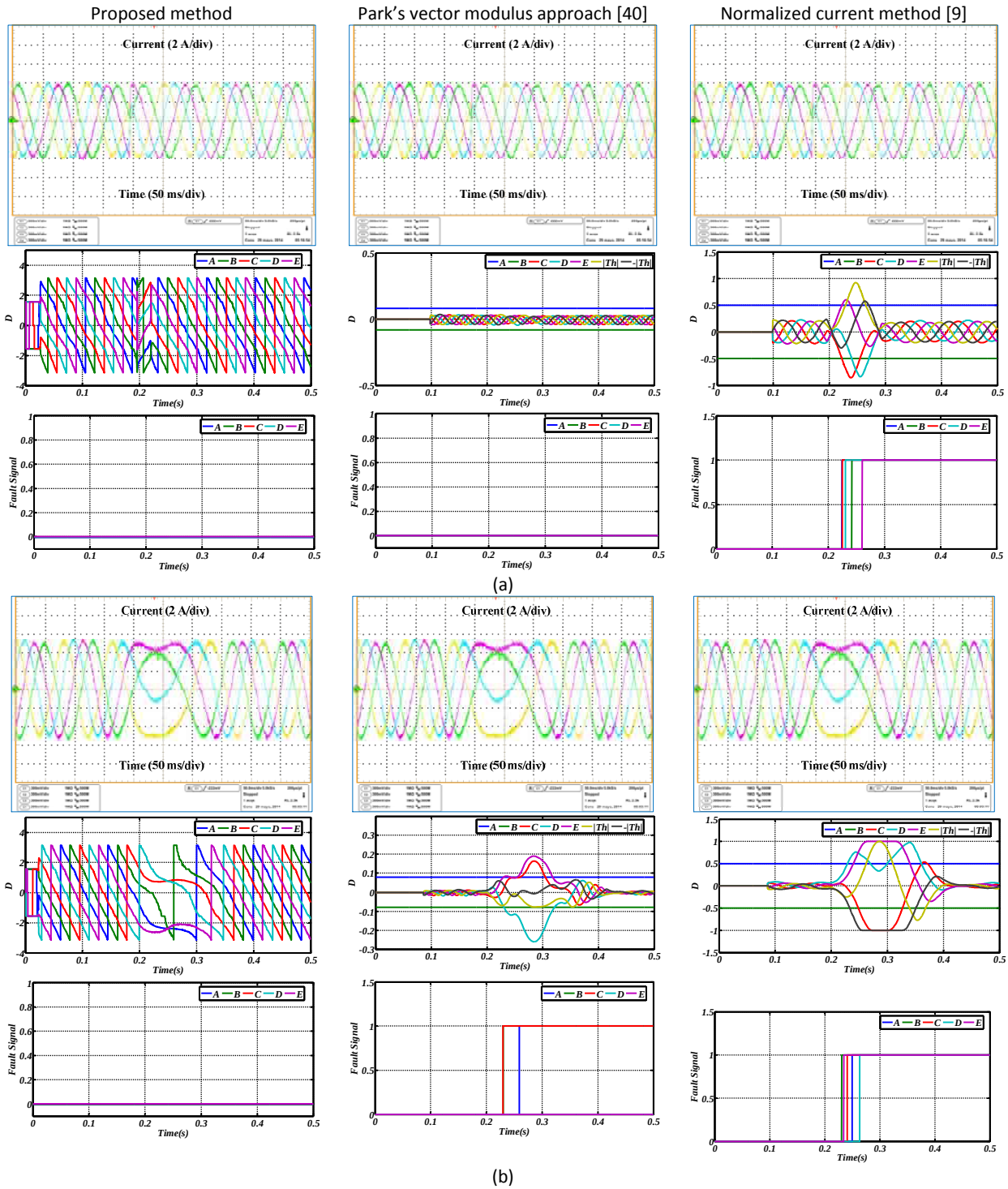

Fig. 4.21. Comparison of FD methods under (a) braking mode. (b) reverse operational mode.

Load Transient:

One important advantage of a high performance FD method is the robustness to the load transients. In this case, motor phase current are once increased about 50 %, after 4 cycles, current values are reduced by 50 %. Experimental waveforms are shown in Fig. 4.22(a). According to the results,

all methods are robust to the load transients. It should be noted that, methods in [9] and [40] can be sensitive to higher transient levels.

Single Switch Fault:

In this case, a single lower switch fault and an upper switch fault are forced in phases *a* and *b* of the five phase inverter, respectively. This case study is a common fault type in VSIs. Experimental results of this case are shown in Fig. 4.22(b). As it can be seen from the fault signal waveform, all methods can detect the fault.

Open Phase Fault:

In the next step, an open phase fault is forced in the inverter. This case was implemented in phase *a*, experimental waveforms are shown in Fig. 4.23(a). According to the results, fault is detected during less than a quarter of one fundamental cycle using the proposed method. Method in [40] is subjected to false alarms. Moreover, presented method in [9] should be equipped with auxiliary variables to detect this fault.

FD under Faulty Mode:

In the last step, FD under faulty mode is considered. To emulate this mode, phase *a* of the motor is disconnected. Control method is updated for one faulty phase mode. A new open switch fault is forced in phase *b*. The results are shown in Fig. 4.23(b). As it can be seen, fault is effectively detected under faulty mode using the proposed method. Other methods generate false alarms in this case. The main reason is due non-sinusoidal unbalanced phase currents. It should be noted that it is necessary to consider a higher threshold value in [40] in order to increase its stability under this operation mode.

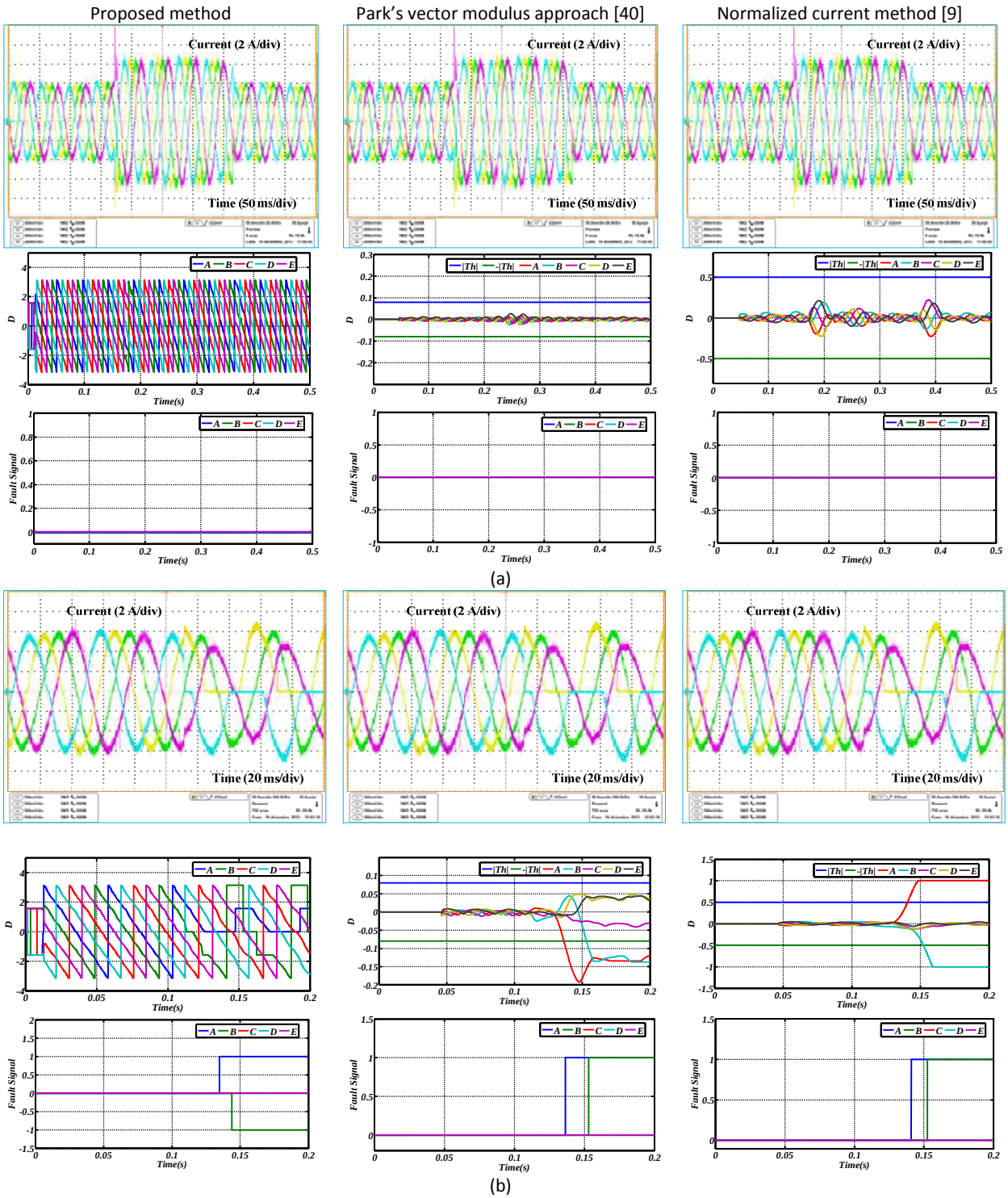

Fig. 4.22. Comparison of FD methods under (a) load transient. (b) multiple single switch fault.

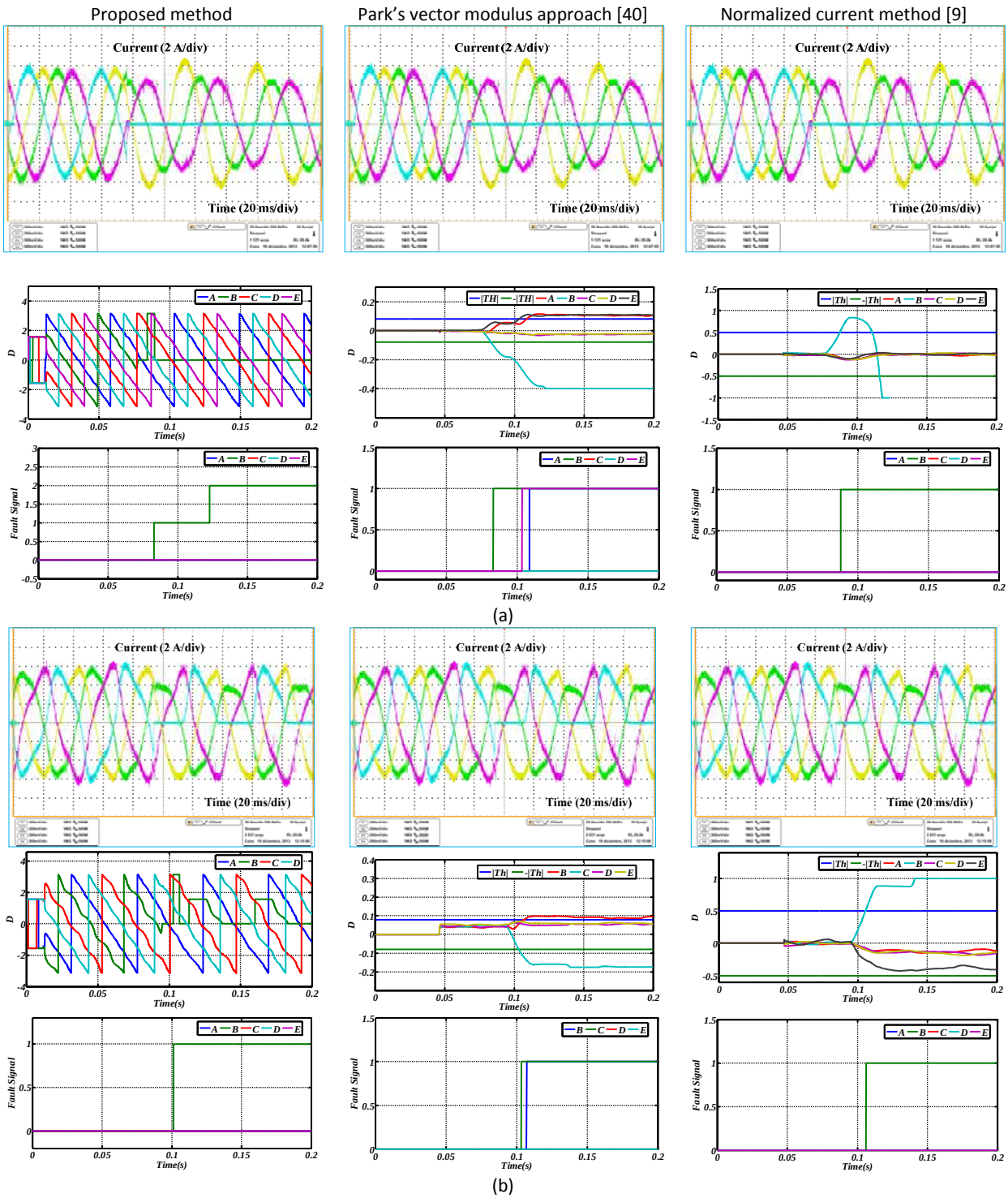

Fig. 4.23. Comparison of FD methods under (a) Open phase fault. (b) Single switch fault in faulty mode.

4.5. Discussion and conclusions

The signal based open switch FD methods are very interesting for industrial applications. Since current signals are usually needed by the control algorithm, they can be used to develop a cost effective FD method. Keeping in mind this point, two novel signal based FD methods are introduced in this thesis. In addition, two fault-tolerant control algorithms are developed with embedded FD method.

Fault Detection and Fault Tolerant Operation of a Five Phase PM Motor Drive Using Adaptive Model Identification Approach

A new open switch FD method based on the signal model identification is presented in this dissertation. An adaptive identification process (i.e. recursive least square method) is used to estimate the current signal, and then a simple FD index was obtained. Resultant value was effectively applied to detect the open switch and open phase faults. It was shown that multiple open switch and open phase faults can be detected in less than a quarter of one period. The proposed FD method is flexible and independent from load parameters.

To address lack of research on fault-tolerant control with embedded FD in multiphase PM machine, reconfiguration of conventional control algorithm is discussed.

Experimental results of a multiphase BLDC motor drive under different faulty modes are shown to validate high performance of the proposed FD technique. The fault-tolerant algorithm was completed by using the presented detection technique.

FPGA Based Robust Open Transistor FD and Fault-Tolerant Sliding Mode Control of a Five-Phase PM Motor Drive

Another, new signal based open transistor FD method was proposed in this theis. Phase angle of the motor phase current is estimated by a simple trigonometric function. The estimated value is used to define an FD index. The FD algorithm was executed inside an FPGA; details of the hardware implementation were explained. The fault signal generated by FPGA is sent to control box in order to update the control method and inverter configuration. The experimental waveforms were presented for a five-phase VSI supplying a PM motor under different operational modes. According to the results, the proposed method is fast, robust and reliable. Furthermore, it is a general, simple and efficient method. It is possible to detect and localize multiple open switch faults. Detection speed less than a quarter of one fundamental cycle may be claimed. However, it depends on the load current at the fault initiation point.

To evaluate the effectiveness of the FD method, SMC was developed to set the current references in a five-phase PM motor with an embedded FD block. The SMC has the advantage of

tracking the reference currents quickly, and accurately. These features are important for the FD strategy. The FD block was included in fault-tolerant control algorithm of a five-phase BLDC motor drive. It was shown that, different remedial strategies can be effectively taken after FD in order to maintain the continuous operation of the motor. A real time fault-tolerant continuous control is achieved.

In this chapter, a comparison was done between a simple signal based open switch FD method based on phase angle estimation with two available high performance methods in literature. Experimental results were conducted under eight relevant operational mode of a motor drive applicable in EV. It was shown that the proposed method is robust to all operational modes in comparison to other methods.

5.

Study and Contributions to FD and Model Predictive FT Control

Due to higher number of phases in multiphase drives in comparison to conventional three phase systems, developing a simple but reliable fault-tolerant control method is necessary. At the same time, a FD method should be used to maintain the continuous operation of the drive. This chapter investigates real time continuous operation of the drive with a novel fault-tolerant control and FD algorithm.

CONTENTS

5.1. Introduction

Due to their fault-tolerant capabilities, five-phase PM motor drives are suitable candidates in applications with high reliability [45], [89], [90-92]. These motors are able to continue their operation after missing up to two phases. The high reliability and continuous operation of the electrical drives under faulty conditions are of great importance in applications such as military, aerospace, electric ship propulsion and hybrid electrical vehicles [45] [93] [94]. Such motors are supplied by five-phase converters. On the other side, inverters are one of the more important units in electrical drives; different fault types may occur in this unit. According to the statistics, 38% of all faults occurring in motor drives are related to the power switches [6]. Therefore, to maintain the continuous operation of a PM motor drive supplied by a multiphase inverter, an FD scheme should be applied.

In order to operate a fault-tolerant motor drive, fast FD and isolation of faulty components in the power converter are of paramount importance. Different FD methods have been investigated in literature. Fault types in the power converters can be divided into open switch and short circuit faults. A comprehensive study has been done on fault types, FD and fault protection methods for VSIs in [7].

In a multiphase motor drive, it is necessary to develop a fault-tolerant control algorithm with an embedded FD scheme. Regarding the control method, FCS-MPC is a high performance solution. There is a lack of research on developing this kind of control methods on multiphase PM motor drives. The simple implementation, high flexibility, and fast dynamic response of the FCS-MPC to implement a fault-tolerant control algorithm are explored in this thesis.

FD in power converter is the complementary part of the fault-tolerant control algorithm. Different methods have been presented in literature to diagnosis the open circuit faults in VSIs. A simple classification in [9] considers these FD methods in three categories such as: model based methods, reference based methods, and signal based methods.

Considering the model based FD methods, the load response to the input signal is predicted by using a load mathematical model. Then difference between the estimated and measured signal is used to define an FD index [19], [53].

Regarding the reference based method, the difference between real signal and reference signal is used to define the FD index [25]. Application of this method is limited to a system with the closed loop control.

Regarding the signal based methods, output voltages or currents of the power converters are measured. Then, by using a signal processing technique, an FD index is calculated [95], [42], [96].

Fault diagnosis and fault-tolerant FCS-MPC of five-phase PMSM in stationary reference frame has been presented in [97]. In this dissertation, a simple open transistor FD method is presented by

using the converter current signal and a simple signal available in the control method. This method is fast, simple and flexible. It can be used in two-level multiphase VSIs. Both open switch and open phase faults can be detected by using this method.

Two main contributions are presented in this chapter. In the first part, the fault-tolerant FCS-MPC is developed for application in a five-phase BLDC motor drive. In the second part, a simple FD scheme is presented; this scheme can detect, localize and isolate the open circuit faults in the power converter feeding a five-phase BLDC motor drive.

5.2. Theoretical approach

Due to its high computational cost, MPC has not been applied extensively at industrial applications in the past. However, with emerging high performance digital signal processors such as DSPs and FPGAs, high amount of calculation is no longer difficult to be implemented by software and hardware. As a result, in recent years MPC has been an attractive control method for researchers. Due to its flexibility, it can be applied to control power electronics converters. The main advantages of this control method are high dynamic performance, simple implementation and flexibility. MPC can be divided into two methods. In the first category, reference voltage waveform is predicted by the system model. After that, the resultant signal is applied to conventional pulse width modulators to produce the reference waveforms. This method is known as dead beat MPC [98]. On the other hand, in the second category, load current waveform is predicted by using available voltage space vectors of the power converter and load parameters. After that, a cost function is calculated. The state vector which minimizes the cost function is chosen as the optimal vector and applied to the power converter during the next switching period. This method is known as FCS-MPC in literature [99]. Using this control method, there is always a steady state error [100]; this error is more relevant at lower switching frequency and small current reference amplitude. This dissertation is focused on FCS-MPC methods.

MPC is a flexible, simple and high dynamic performance control method. It can be used as an alternative for inner control loop of the power converters for any application such as motor drives, grid connected converters, DC-DC converters, power quality conditioners, etc. However, at any application, a cost function can be designed based on required control objectives; this is due to its flexibility. All aforementioned applications of the power converter controlled by FCS-MPC were demonstrated in [98], where a comparison with traditional methods based on PWM was shown. A review regarding state of the art emerging FCS-MPC in power electronics is shown in [99], [101] and [102].

Based on FCS-MPC method, at each sampling period, the current is predicted for all possible switching states of the converter; the load model is used to predict this current. Then, the error between the predicted current values and the reference current is calculated [102]. It should be noted that the reference current is calculated by an outer controller. Using these error values, a cost function is calculated. After that, a switch vector which minimizes the cost function is chosen as an optimal and applied during the next switching period. The control method is shown in Fig. 5.1; it has been used to implement a fault-tolerant control of a five-phase PM motor. It should be noted that the control method of Fig. 5.1 is general and it can be applied to any application area; in this thesis, only motor drive subject is studied. To implement this control method in multiphase drives, several points should be considered as following. By increasing the number of the switching vectors, amount of calculation is increased. The

cost function should be designed based on desirable control purposes considering the constraints. Inaccurate model parameters can lead to non-accurate predicted current values. Keeping in mind these criteria, theory of the control method is explained in the following section.

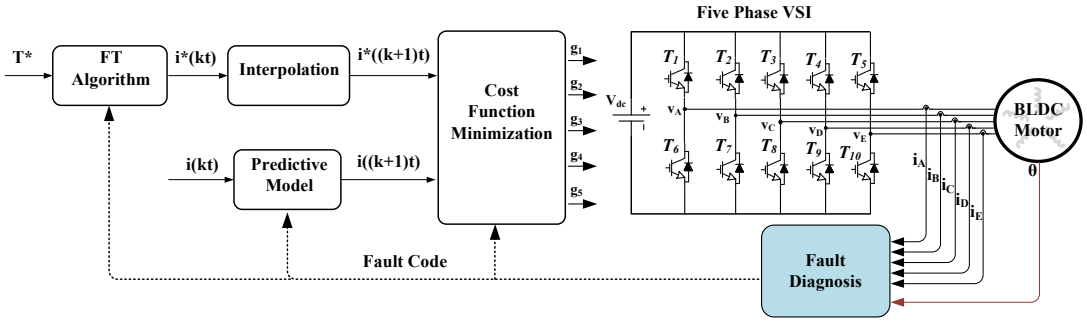

Fig. 5.1. The fault-tolerant FCS-MPC of the five-phase converter supplying PM motor

5.2.1. FCS-MPC of Five-Phase Converter Supplying BLDC Motor Drive:

In this thesis, a five-phase converter supplying a BLDC motor is considered as the case study. The considered system is shown in Fig. 5.1. The five-phase motor drive is a fault-tolerant system; it can tolerate up to two faulty phases. In the following, its mathematical model is discussed.

A five-phase motor connected to a VSI can be modeled under healthy operational mode as:

$$\begin{bmatrix} v_a - e_a - v_x \\ v_b - e_b - v_x \\ v_c - e_c - v_x \\ v_d - e_d - v_x \\ v_e - e_e - v_x \end{bmatrix} = \left(\begin{bmatrix} r_a & 0 & 0 & 0 & 0 \\ 0 & r_b & 0 & 0 & 0 \\ 0 & 0 & r_c & 0 & 0 \\ 0 & 0 & 0 & r_d & 0 \\ 0 & 0 & 0 & 0 & r_e \end{bmatrix} + \begin{bmatrix} l_a & m_1 & m_2 & m_2 & m_1 \\ m_1 & l_b & m_1 & m_2 & m_2 \\ m_2 & m_1 & l_c & m_1 & m_2 \\ m_2 & m_2 & m_1 & l_d & m_1 \\ m_1 & m_2 & m_2 & m_1 & l_e \end{bmatrix} \frac{d}{dt} \right) \begin{bmatrix} i_a \\ i_b \\ i_c \\ i_d \\ i_e \end{bmatrix} \quad (5.1)$$

where *i* is the phase current, *v* is the voltage of each phase, *r* is the phase equivalent resistance, *l* is the phase equivalent inductance, m_1 is mutual inductance between two adjacent phases, m_2 is mutual inductance between two nonadjacent phases, *e* is the back EMF in each phase of the motor, and v_x is the neutral voltage. The back-EMF can be estimated as follows:

$$\begin{bmatrix} e_a \\ e_b \\ e_c \\ e_d \\ e_e \end{bmatrix} = \lambda_{m1} \omega_e \begin{bmatrix} \cos(\vartheta) \\ \cos(\vartheta - 2\pi/5) \\ \cos(\vartheta - 4\pi/5) \\ \cos(\vartheta - 6\pi/5) \\ \cos(\vartheta - 8\pi/5) \end{bmatrix} + \lambda_{m3} \omega_e \begin{bmatrix} \cos(3\vartheta) \\ \cos 3(\vartheta - 2\pi/5) \\ \cos 3(\vartheta - 4\pi/5) \\ \cos 3(\vartheta - 6\pi/5) \\ \cos 3(\vartheta - 8\pi/5) \end{bmatrix}. \quad (5.2)$$

where λ_{m1} and λ_{m3} are the first and third harmonic amplitudes of the rotor flux linkage; ω_e is the electrical rotational velocity, and Θ is the rotor electrical angle.

To simplify the model under healthy and faulty mode, a modification is applied to (5.1). Model is redefined in terms of voltage difference between machine's terminals as follow:

$$\begin{bmatrix} v_{ab} \\ v_{bc} \\ v_{cd} \\ v_{de} \end{bmatrix} = \begin{bmatrix} r_a & -r_b & 0 & 0 \\ 0 & r_b & -r_c & 0 \\ 0 & 0 & r_c & -r_d \\ r_e & r_e & r_e & r_d + r_e \end{bmatrix} \begin{bmatrix} i_a \\ i_b \\ i_c \\ i_d \end{bmatrix} + \begin{bmatrix} e_{ab} \\ e_{bc} \\ e_{cd} \\ e_{de} \end{bmatrix} + \begin{bmatrix} l_a + m_2 - 2m_1 & m_2 - l_b & 2m_2 - 2m_1 & m_2 - m_1 \\ m_1 - m_2 & l_b - m_1 & m_1 - l_c & m_2 - m_1 \\ m_1 - m_2 & 2m_1 - 2m_2 & l_c - m_2 & 2m_1 - m_2 - l_d \\ l_e + m_2 - 2m_1 & l_e - m_1 & l_e - m_2 & l_e + l_d - 2m_1 \end{bmatrix} \frac{d}{dt} \begin{bmatrix} i_a \\ i_b \\ i_c \\ i_d \end{bmatrix}. \quad (5.3)$$

As it can be seen in (5.3), it is no longer necessary to consider the neutral voltage. This advantage can be utilized to model the machine. Considering an open phase fault in phase *a*, model under one faulty phase is simply derived from (5.1) as:

$$\begin{bmatrix} v_{bc} \\ v_{cd} \\ v_{de} \end{bmatrix} = \begin{bmatrix} r_b & -r_c & 0 \\ 0 & r_c & -r_d \\ r_e & r_e & r_d + r_e \end{bmatrix} \begin{bmatrix} i_b \\ i_c \\ i_d \end{bmatrix} + \begin{bmatrix} e_{bc} \\ e_{cd} \\ e_{de} \end{bmatrix} + \begin{bmatrix} l_b - m_1 & m_1 - l_c & m_2 - m_1 \\ 2m_1 - 2m_2 & l_c - m_2 & 2m_1 - m_2 - l_d \\ l_e - m_1 & l_e - m_2 & l_e + l_d - 2m_1 \end{bmatrix} \frac{d}{dt} \begin{bmatrix} i_b \\ i_c \\ i_d \end{bmatrix}. \quad (5.4)$$

As seen in (5.4), only row and column related to the faulty phase are removed from (5.1), and then the faulty model is obtained. Similarly, the machine model under two adjacent faults in phases *a* and *b* is calculated as:

$$\begin{bmatrix} v_{cd} \\ v_{de} \end{bmatrix} = \begin{bmatrix} r_c & -r_d \\ r_e & r_d + r_e \end{bmatrix} \begin{bmatrix} i_c \\ i_d \end{bmatrix} + \begin{bmatrix} e_{cd} \\ e_{de} \end{bmatrix} + \begin{bmatrix} l_c - m_2 & 2m_1 - m_2 - l_d \\ l_e - m_2 & l_e + l_d - 2m_1 \end{bmatrix} \frac{d}{dt} \begin{bmatrix} i_c \\ i_d \end{bmatrix}. \quad (5.5)$$

As it is shown, using the described model, it is possible to treat the inverter as a five-phase, a four-phase and a three-phase inverter under healthy mode, one faulty phase mode, and two-faulty phase mode, respectively. It should be noted that using this simplification, the neutral voltage is no longer important. On the other side, implementation of the control algorithm on *abcde* frame is an advantage due to two reasons. Firstly, modeling of the machine under the faulty mode is easier. Secondly, no transformation is necessary. So, less calculation is the second advantage of this method.

Modulation Strategy:

To produce the reference currents using FCS-MPC, a simple modulation strategy is used in this thesis. The theory of the control method is presented in the following.

In order to realize the control algorithm, the current at the end of each switching step is predicted as:

$$\boldsymbol{i}(k+1) = \boldsymbol{L}^{-1} \times \boldsymbol{T}_{samp} \times (\boldsymbol{v}(k) - \boldsymbol{e}(k) - \boldsymbol{R} \times \boldsymbol{i}(k)) + \boldsymbol{i}(k) \quad (5.6)$$

where T_{samp} is the sampling frequency. It should be noted that (5.6) is the general form of the machine model given in (5.3)-(5.5). After the current prediction, the current is predicted for all switching vectors of the power converter as:

$$\boldsymbol{i}(\boldsymbol{k}+2)=\boldsymbol{L}^{-1}\times\boldsymbol{T}_{\boldsymbol{samp}}\times(\boldsymbol{v}(\boldsymbol{k})-\boldsymbol{e}(\boldsymbol{k})-\boldsymbol{R}\times\boldsymbol{i}(\boldsymbol{k}+1))+\boldsymbol{i}(\boldsymbol{k}+1) \qquad (5.7)$$

After that, a cost function is calculated for each switching vector of the VSI. Here, the cost function is simply defined as difference between the reference and predicted currents of the motor during each sampling period as:

$$\begin{aligned}\boldsymbol{g}_{5\boldsymbol{ph}}&=(\boldsymbol{i}_{\boldsymbol{a}}^{\boldsymbol{ref}}-\boldsymbol{i}_{\boldsymbol{a}}^{\boldsymbol{k}+2})^2+(\boldsymbol{i}_{\boldsymbol{b}}^{\boldsymbol{ref}}-\boldsymbol{i}_{\boldsymbol{b}}^{\boldsymbol{k}+2})^2+\\&(\boldsymbol{i}_{\boldsymbol{c}}^{\boldsymbol{ref}}-\boldsymbol{i}_{\boldsymbol{c}}^{\boldsymbol{k}+2})^2+(\boldsymbol{i}_{\boldsymbol{d}}^{\boldsymbol{ref}}-\boldsymbol{i}_{\boldsymbol{d}}^{\boldsymbol{k}+2})^2+(\boldsymbol{i}_{\boldsymbol{e}}^{\boldsymbol{ref}}-\boldsymbol{i}_{\boldsymbol{e}}^{\boldsymbol{k}+2})^2\end{aligned} \qquad (5.8)$$

where g is the cost function. Since, there are 32 possible switching vectors in a five-phase converter, the cost function is calculated for all the vectors. At each sampling period, the optimal switching vector with the minimum cost is chosen and applied to the VSI.

As it can be seen from (5.8), the reference current is calculated at time $k+2$. Similar to [104], here a fourth order Lagrange extrapolation is used to calculate the future reference current as:

$$\boldsymbol{i}^{*}(\boldsymbol{k}+1)=4\boldsymbol{i}^{*}(\boldsymbol{k})-6\boldsymbol{i}^{*}(\boldsymbol{k}-1)+4\boldsymbol{i}^{*}(\boldsymbol{k}-2)-\boldsymbol{i}^{*}(\boldsymbol{k}-3) \qquad (5.9)$$

Under faulty mode, inverter configuration can be either a four-phase converter or a three-phase converter. The cost function in (5.8) is modified to include only the fault free phase currents as:

$$\begin{aligned}\boldsymbol{g}_{4\boldsymbol{ph}}&=(\boldsymbol{i}_{\boldsymbol{b}}^{\boldsymbol{ref}}-\boldsymbol{i}_{\boldsymbol{b}}^{\boldsymbol{k}+2})^2+(\boldsymbol{i}_{\boldsymbol{c}}^{\boldsymbol{ref}}-\boldsymbol{i}_{\boldsymbol{c}}^{\boldsymbol{k}+2})^2+\\&(\boldsymbol{i}_{\boldsymbol{d}}^{\boldsymbol{ref}}-\boldsymbol{i}_{\boldsymbol{d}}^{\boldsymbol{k}+2})^2+(\boldsymbol{i}_{\boldsymbol{e}}^{\boldsymbol{ref}}-\boldsymbol{i}_{\boldsymbol{e}}^{\boldsymbol{k}+2})^2\end{aligned} \qquad (5.10)$$

$$\boldsymbol{g}_{3\boldsymbol{ph}}=(\boldsymbol{i}_{\boldsymbol{c}}^{\boldsymbol{ref}}-\boldsymbol{i}_{\boldsymbol{c}}^{\boldsymbol{k}+2})^2+(\boldsymbol{i}_{\boldsymbol{d}}^{\boldsymbol{ref}}-\boldsymbol{i}_{\boldsymbol{d}}^{\boldsymbol{k}+2})^2+(\boldsymbol{i}_{\boldsymbol{e}}^{\boldsymbol{ref}}-\boldsymbol{i}_{\boldsymbol{e}}^{\boldsymbol{k}+2})^2 \qquad (5.11)$$

where g_{4ph} and g_{3ph} are the cost function for a four-phase and a three-phase converter, respectively. It should be noted that the number of switching vectors is equal to 16 and 8, for a four-phase and a three-phase inverter, respectively. The all possible switching vectors of a five-phase inverter are shown in Fig. 5.2.

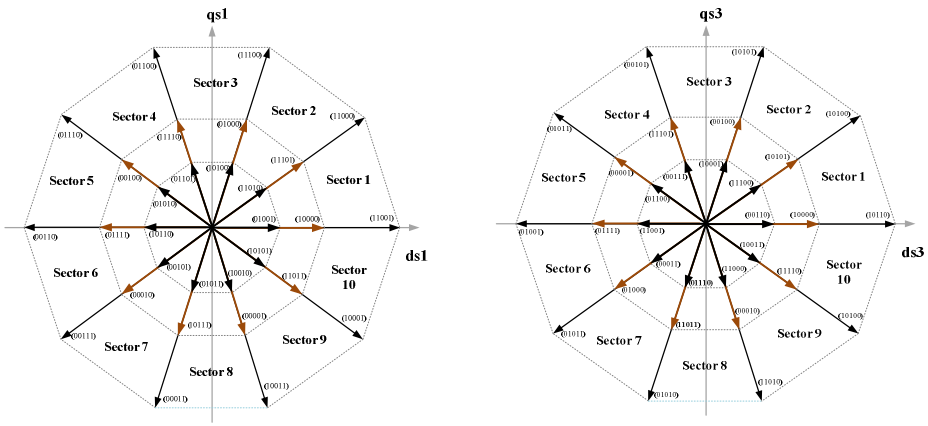

Fig. 5.2. switching vectors of the five-phase inverter

5.2.2. Fault Detection Method

In order to implement the fault-tolerant control algorithm of the multiphase drive, it is necessary to provide an FD unit. This unit detects the fault. After that, the control method is updated according to the faulty mode of the power converter, as it has been shown in Fig. 5.1. The theory of the developed open switch FD method is explained in the following.

In the case of an open switch fault in the power converter, the faulty switch cannot be turned on. So, the vectors including on-state of the faulty switch cannot be produced by the converter. As a result, the cost function value in FCS-MPC for these vectors will be as high as possible. This idea is used to propose a novel FD method in this thesis.

In order to diagnosis a fault, a simple fault alarm is proposed. For this purpose, the highest cost function and corresponding switching vector in each execution of the control algorithm is calculated. After that, using the later switching vector and the reference currents at the previous step, phase current under healthy operation mode of the motor is predicted at next switching period as:

$$\begin{bmatrix} i_{ap}^{ref}(k) \\ i_{bp}^{ref}(k) \\ i_{cp}^{ref}(k) \\ i_{dp}^{ref}(k) \end{bmatrix} = T_{samp} \times L^{-1} \times \left(\begin{bmatrix} v_{ab} - e_{ab} \\ v_{bc} - e_{bc} \\ v_{cd} - e_{cd} \\ v_{de} - e_{de} \end{bmatrix} - \begin{bmatrix} r_a & -r_b & 0 & 0 \\ 0 & r_b & -r_c & 0 \\ 0 & 0 & r_c & -r_d \\ r_e & r_e & r_e & r_d + r_e \end{bmatrix} \begin{bmatrix} i_a \\ i_b \\ i_c \\ i_d \end{bmatrix} \right) + \begin{bmatrix} i_a^*(k-1) \\ i_b^*(k-1) \\ i_c^*(k-1) \\ i_d^*(k-1) \end{bmatrix} \tag{5.12}$$

A reference cost function is defined as:

$$g_{5ph}^{ref} = (i_{ap}^{ref} - i_a^*)^2 + (i_b^{ref} - i_b^*) + (i_{cp}^{ref} - i_c^*) + (i_{dp}^{ref} - i_d^*) + (i_{ep}^{ref} - i_e^*) \tag{5.13}$$

Similarly, the reference cost function can be calculated under the faulty mode control of the motor drive. Under the healthy condition, the highest cost function is equal to the reference cost function. Under the faulty mode, the reference cost function still maintains a small tracking error, while the cost function value is increased significantly.

In order to produce the fault alarm, a simple detection index showing the fault alarm (FADI) is proposed in this thesis as:

$$FADI = \frac{\left| g_{5ph}^{ref} - g_{5ph} \right|}{g_{5ph}^{ref}} \tag{5.14}$$

It should be note that, the proposed normalization method of the cost function in (5.14) was deduced from the presented method in [6]; authors used this method to define a FD index from the motor phase currents.

The proposed FADI is equal to zero under the healthy mode; its value is increased to g_{5ph} value under the faulty mode. Therefore, a FADI higher than zero can be interpreted as a fault alarm.

The FADI is compared to a threshold value. If its value is higher than the threshold value, a fault alarm is produced.

$$\boldsymbol{Fault\ Alarm} = \begin{cases} \boldsymbol{Fault} & \boldsymbol{FADI > th} \\ \boldsymbol{Healthy} & \boldsymbol{FADI < th} \end{cases} \qquad (5.15)$$

where *th* denotes the threshold value; the theoretical value of the *th* is equal to zero.

Alarm signal is used to enable the fault localization block. In the second step, after fault detection, the fault localization block is evaluated to locate the faulty switch. The proposed fault localization method is explained in the following part.

Fault Localization Method:

A simple fault localization method is described as follows. This method can detect multiple single switch and open phase faults. Since the reference currents in a FCS-MPC are always available, taking into account this advantage, an FD index is proposed as follows:

$$\boldsymbol{D_j} = \left| \frac{\boldsymbol{i_j}}{\max(|\boldsymbol{i_j}|, |\boldsymbol{i_j^*}|)} \right| , \quad \boldsymbol{j = a,b,c,d,e} \qquad (5.16)$$

where *D* is the FD index, *i* and *i** are the real and reference currents in each phase of the power converter, respectively. The FD index is equal to 1 under healthy mode, while it is reduced to zero under faulty mode. Due to the normalization, it is not sensitive to transients. It is possible to detect both open switch and open phase faults using (5.16). In order to improve the robustness of the FD method against the noise and transients, FD is done after a time delay.

A high performance FD method should localize the faulty components. Considering a leg of the power converter, fault type can be either upper switch fault, or lower switch fault or open phase fault. When there is a fault in a switch in one leg of the converter, current will be zero for half of one period. It means that real current is zero while reference current is nonzero. Therefore, the faulty component can be localized simply from sign of the reference current as:

$$\boldsymbol{Sign(i^*)} = \begin{cases} + & \boldsymbol{lower\ switch\ fault} \\ - & \boldsymbol{upper\ switch\ fault} \end{cases} \qquad (5.17)$$

Using (5.17), it is possible to localize both upper switch and lower switch faults. Under the open phase fault, *D* value is zero. To localize this fault, average value of *D* is measured during one

fundamental cycle after FD. If the resultant value is zero, then the fault type is an open phase fault. This index is defined as:

$$D_1 = \frac{1}{T}\int_0^T D dt \qquad (5.18)$$

It should be noted that the fault localization in case of a single switch fault is done one sample after FD, while open phase fault is localized about one fundamental cycle after FD. The block diagrams of the fault-tolerant control and FD method are shown in Fig. 5.3.

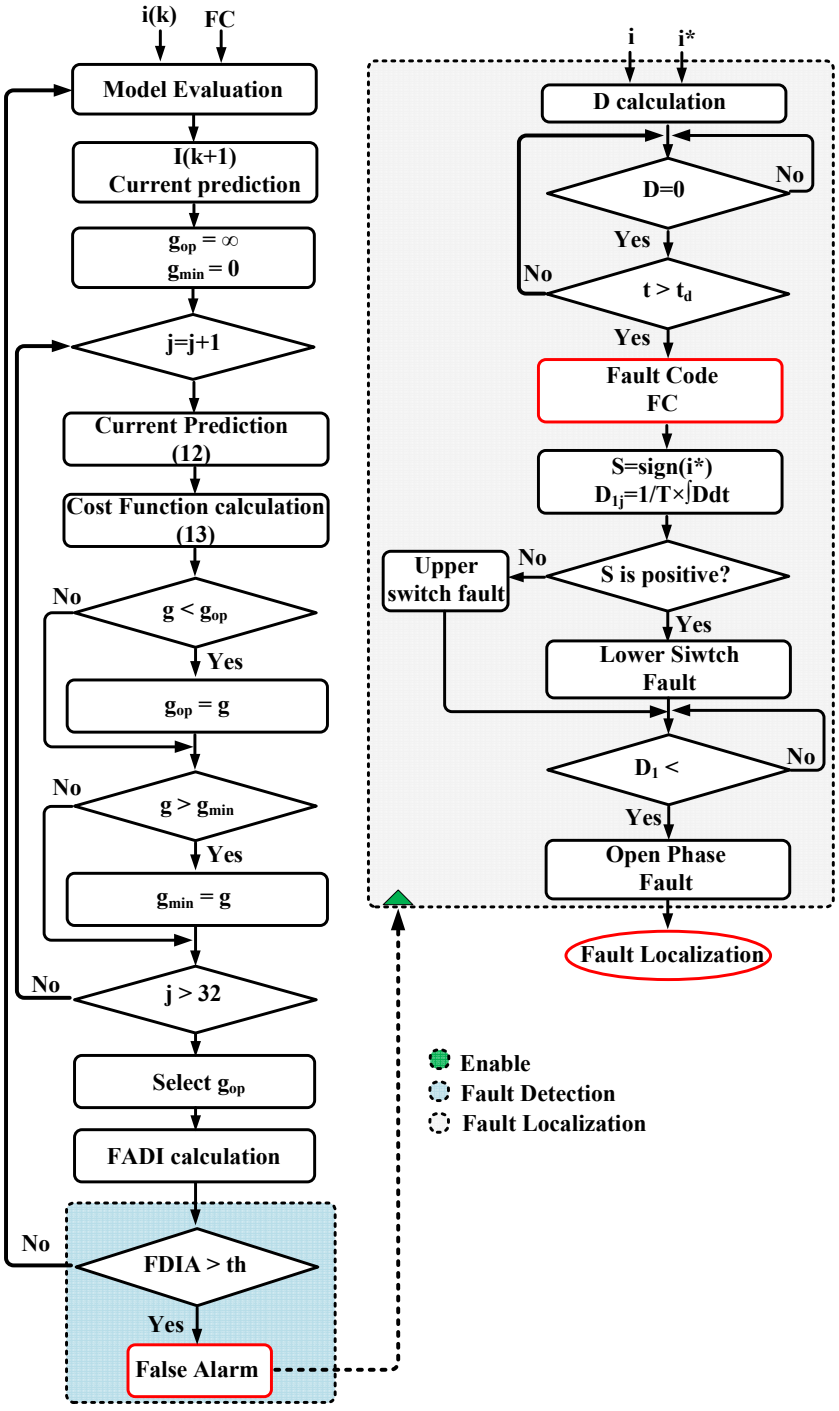

Fig. 5.3. Modulation strategy, FD and localization algorithm

As it can be seen, at each sampling time, a cost function is evaluated to determine the fault alarm. If the fault alarm is activated, then the faulty component is determined by the fault localization block. This block generate a fault operation code (i.e. FC); besides faulty components are localized. The FC is used to update the fault-tolerant control, modulation strategy, and cost minimization block. At the same time, the faulty leg is isolated by removing the gate signal for the remaining healthy switches.

5.3. Simulation results

In order to validate the effectiveness of the proposed FD and fault-tolerant control method, a fault-tolerant control algorithm of a five-phase BLDC motor drive has been simulated with the proposed method. It should be noted that this motor can continuously work in case of one faulty phase, two adjacent faulty phases and two nonadjacent faulty phases. Therefore, two cases studies are considered for simulation including the healthy operational mode and faulty mode control.

In the first step, detection performance of the FD method under load transients is evaluated. The cost function is denoted by C_f. Besides, phases of the VSI are denoted by indexes *a*, *b*, *c*, *d*, and *e*, respectively. Two step transients are applied to the load current at times 0.16 s and 0.32 s, respectively. The simulated results for this case are shown in Fig. 5.4(a); as it can be seen, FADI is always close to zero. However, in the transient, its amplitude is higher than the threshold value during a very short time. As it can be seen, FD method is robust to this transient, since the fault is detected after a short delay.

A single switch open circuit fault in phase *a* and an open phase fault in phase *b* are forced on the inverter at time 0.2 s. Results of this case are shown in Fig. 5.4(b). As seen, the cost function increases after the fault. The *D* index is also reduced to zero value after the fault. According to the results presented in Fig. 5.4(b), an open switch fault in both phases is detected and localized in less than a quarter of one cycle. However, the open phase fault is localized after one fundamental cycle.

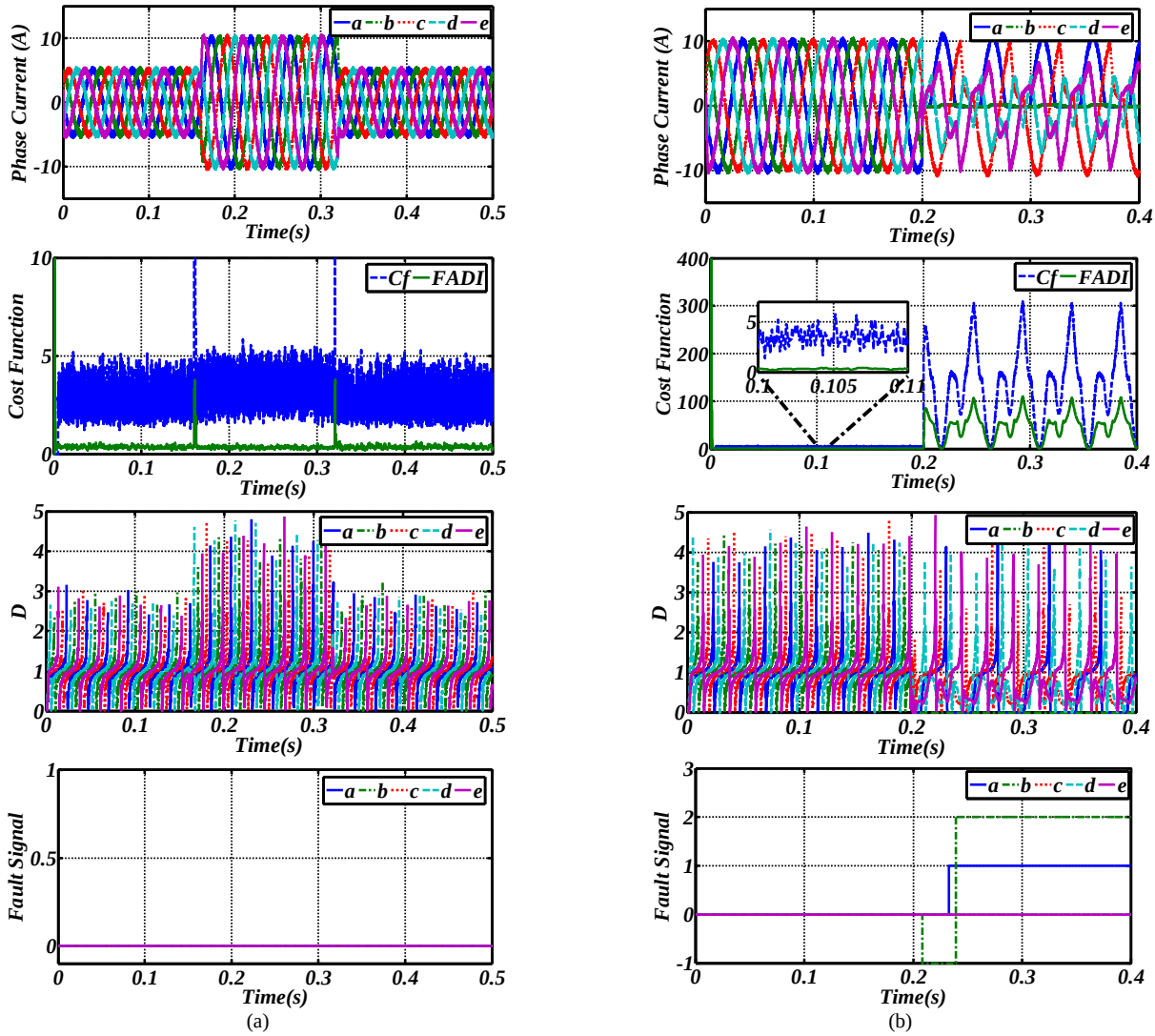

Fig. 5.4. Performance evaluation of FD method (a) under load transients (b) under open switch FD

5.4. Experimental results

To validate the presented theory, experimental results are carried out on a five-phase BLDC motor drive. The results are presented in two parts. In the first one, different fault types are forced in the inverter. The performance of the FD block is evaluated under different faulty modes. Then, the motor is controlled with the developed fault-tolerant algorithm.

Performance Evaluation of the Control Algorithm with FD Block:

To validate the simulation results, experimental results are presented to show the effectiveness of the developed FD block. A high performance FD method should be robust to the load transients. To evaluate this case, motor was operated under healthy mode. Two current steps were imposed on the load current. Experimental results of this case are shown in Fig. 5.5(a); as it can be seen, FD block is robust to the transients. Moreover, the cost function is consistently the same during the transients.

In the second step, an open switch fault is forced in the phase *a* of the power converter. Results of this case are displayed in Fig. 5.5(b); as it can be seen, the fault is detected and localized during less than a quarter of one cycle.

In the third step, an open phase fault is considered in phase *a*. Corresponding experimental waveforms are shown in Fig. 5.5(c). As it can be seen, the fault is detected successfully. In comparison to the single switch fault, the cost function value is more distorted after the fault.

Since a five-phase BLDC motor can be operated with two faulty phases, the FD block should be even able to detect the fault under faulty mode. Therefore, the motor was operated with the control algorithm under one faulty phase mode. An open switch fault was forced in phase *b*. The experimental results under this mode are shown in Fig. 5.5(d). As it can be seen, the fault is detected and localized successfully.

In order to validate the effectiveness of the proposed system in this thesis against fault alarms, two case studies are considered. In the first one, a single switch fault is forced in phase *a* of the inverter. The result of this case is shown in Fig. 5.5(e); as it can be seen, after fault, FADI is higher than zero. Besides, it can be seen that the fault signal is produced during less than a quarter of one period. Similarly, the experimental results are done in presence of an open phase fault in phase *a*. As it can be seen from Fig. 5.5(f), the fault alarm is successfully generated following the open phase fault.

Due to the limited number of oscilloscope channels, here experimental results for different case studies are repeated. The effect of the faulty mode control on the remaining healthy phases of the motor is presented in Fig. 5.6. As it can be seen from Fig. 5.6(b), after open switch fault in phase *a*, a distortion and DC value appear in the remaining healthy phases. In case of simultaneous single switch and open phase faults shown in Fig. 5.6(c), the cost function value is even higher. At the same time poor

tracking performance of the reference current can be observed in the healthy phase currents. Finally, the results of the faulty mode control as shown in Fig. 5.6(d) have the lowest performance among other cases.

According to the presented experimental results, fault is detected in all phases. Besides, the FD index is robust to the transients. Performance of the control method is also reduced under faulty mode; this requires fast FD and isolation. So, secondary effects due to the faulty mode control can be avoided. In the following section, the fault-tolerant control algorithm with embedded FD unit is used to maintain the continuous operation of the motor drive under faulty mode.

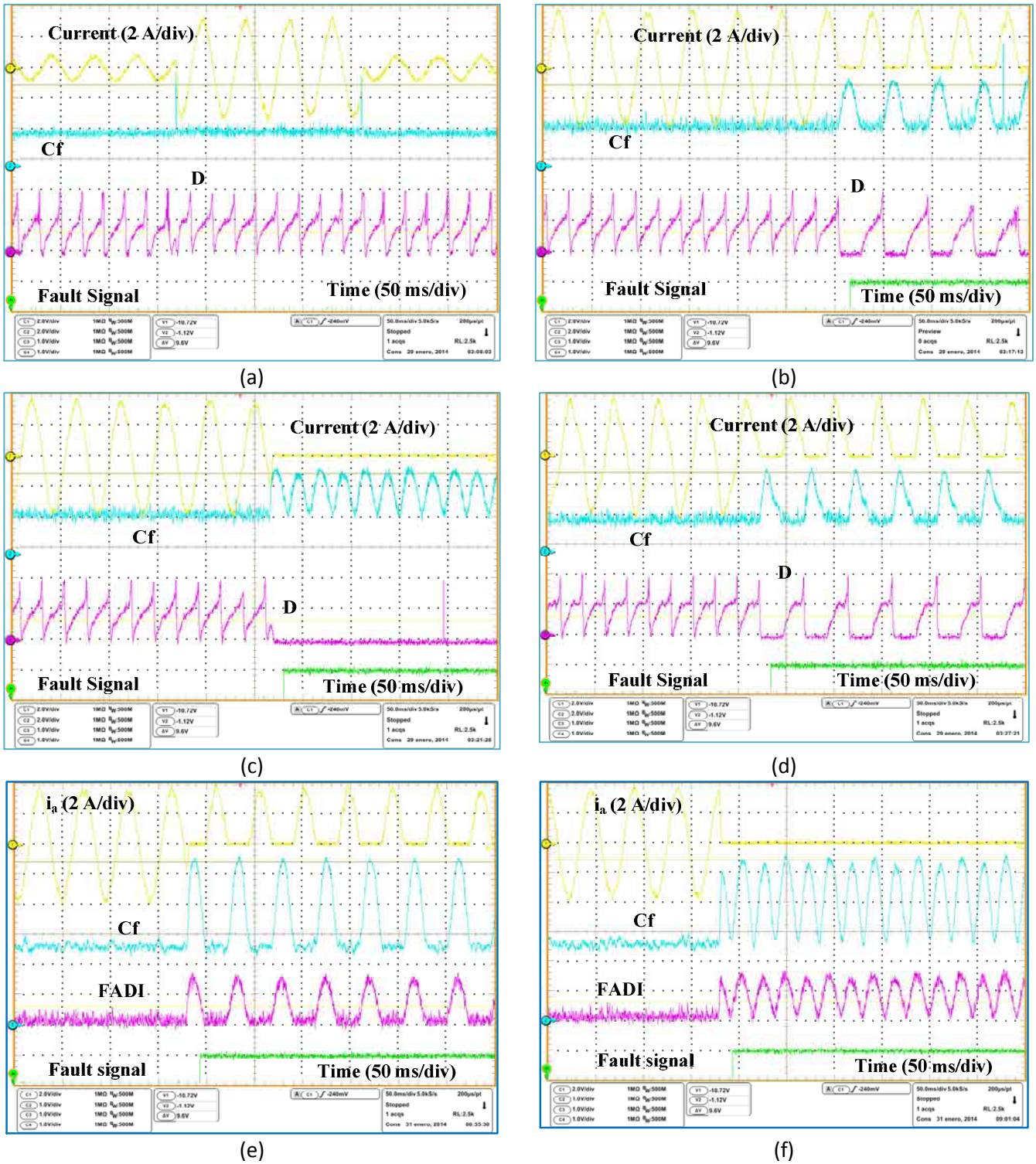

Fig. 5.5. Experimental results of the FD block (a) under load transients. (b) under open switch FD. (c) under open phase fault (d) under faulty mode. (e) FADI under single switch fault. (f) FADI under open phase fault.

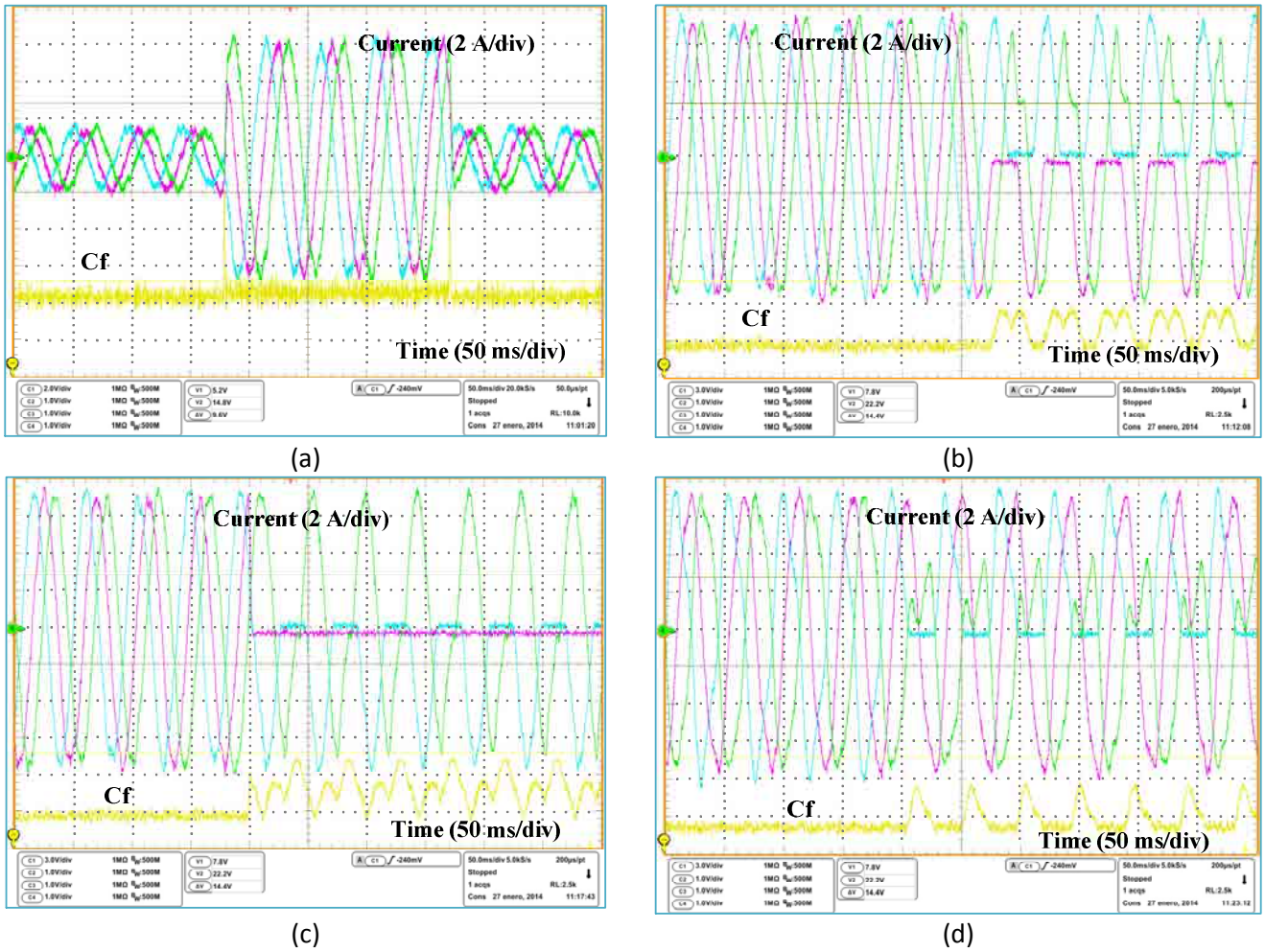

Fig. 5.6. Performance evaluation of FCS-MPC (a) under load transients. (b) Open switch FD. (c) Under open phase faulty. (d) Under faulty mode control.

Fault-Tolerant Operation of the Five-Phase BLDC Motor Drive:

The developed FD block is included in the fault-tolerant control algorithm of a five-phase BLDC motor. The presented FCS-MPC is used to control the motor. In the first experiment, the motor is operated under healthy mode. After that, a new fault is forced in phase *a* of the power converter. This fault is detected during less than a quarter of one cycle. The corresponding fault code in this case is equal to 2. After nine cycles, a new fault is forced in phase *c*. The corresponding fault code in this case is equal to 4. The experimental results of this case are shown in Fig. 5.7. As it can be seen, in both cases, the fault is detected successfully. Moreover, under each faulty mode, the control algorithm is updated with the corresponding control method. The cost function during the faulty mode is increased beyond the threshold value. At steady state, its value under one faulty phase mode is less than the healthy mode. Also, C_f value under two-faulty phase control mode is less than under one faulty phase control mode.

According to the presented experimental results, the motor was operated successfully under different faulty modes. Therefore, the developed FCS-MPC and FD method can present a high performance for a fault-tolerant control application.

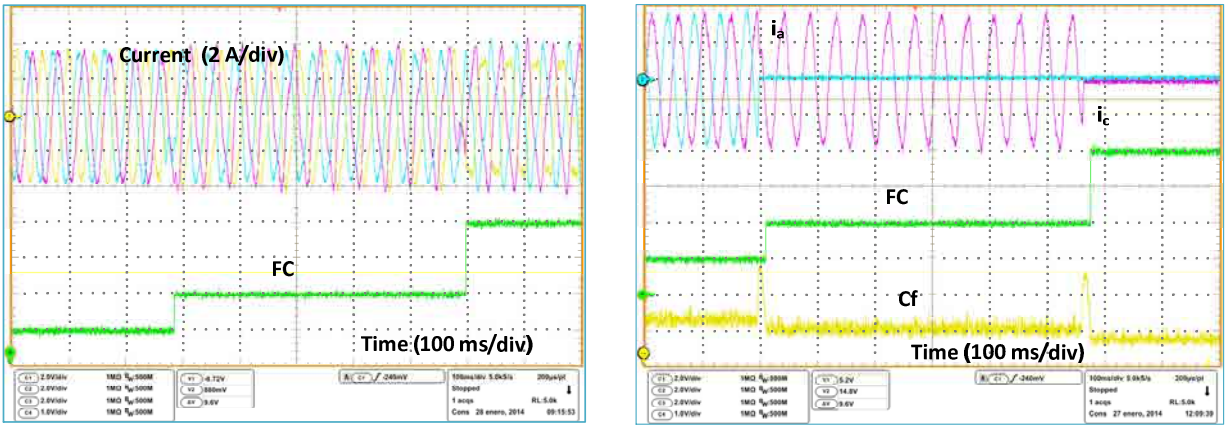

(a) (b)

Fig. 5.7. Experimental results of the fault-tolerant control under two non-adjacent faulty phases (a) healthy current waveforms and fault code (b) faulty current waveforms, fault code, and cost function.

5.5. Discussion and conclusions

A fault-tolerant FCS-MPC of a five-phase BLDC motor was developed in this chapter. It was shown that due to its flexibility, FCS-MPC can be easily implemented under both healthy and faulty operational mode of the machine. Moreover it is possible to simply include the different constraints on the control algorithm. A simple modulation method was developed to control the power converter.

Furthermore, a new open transistor FD method for VSIs was proposed. Based on this method, a cost function value, which is the output of the modulation scheme in the FCS-MPC, is used to detect the faults. Then, a simple method was presented to locate the faulty switch. Advantages of the presented idea in comparison to the methods in literature are less computational cost, flexibility, and simplicity. This method is considered as a signal based FD method.

Effectiveness of the proposed FD technique was demonstrated through simulation results. Moreover, the FD algorithm was effectively embedded in a fault-tolerant control algorithm for a five-phase BLDC motor drive. Experimental results on a five-phase BLDC motor drive validated the developed theory. According to the presented approach, it is possible to realize real time continuous operation of the motor drive under healthy and faulty mode.

6.

General Conclusions and Future Work

The main contributions of this dissertation, as well as the conclusions and future work, are presented in this chapter.

CONTENTS:

6.1. General conclusions

The aims and objectives, as well as the initial hypotheses, have determined the steps throughout this research work. The investigation and proposal of novel, effective and systematic fault detection methods and control algorithms – to maintain continuous operation of a multiphase motor drive – has been the general approach in this thesis.

A thoroughly review was conducted on open switch fault detection methods in literature. These methods can be considered in three different categories including signal based methods, model based methods and reference based methods. Almost all these methods investigate fault detection in a three phase systems, where a three phase load is supplied with balanced sinusoidal currents. The fault tolerant capability of these systems is often limited to a single switch or single phase faults. On the other side, multiphase systems are able to tolerate multiple types. Due to this, conventional fault detection methods - presented in literature - are less effective for application in multiphase systems.

Regarding the presented FD methods, the voltage based methods measuring the real voltage with extra sensors are able to detect open switch or short circuit faults so fast. However, implementations cost and complexity of these methods are high. As a result, FD methods which use available signals in the control algorithm are more interesting for industrial applications. Keeping in mind this feature, novel FD methods with low implementation cost and effort are investigated. The proposed methods are briefly addressed in the following section.

Observer based open switch fault detection

It is possible to predict the motor drive signals using standard observers. This technique can be either used for control purposed and fault detection. Considering both of these features, an observer based FD method was proposed. This method can be used simultaneously for condition monitoring of the motor. At the same time, the identified model of the motor can be used to adaptively design the PI controller. The results of this method were presented in chapter 3 of this dissertation.

Signal based open switch fault detection

As before mentioned, FD based on the current signal is a cost effective methods. Here the current signal in each phase of the motor drive is used to define a suitable FD index. Two contributions were presented in this section. According to the first method, phase angle in each phase of the motor was estimated using a simple trigonometric function. It was shown that this index is robust to load and speed variations in the motor drives. Therefore, it can effectively be used to detect the faulty condition.

Besides, an adaptive model identification approach was proposed. This method measures the harmonic components of the phase current at each time. Since under faulty mode, phase current is no longer a standard signal, the faulty phase current can be easily identified from a standard healthy current. Both presented methods can be individually done in each phase of the motor. As a result, these methods are general.

The implementation of conventional methods to realize fault-tolerant control in five phase converter was also discussed. Moreover, the SMC was developed to control the power converter under each operational mode. The results of these methods were presented in chapter 4 of this thesis.

Fault-tolerant control and fault diagnosis

Developing a high performance method for fault-tolerant control is of high paramount importance. Finite control set model predictive control is a newly well accepted method in industrial applications in order to control the motor drive. The main reasons are high flexibility, simple implementation, fast dynamic response, and remarkable progress in digital signal processors and power switching devices. Therefore, as the last contribution of this dissertation, this method was extended for application in a five-phase BLDC motor. It has been demonstrated that the information from this control method can be used to diagnose the faults in the power converter. The main advantage of the introduced fault detection method is less computation cost. Therefore, more calculation is not necessary to extract a fault detection index. The results of this method were presented in chapter 5 of this thesis.

All presented fault detection methods and control algorithms in this dissertation are robust to load and speed transients in a variable speed drive applicable for electric or hybrid electric vehicles. Due to avoid extra sensors, these methods are also cost effective. Furthermore, the proposed methods are flexible and can be used in any 2-level multiphase power converter. At the same time, simultaneous faults can be detected using these methods; this feature is very important in multiphase machines. According to presented simulation and experimental results, it was possible to maintain continuous operation of the motor drive due to fast fault detection capability of the proposed methods. The minimum fault detection in all cases was around one quarter of a fundamental cycle. The fault localization in case of single switch faults in all samples was done one sample after fault detection. On the other side, it takes around one fundamental cycle to localize the open phase faults.

6.2. Future work

During the development of this research work, although the defined aims and objectives have been covered, some points have been detected that could be further investigated to increase the progress and advances in the field.

Fault diagnosis considering faults in current sensor, power converter, speed sensor and motor windings

The focus of this thesis is mainly on open switch fault diagnosis in power converters. However, a traction motor drive can be subjected to other faults in measurement sensors, such as speed and current sensors or in the motor windings. In case of a fault in the current sensor, signal based open switch fault detection methods fail to distinguish such fault from open switch fault. Besides, in this specific case, the sensorless method can be used to maintain continuous operation of the motor drive without fault isolation. The same robustness of FD methods can be considered in case of a fault in the speed sensor or motor windings.

Fault diagnosis in other topologies of fault-tolerant power converters applicable in multiphase motor drives such as matrix converter, high frequency AC-link converters, multi-level multi-phase converters

There are some power converter topologies with high fault-tolerant capability and reliability being able to supply the multiphase machines. The different topologies of matrix converters, multilevel multiphase converters, and high frequency AC-link converters are the most important topologies among others. Due to harsh environment and limited space in automotive industry, these converters feature specific characteristics for motor drive application. In case of fault in the power converter, it is necessary to locate the faulty component exactly in order to reconfigure the system. The difference with two level converters is the complexity of configuration. Here, due to higher fault tolerant capability, even more level of reliability can be achieved.

Develop a condition monitoring systems to detect fault in the power converter

In an industrial application such as automotive industry, in order to meet the safety requirements set by ISO26262 standard, different fault types should be considered in the traction drive. Due to different possible fault types and detection methods, it is of paramount importance to develop an optimized algorithm for fault detection, isolation and fault tolerant control algorithm. The condition

monitoring system should consider all fault signals at the same time. A successful system can contribute to higher safety levels and reduced maintenance costs of the vehicle.

Open circuit fault diagnosis based on field data and thermal model of the power switch

Field data of the power switch can be directly used to detect the different fault types at the same time. Open switch fault due to wire bond lift up or rapture can be detected or even in advance predicted by evaluating the thermal data of the power switch. Due to variable operational condition of the motor and high noise level, the fault detection method should be robust to the presence of false alarms. At the same time, implementation should be done with minimum extra cost and hardware. Developing suitable models to distinguish healthy mode from faulty mode is very important.

Open circuit fault diagnosis able to detect and distinguish combination of open switch and short circuit fault

This thesis has only focused on permanent open switch fault detection methods in power converters. However, the fault can also be a permanent short circuit fault. There are three important research topics in this case: developing software based methods to diagnosis the short circuit fault, isolation and reconfiguration strategy of the fault in the power converter by minimum cost and simple circuit breakers such as back to back connected TRIAC, and study of FD methods able to distinguish open switch and short circuit faults. The last feature is important in order to set the isolation strategy of the faulty components.

7.

Thesis Results Dissemination

The direct contributions resulting from this Thesis work, in international journals as wells as in specialized conferences, are collected in this Chapter. Additionally, the contributions in research projects related with the Thesis topic are also briefly exposed.

CONTENTS:

7.1. Publications

Publications directly related with the thesis contributions

Journals

M. Salehifar, R. S. Arashloo, J. M. Moreno, V. Sala, L. Romeral, "Fault Detection and Fault Tolerant Operation of a Five Phase PM Motor Drive Using Adaptive Model Identification Approach", IEEE Journal of Emerging and Selected Topics on Power Electronics, vol. 2, no. 2, pp. 212-223, Jun. 2014.

M. Salehifar, J. M. Moreno, R. S. Arashloo, V. Sala, L. Romeral, "Observer Based Open Transistor Fault Diagnosis and Fault-Tolerant Control of Five-Phase PM Motor Drive for Application in Electric Vehicles", A major revision has been submitted to IET Power Electronics Journal.

M. Salehifar, J. M. Moreno, V. Sala, "Fault Diagnosis and Fault Tolerant Finite Control Set Model Predictive Control of a Multiphase Voltage Source Inverter Supplying PM Motor", Submitted to ISA Transaction - Elsevier.

M. Salehifar, J. M. Moreno, R. S. Arashloo, V. Sala, "FPGA Based Robust Open Transistor Fault Diagnosis and Fault Tolerant Sliding Mode Control of a Five-Phase PM Motor Drive", A major revision has been submitted to Journal of Power Electronic (JPE) - South Korea.

M. Salehifar, J. M. Moreno, V. Sala, "Simplified Fault Tolerant Finite Control Set Model Predictive Control of Five-Phase Voltage Source Inverter", preparing for submission to IEEE Transactions on Power Electronics.

Conferences

M. Salehifar, R. S. Arashloo, J. M. Moreno, V. Sala, L. Romeral, "Fault Tolerant Operation of a Five Phase Converter for PMSM Drives", Applied Power Electronics Conference and Exposition (APEC), IEEE, 2013, USA.

M. Salehifar, R. S. Arashloo, J. M. Moreno, V. Sala, "Open Circuit Fault Detection Based on Emerging FCS-MPC in Power Electronics Systems", Power Electronics and Applications European Conference on (EPE-ECCE), 2013, France.

M. Salehifar, J. M. Moreno, V. Sala, R. S. Arashloo, "Fault Detection in Multi-Phase Two Level Inverters Using Caushy Distribution of Normalized Phase Currents", Industrial electronics Society, 39th annual Conference of IEEE (IECON), 2013, France.

M. Salehifar, R. S. Arashloo, J. M. Moreno, V. Sala, L. Romeral, “A Simple and Robust Method for Open Switch Fault detection in Power Converters”, Diagnosic for Electrical Machines, Power Electronics and Drives (SDEMPED), IEEE, 2013, Spain.

M. Salehifar, J. M. Moreno, V. Sala, R. S. Arashloo, L. Romeral, “Improved Open Switch Fault Detection Based on Normalized Current Analysis in Multiphase Fault Tolerant Converters”, Diagnosic for Electrical Machines, Power Electronics and Drives (SDEMPED), IEEE, 2013, Spain.

Publication resulting from additional collaborations related with the thesis work

Journals

R. Salehi Arashloo, L. Romeral, **M. Salehifar**, J. M. Moreno, "Genetic Algorithm Based Output Power Optimization of Fault Tolerant Five-Phase BLDC Drives Applicable for Electrical and Hybrid Electrical Vehicles", IET journal of Electric Power Application (EPA), to be published.

R. Salehi Arashloo, **M. Salehifar**, H. Saavedra, L. Romeral, "Efficiency Evaluation of Five-Phase Outer-Rotor Fault-Tolerant BLDC Drives under Healthy and Open-Circuit Faulty Conditions", AECE journal – Advances in electrical and Computer Engineering, vol. 14, no. 2, pp. 145-152, May. 2014.

R. Salehi Arashloo, L. Romeral, **M. Salehifar**, V. Sala, "Impact of Neutral Point Current Control on Copper Loss Distribution of Five Phase PM Generators Used in Wind Power Plants", AECE journal – Advances in electrical and Computer Engineering, vol. 14, no. 2, pp. 89-96, May. 2014.

R. Salehi Arashloo, **M. Salehifar**, L. Romeral, V. Sala, "A Robust Predictive Deadbeat Current Control for Five-Phase BLDC Drives under Healthy and Open-Circuit Faulty Conditions ", Submitted to IET journal of Electric Power Application (EPA).

Conferences

M. Salehifar, J. M. Moreno, V. Sala, L. Romeral, “A Novel AC-AC Converter Based SiC For Domestic Induction Cooking applications”, *Applied Power Electronics Conference and Exposition (APEC)*, IEEE, 2013, USA.

R. S. Arashloo, **M. Salehifar**, L. Romeral, V. Sala, “Ripple Free Fault Tolerant Control of Five Phase Permanent Magnet Machines”, *Power electronics and Applications European Conference on (EPE-ECCE)*, IEEE, 2013, France.

R. S. Arashloo, **M. Salehifar**, L. Romeral, V. Sala, “Fault Tolerant Model Predictive Control of Five Phase Permanent Magnet Motors”, *Industrial electronics Society, 39th annual Conference of IEEE (IECON)*, 2013, Austria.

R. S. Arashloo, **M. Salehifar**, L. Romeral, "On the Effect of the Accessible Neutral Point in Fault Tolerant Five Phase PMSM Drives", *Industrial electronics Society, 39th annual Conference of IEEE (IECON)*, 2012, Canada.

R. S. Arashloo, L. Romeral, **M. Salehifar**, "A Novel Broken Rotor Bar Fault Detection Method Using Park's Transform and Wavelet Decomposition", *Diagnosic for Electrical Machines, Power Electronics and Drives (SDEMPED)*, IEEE, 2013, Spain.

R. S. Arashloo, L. Romeral, **M. Salehifar**, J. M. Moreno, "Model Predictive Current Control of Five Phase Permanent Magnet Motor", *Power electronics and Applications European Conference on (EPE-ECCE)*, IEEE, 2013, France.

Patent

M. Salehifar et al. A patent is under review.

7.2. Collaboration in technologic transfer projects

European projects

Project Title: Design and Implementation of Power Supply for Barrier Electric Discharge (DBD) Excimer Lamp.

Founding entity: Fraunhofer IGB, Stuttgart, Germany.

Partners: UPC

Duration: from 01/9/2013 to present

Tasks description: Simulation, Design and Implementation of the Power Supply.

National projects

Project Title: Research on Induction Heating by Resonant Power Converters for Application in Wooden Machinery.

Founding entity: Ministerio de Educación y Ciencia, Proyecto CENIT.
Education and Science Ministry, CENIT project.

Partners: UPC, CTM.

Duration: from 01/9/2011 to 01/02/2014

Tasks description: Simulation, Design and Implementation of the Resonant Power Converter and Magnetic Coils.

References

[1] H. Wang, M. Liserre, and F. Blaabjerg, "Toward Reliable Power Electronics," *IEEE Ind. Electron. Mag.*, vol. 7, no. 2, pp. 17-26, Jun. 2013.

[2] www.turbo.fr

[3] Wenping Zhang, Dehong Xu, Prasad N. Enjeti, Haijin Li, Joshua T. Hawke, and Harish S. Krishnamoorthy, "Survey on Fault-Tolerant Techniques for Power Electronic Converters," *IEEE Trans. Power electron*., 2014, to be published.

[4] H. Guzman, M. J. Duran, F. Barrero, B. Bogado, and S. Toral, "Speed Control of Five-Phase Induction Motors With Integrated Open-Phase Fault Operation Using Model-Based Predictive Current Control Techniques," *IEEE Trans. Ind. Electron.*, vol. 61, no. 9, pp. 4474-4484, Sep. 2014.

[5] Yantao Song and Bingsen Wang, "Survey on Reliability of Power Electronic Systems," *IEEE Trans. Power Electron.*, vol. 28, no. 1, pp. 591-604, Jan. 2013.

[6] Shaoyong Yang, Angus Bryant, Philip Mawby, Dawei Xiang, Li Ran, and Peter Tavner, "An Industry-Based Survey of Reliability in Power Electronic Converters," *IEEE Trans. Ind. Appl.*, vol. 47, no. 3, pp. 1441-1451, Jun. 2011.

[7] B. Lu and S. Sharma, "A literature review of IGBT fault diagnostic and protection methods for power inverters," *IEEE Trans. Ind. Appl.*, vol. 45, no. 5, pp. 1770–1777, Oct. 2009.

[8] Huai Wang, Marco Liserre, Frede Blaabjerg, Peter de Place Rimmen, John B. Jacobsen, Thorkild Kvisgaard, and Jørn Landkildehus, "Transitioning to Physics-of-Failure as a Reliability Driver in Power Electronics," *IEEE Journal OF Emerging and Selected Topics in Power Electron.*, vol. 2, no. 1, pp. 97-114, Mar. 2014.

[9] Wojciech Sleszynski, Janusz Nieznanski, and Artur Cichowski, "Open-Transistor Fault Diagnostics in Voltage-Source Inverters by Analyzing the Load Currents," *IEEE Trans. Ind. Electron.*, vol. 56, no. 11, pp. 4681–4688, Nov. 2009.

[10] Min-Sub Kim; Byoung-Gun Park; Rae-Young Kim; Dong-Seok Hyun, "A Novel Fault Detection Circuit for Short-circuit Faults of IGBT," *Applied Power Electronics Conference and Exposition (APEC), 2011 Twenty-Sixth Annual IEEE*, pp: 359 – 363, 2011.

[11] M. A. Rodriguez-Blanco, A. Claudio-Sanchez, D. Theilliol, L. G. Vela Valdes, P. Sibaja-Teran, L. Hernandez-Gonzalez, J. Aguayo "A failure-detection strategy for IGBT based on gate voltage behavior applied to a motor drive system," *IEEE Trans. on Ind. Electrons*, vol. 58, no. 5, pp. 1625-1633, May 2011.

[12] F. Blaabjerg, J. K. Pedersen, U. Jaeger, and P. Thoegersen, "Single current sensor technique in the DC link of three-phase PWM-VS inverters: A review and a novel solution," *IEEE Trans. Ind. Appl.*, vol. 33, no. 5, pp. 1241–1253, Oct. 1997.

[13] F. Huang and F. Flett, "IGBT fault protection based on di/dt feedback control," in *Proc. IEEE Power Electron. Spec. Conf.*, 2007, pp. 1478–1484.

[14] A. M. S. Mendes and A. J. Marques Cardoso, "Voltage source inverter fault diagnosis in variable speed ac

drives, by the average current Park's vector approach," in *Proc. IEMDC*, 1999, pp. 704–706.

[15] F. Richardeau, P. Baudesson, and T. A. Meynard, "Failures-tolerance and remedial strategies of a PWM multicell inverter," *IEEE Trans. Power Electron.*, vol. 17, no. 6, pp. 905–912, Nov. 2002.

[16] Kazufumi Yuasa, Soh Nakamichi and Ichiro Omura , "Ultra High Speed Short Circuit Protection for IGBT with Gate Charge Sensing," *Proceedings of The 22nd International Symposium on Power Semiconductor Devices & ICs, Hiroshima*.

[17] Takuya Tanimura, Kazufumi Yuasa and Ichiro Omura, "Full Digital Short Circuit Protection for Advanced IGBTs," *Proceedings of the 23rd International Symposium on Power Semiconductor Devices & IC's May 23-26, 2011 San Diego, CA*.

[18] K. S. Smith, L. Ran and J. Penman, "Real-time detection of intermittent misfiring in a voltage-fed PWM inverter induction-motor drive", *IEEE Trans. Ind. Electron.*, vol. 44, no. 4, pp. 468-476, Aug. 1997.

[19] D. U. Campos-Delgado and D. R. Espinoza-Trejo, "An observer-based diagnosis scheme for single and simultaneous open-switch faults in induction motor drives", *IEEE Trans. Ind. Electron.*, vol. 58, no. 2, pp. 671-679, Feb. 2011.

[20] D. R. Espinoza-Trejo, D. U. Campos-Delgado and A. Loredo-Flores, "A Novel Fault Diagnosis Scheme for FOC Induction Motor Drives by Using Variable Structure Observers", *Industrial Electronics (ISIE), 2010 IEEE International Symposium on* , pp. 2601-2606, 2010.

[21] M. A. Masrur, Z. Chen, B. Zhang, and Y. L. Murphey, "Model-based fault diagnosis in electric drive inverters using artificial neural network," *in Proc. IEEE Gen. Meeting Power Eng. Soc.*, 2007, pp. 1–7.

[22] Yi Lu Murphey, M. Abul Masrur, Zhi Hang Chen, and Baifang Zhang, "Model-Based Fault Diagnosis in Electric Drives Using Machine Learning," *IEEE/ASME Trans. Mechatronics*, vol. 11, no. 3, pp. 290 – 303, Jun. 2006.

[23] Shin-Myung Jung, Jin-Sik Park, Hag-Wone Kim, Kwan-Yuhl Cho, and Myung-Joong Youn, "An MRAS-Based Diagnosis of Open-Circuit Fault in PWM Voltage-Source Inverters for PM Synchronous Motor Drive Systems," *IEEE Trans. Power Electron.*, vol. 28, no. 5, pp. 2514-2526, May 2013.

[24] C. Kral and K. Kafka, "Power electronics monitoring for a controlled voltage source inverter drive with induction machines," *IEEE Power Electron. Specialists Conf.*, vol. 1, pp. 213-217, 2000.

[25] J. O. Estima and A. J. M. Cardoso, "A New Algorithm for Real-Time Multiple Open-Circuit Fault Diagnosis in Voltage-Fed PWM Motor Drives by the Reference Current Errors," *IEEE Trans. Ind. Electron.*, vol. 60, no. 8, pp. 3496-3505, Aug. 2013.

[26] M. A. Rodriguez-Blanco, A. Claudio-Sanchez, D. Theilliol, L. G. Vela Valdes, P. Sibaja-Teran, L. Hernandez-Gonzalez, J. Aguayo "A failure-detection strategy for IGBT based on gate voltage behavior applied to a motor drive system", *IEEE Trans. Ind. Electron.*, vol. 58, no. 5, pp. 1625-1633, May 2011.

[27] Q.-T. An, L.-Z. Sun, K. Zhao and L. Sun, "Switching function model based fast-diagnostic method of open-switch faults in inverters without sensors", *IEEE Trans. Power Electron.*, vol. 26, no. 1, pp. 119-126, Jan. 2011.

[28] O. S. Yu, N. J. Park, D. S. Hyun, "A novel fault detection scheme for voltage fed PWM inverter," *in Proc. IEEE Ind. Electron. Conf.*, 2006, pp.2654-2659.

[29] M. Trabelsi, M. Boussak , P. Mestre, M. Gossa, "Pole Voltage Based-Approach for IGBTs Open-Circuit Fault

Detection and Diagnosis in PWM-VSI-Fed Induction Motor Drives," *Proceedings of the 2011 International Conference on Power Engineering, Energy and Electrical Drives* , 2011.

[30] R. L. A. Ribeiro, C. B. Jacobina, E. R. C. Silva, and A. M. N. Lima, "Fault detection of open-switch damage in voltage-fed PWM motor drive systems," *IEEE Trans. Power Electron.*, vol. 18, no. 2, pp. 587–593, Mar. 2003.

[31] S. Karimi, P. Poure, and S. Saadate, "Fast power switch failure detection for fault tolerant voltage source inverters using FPGA," *IET Power Electron.*, vol. 2, no. 4, pp. 346–354, Jul. 2009.

[32] S. Karimi, A. Gaillard, P. Poure, and S. Saadate, "FPGA-Based Real-Time Power Converter Failure Diagnosis for Wind Energy Conversion Systems," *IEEE Trans. Ind. Electron.*, vol. 55, no. 12, pp. 4299-4308, Dec. 2008.

[33] S. Karimi, P. Poure, S. Saadate, "FPGA-based fully digital fast power switch fault detection and compensation for three-phase shunt active filters," Electric Power Systems Research 78 (2008) 1933–1940.

[34] M. Shahbazi, P. Poure, S. Saadate, M. R. Zolghadri, "FPGA-based Fast Detection with Reduced Sensor Count for a Fault-Tolerant Three-Phase Converter ," *IEEE Trans. Ind. Inform.*, vol. 9, no. 3, pp. 1343-1350, Aug. 2012.

[35] R. L. A. Ribeiro, C. B. Jacobina, E. R. C. Silva, and A. M. N. Lima, "Fault detection of open-switch damage in voltage-fed PWM motor drive systems," *IEEE Trans. Power Electron.*, vol. 18, no. 2, pp. 587–593, Mar. 2003.

[36] Raphael Peuget, Stephane Courtine, and Jean-Pierre Rognon, "Fault Detection and Isolation on a PWM Inverter by Knowledge-Based Model," *IEEE Trans. Ind. Appl.*, Vol. 34, No. 6, pp. 1318-1326, Dec. 1998.

[37] K. Rothenhagen and F. W. Fuchs, "Performance of diagnosis methods for IGBT open circuit faults in three phase voltage source inverters for ac variable speed drives," *in Proc. Eur. Power Electron. Appl. Conf.*, 2005, pp. 1–10.

[38] M. Trabelsi, M. Boussak, and M. Gossa, "Multiple IGBTs open circuit faults diagnosis in voltage source inverter fed induction motor using modified slope method," *in Proc. XIX Int. Conf. Elect. Mach.*, Sep. 6–8, 2010, pp. 1–6.

[39] M. Aktas, V. Turkmenoglu, "Wavelet-based switching faults detection in direct torque control induction motor drives," *IET Sci. Meas. Technol.,* 2010, Vol. 4, Iss. 6, pp. 303–310.

[40] Jorge O. Estima and Antonio J. Marques Cardoso, "A New Approach for Real-Time Multiple Open-Circuit Fault Diagnosis in Voltage-Source Inverters," *IEEE Trans. Ind. Appl.*, vol. 47, no. 6, pp. 2487-2494, Dec. 2011.

[41] Jorge Nuno M. A. Freire, Jorge O. Estima, A. J. Marques Cardoso, "Multiple Open-Circuit Fault Diagnosis in Voltage-Fed PWM Motor Drives Using the Current Park's Vector Phase and the Currents Polarity," *Diagnostics for Electric Machines, Power Electronics & Drives (SDEMPED), 2011 IEEE International Symposium on*, pp: 397-404, 2011.

[42] Nuno M. A. Feire, J. O. Estima, and A. J. M. Cardoso, "Open-Circuit Fault Diagnosis in PMSG Drives for Wind Turbine Applications," *IEEE Trans. Ind. Electron.,* Vol. 60, No. 9, pp. 3957-3967, Sept. 2013.

[43] M. Shahbazi, E. Jamshidpour, P. Poure, S. Saadate, M. Zolghadri, "Open and Short-Circuit Switch Fault

Diagnosis for Non-Isolated DC-DC Converters Using Field Programmable Gate Array," *IEEE Trans. Ind. Electron.,* vol. 60, no. 9, pp. 4136-4146, Sept. 2013.

[44] Yantao Song and Bingsen Wang, "Survey on Reliability of Power Electronic Systems," *IEEE Trans. Power Electron.*, vol. 28, no. 1, pp. 591-604, Jan. 2013.

[45] A. Mohammadpour, S. Sadeghi, and L. Parsa, "A Generalized Fault-Tolerant Control Strategy for Five-Phase PM Motor Drives Considering Star, Pentagon, and Pentacle Connections of Stator Windings," *IEEE Trans. Ind. Electron.*, vol. 61, no. 1, pp. 63-74, Jan. 2014.

[46] M. Shahbazi, P. Poure, S. Saadate, M. R. Zolghadri, "FPGA-based Fast Detection with Reduced Sensor Count for a Fault-Tolerant Three-Phase Converter," *IEEE Trans. Ind. Informatics*, vol. 9, no. 3, pp. 1343-1350, Aug. 2013.

[47] C. Choi W. Lee, "Design and evaluation of voltage measurement-based sectoral diagnosis method for inverter open switch faults of permanent magnet synchronous motor drives," *IET Electr. Power Appl.*, 2012, Vol. 6, Iss. 8, pp. 526–532.

[48] F. Meinguet, P. Sandulescu, X. Kestelyn, and E. Semail, "A Method for Fault Detection and Isolation based on the Processing of Multiple Diagnostic Indices: Application to Inverter Faults in AC Drives," *IEEE Trans. Veh. Technol.*, vol. 62, no. 3, pp. 995 – 1009, Mar. 2013.

[49] D. Ulises Campos-Delgado, J. Angel Pecina-Sanchez, D. Rivelino Espinoza-Trejo, E. Roman Arce-Santana, "Diagnosis of open-switch faults in variable speed drives by stator current analysis and pattern recognition," *IET Electr. Power Appl.*, 2013, Vol. 7, Iss. 6, pp. 509–522.

[50] D. Rivelino Espinoza-Trejo, D. Ulises Campos-Delgado, G. Bossio, Ernesto Barcenas, J. Enrique Hernandez-Diez, L. Felipe Lugo-Cordero, "Fault diagnosis scheme for open-circuit faults in field-oriented control induction motor drives," *IET Power Electron.*, 2013, vol. 6, Iss. 5, pp. 869–877.

[51] D. R. Espinoza-Trejo, D. U. Campos-Delgado, E. Barcenas, F. J. Martinez-Lopez, "Robust fault diagnosis scheme for open-circuit faults in voltage source inverters feeding induction motors by using non-linear proportional-integral observers," *IET Power Electron.*, 2012, vol. 5, Iss. 7, pp. 1204–1216.

[52] D. U. Campos-Delgado, and D. R. Espinoza-Trejo, "An Observer- Based Diagnosis Scheme for Single and Simultaneous Open-Switch Faults in Induction Motor Drives," *IEEE Trans. Ind. Electron.*, vol. 58, no. 2, pp. 671-679, Feb. 2011.

[53] Nuno M. A. Freire, Jorge O. Estima, and A. J. Marques Cardoso, "A Voltage-Based Approach without Extra Hardware for Open-Circuit Fault Diagnosis in Closed-Loop PWM AC Regenerative Drives," *IEEE Trans. Ind. Electron.*, vol. 61, no. 9, pp. 4960-4970, Sep. 2014.

[54] Shuai Shao, Patrick W. Wheeler, Jon C. Clare, and Alan J. Watson, "Fault detection for Modular Multilevel Converters Based on Sliding Mode Observer," *IEEE Trans. Power Electron.*, vol. 28, no. 11, pp. 4867 - 4872, Nov. 2013.

[55] M. Villani, M. Tursini, G. Fabri, and L. Castellini, "High Reliability Permanent Magnet Brushless Motor Drive for Aircraft Application," *IEEE Trans. Ind. Electron.*, vol. 59, no. 5, pp. 2073-2081, May 2012.

[56] Taehyun Shim, Sehyun Chang, and Seok Lee, "Investigation of Sliding-Surface Design on the Performance of Sliding Mode Controller in Antilock Braking Systems," *IEEE Trans. Veh. Technol.*, vol. 57, no. 2, pp. 747-759, Mar. 2008.

[57] Zhaowei Qiao, Tingna Shi, Yindong Wang, Yan Yan, Changliang Xia, and Xiangning He, "New Sliding-Mode Observer for Position Sensorless Control of Permanent-Magnet Synchronous Motor," *IEEE Trans. Ind. Electron.*, vol. 60, no. 2, pp. 710-719, Feb. 2013.

[58] L. Zarri, M. Mengoni, Y. Gritli, A. Tani, F. Filippetti, G. Serra, and D. Casadei, "Detection and Localization of Stator Resistance Dissymmetry Based on Multiple Reference Frame Controllers in Multiphase Induction Motor Drives," *IEEE Trans. Ind. Electron.*, vol. 60, no. 8, pp. 3506-3518, Aug. 2013.

[59] Gianluca Gatto, Ignazio Marongiu, and Alessandro Serpi, "Discrete-Time Parameter Identification of a Surface-Mounted Permanent Magnet Synchronous Machine," *IEEE Trans. Ind. Electron.*, vol. 60, no. 11, pp. 4869-4880, Nov. 2013.

[60] Elhanan Elboher and Michael Werman, "Asymmetric Correlation: A Noise Robust Similarity Measure for Template Matching," *IEEE Trans. Imag. Process.*, vol. 22, no. 8, pp. 3062-3073, Aug. 2013.

[61] M. Salehifar, R. Salehi Arashloo, J. M. Moreno, V. Sala, L. Romeral, "Fault Detection and Fault Tolerant Operation of a Five Phase PM Motor Drive Using Adaptive Model Identification Approach," *IEEE Journal of Emerging and Selected Topics on Power Electronics*, vol. 2, no. 2, pp.212-223, Jun. 2014.

[62] L. Rodrigues Limongi, R. Bojoi, G. Griva, and A. Tenconi, "Comparing the Performance of Digital Signal Processor-Based Current Controllers for Three-Phase Active Power Filters," *IEEE Ind. Electron. Mag.*, 2009, Digital Object Identifier 10.1109/MIE.2009.931894

[63] Yaoqin Jia, Jiqian Zhao, and Xiaowei Fu, "Direct Grid Current Control of LCL-Filtered Grid-Connected Inverter Mitigating Grid Voltage Disturbance," *IEEE Trans. Power Electron.*, vol. 29, no. 3, pp. 1532-1541, Mar. 2014.

[64] A. G. Yepes, F. D. Freijedo, J. Doval-Gandoy, O. Lopez, J. Malvar, and P. Fernandez-Comesana, "Effects of Discretization Methods on the Performance of Resonant Controllers," *IEEE Trans. Power Electron.*, vol. 25, no. 7, pp. 1692-1712, Jul. 2010.

[65] Chenlei Bao, Xinbo Ruan, Xuehua Wang, , Weiwei Li, , Donghua Pan, and Kailei Weng, "Step-by-Step Controller Design for LCL-Type Grid-Connected Inverter with Capacitor–Current-Feedback Active-Damping," *IEEE Trans. Power Electron.*, vol. 29, no. 3, pp. 1239-1253, Mar. 2014.

[66] D. G. Holmes, T. A. Lipo, B. P. McGrath, and W. Y. Kong, "Optimized Design of Stationary Frame Three Phase AC Current Regulators," *IEEE Trans. Power Electron.*, vol. 24, no. 11, pp. 2417-2426, Nov. 2009.

[67] Yantao Song and Bingsen Wang, "Survey on Reliability of Power Electronic Systems," *IEEE Trans. Power Electron.*, vol. 28, no. 1, pp. 591-604, Jan. 2013.

[68] M. Villani, M. Tursini, G. Fabri, and L. Castellini, "High Reliability Permanent Magnet Brushless Motor Drive for Aircraft Application," *IEEE Trans. Ind. Electron.*, vol. 59, no. 5, pp. 591-604, May 2012.

[69] A. Mohammadpour, L. Parsa, "A Unified Fault-Tolerant Current Control Approach for Five-Phase PM Motors With Trapezoidal Back EMF Under Different Stator Winding Connections," *IEEE Trans. Power Electron.*, vol. 28, no. 7, pp. 3517 - 3527, Jul. 2013.

[70] L. Parsa and H. Toliyat, " Five-phase permanent-magnet motor drives," *IEEE Trans. Ind. Appl.*, vol. 41, no. 1, pp. 30-37, Jan. 2005.

[71] D. R. Espinoza-Trejo, D. U. Campos-Delgado, E. Barcenas, F.J. Martınez-Loipez, "Robust fault diagnosis

scheme for open-circuit faults in voltage source inverters feeding induction motors by using non-linear proportional-integral observers," *IET Power Electron.*, 2012, vol. 5, Iss. 7, pp. 1204–1216.

[72] M. Shahbazi, P. Poure, S. Saadate, M. R. Zolghadri, "FPGA-based Fast Detection with Reduced Sensor Count for a Fault-Tolerant Three-Phase Converter," *IEEE Trans. Ind. Informat.*, vol. 9, no. 3, pp. 1343-1350, Aug. 2013.

[73] Songsong Nie, Xuejun Pei, Yu Chen, and Yong Kang, "Fault Diagnosis of PWM DC-DC Converters Based on Magnetic Component Voltages Equation," *IEEE Trans. Power Electron.*, vol .29, no. 9, pp. 4978-4988, Sept. 2014.

[74] Pan Duan, Kai-gui Xie, Li Zhang, and Xianliang Rong, "Open-Switch Fault Diagnosis and System Reconfiguration of Doubly fed Wind Power Converter Used in a Microgrid," *IEEE Trans. Power Electron.*, vol. 26, no. 3, pp. 816-821, Mar. 2011.

[75] I. Sadinezhad and V. G. Agelidis, "Real-Time Power System Phasors and Harmonics Estimation Using a New Decoupled Recursive-Least-Squares Technique for DSP Implementation," *IEEE Trans. Ind. Electron.*, vol. 60, no. 6, pp. 2295-2308, Jun. 2013.

[76] Gaolin Wang, Tielian Li, Guoqiang Zhang, Xianguo Gui and Dianguo Xu, "Position Estimation Error Reduction Using Recursive-Least-Square Adaptive Filter for Model-Based Sensorless Interior Permanent Magnet Synchronous Motor Drives," *IEEE Trans. Ind. Electron.*, vol 61, no. 9, pp. 5115-5125, Sept. 2014.

[77] M. Beza, and M. Bongiorno, "Application of Recursive Least Square (RLS) Algorithm with Variable Forgetting Factor for Frequency Components Estimation in a Generic Input Signal," *IEEE Trans. Ind. Appl.*, to be published.

[78] M. Salehifar, R. Salehi Arashloo, M. Moreno-Eguilaz, V. Sala, L. Romeral, "Fault Tolerant Operation of a Five Phase Converter for PMSM Drives," *Applied Power Electronics Conference and Exposition (APEC), 2013 Twenty-Eighth Annual IEEE*, pp. 1177 – 1184, 2013.

[79] E. Levi, N. W. Satiawan, N. Bodo, and M. Jones, "A Space-Vector Modulation Scheme for Multilevel Open-End Winding Five-Phase Drives," *IEEE Trans. Energy Conv.*, vol. 27, no. 1, pp. 1-10, Mar. 2012.

[80] D. Dujic, G. Grandi, M. Jones, and E. Levi, "A Space Vector PWM Scheme for Multi frequency Output Voltage Generation With Multiphase Voltage-Source Inverters," *IEEE Trans. Ind. Electron.*, vol. 55, no. 5, pp. 1943-1955, May 2008.

[81] A. Iqbal, and S. Moinuddin, "Comprehensive Relationship Between Carrier-Based PWM and Space Vector PWM in a Five-Phase VSI," *IEEE Trans. Power Electron.*, vol. 24, no. 10, pp. 2379-2390, Oct. 2009.

[82] R. Salehi Arashloo, M. Salehifar, L. Romeral, V. Sala, "Ripple Free Fault Tolerant Control of Five Phase Permanent Magnet Machines," *15th European conference on Power Electronics and Applications (EPE) 2013*, pp. 1-5.

[83] A. Khalick Mohammad, N. Uchiyama, and S. Sano, "Reduction of Electrical Energy Consumed by Feed-Drive Systems Using Sliding-Mode Control With a Nonlinear Sliding Surface," *IEEE Trans. Ind. Electron.*, vol. 61, no. 6, pp. 2875-2882, Jun. 2014.

[84] T. Bernardes, V. F. Montagner, H. A. Gründling, and H. Pinheiro, "Discrete-Time Sliding Mode Observer for

Sensorless Vector Control of Permanent Magnet Synchronous Machine," *IEEE Trans. Ind. Electron.*, vol. 61, no. 4, pp. 1679-1691, Apr. 2014.

[85] X. Zhang, Lizhi Sun, Ke Zhao, and Li Sun, "Nonlinear Speed Control for PMSM System Using Sliding-Mode Control and Disturbance Compensation Techniques," *IEEE Trans. Power Electron.*, vol. 28, no. 3, pp. 1358-1365, Mar. 2013.

[86] J. R. Domınguez, A. Navarrete, M. Meza, A. Loukianov and J. Canedo, "Digital Sliding Mode Sensorless Control for Surface Mounted PMSM," *IEEE Trans. Ind. Inform.*, vol. 10, no. 1, pp. 137-151, Feb. 2014.

[87] O. Jimenez, O. Lucia, I. Urriza, L. A. Barragan, P. Mattavelli, and D. Boroyevich, "An FPGA-Based Gain-Scheduled Controller for Resonant Converters Applied to Induction Cooktops," *IEEE Trans. Power Electron.*, vol. 29, no. 4, pp. 2143-2152, Apr. 2014.

[88] A. Damiano, G. Gatto, I. Marongiu, A. Perfetto, and A. Serpi, "Operating Constraints Management of a Surface-Mounted PM Synchronous Machine by Means of an FPGA-Based Model Predictive Control Algorithm," *IEEE Trans. Ind. Inform.*, vol. 10, no. 1, pp. 243-255, Feb. 2014.

[89] J. Karttunen, S. Kallio, P. Peltoniemi, P. Silventoinen, and O. Pyrhonen, "Decoupled Vector Control Scheme for Dual Three-Phase Permanent Magnet Synchronous Machines," *IEEE Trans. Ind. Electron.*, vol. 61, no. 5, pp. 2185-2196, May. 2014.

[90] Talaeizadeh V, Kianinezhad R, Seyfossadat S G, Shayanfar H A. "Direct torque control of six-phase induction motors using three-phase matrix converter. Energy Conversion and Management; 51:2482-2491.

[91] Singh G K, Senthil Kumar A, Saini R P. Performance analysis of a simple shunt and series compensated six-phase self-excited induction generator for stand-alone renewable energy generation. Energy Conversion and Management; 52:1688-1699.

[92] Fatiha Mekri, Seifeddine Ben Elghali, and Mohamed El Hachemi Benbouzid, "Fault-Tolerant Control Performance Comparison of Three- and Five-Phase PMSG for Marine Current Turbine Applications," *IEEE Trans. Sustainable Energy*, vol. 4, no. 2, pp. 425-433, Apr. 2013.

[93] H. Seng Che, E. Levi, M. Jones, M. J. Duran, Wooi-Ping Hew, and Nasrudin Abd. Rahim, "Operation of a Six-Phase Induction Machine Using Series-Connected Machine-Side Converters," *IEEE Trans. Ind. Electron.*, vol. 61, no. 1, pp. 164-176, Jan. 2014.

[94] Ayman S. Abdel-Khalik, Ahmed S. Morsy, Shehab Ahmed, and Ahmed M. Massoud, "Effect of Stator Winding Connection on Performance of Five-Phase Induction Machines," *IEEE Trans. Ind. Electron.*, vol. 61, no. 1, pp. 3-19, Jan. 2014.

[95] J. Zhang, Jin Zhao, D. Zhou, and C. Huang, "High Performance Fault Diagnosis in pwm Voltage Source Inverters for Vector Controlled Induction Motor Drives," *IEEE Trans Power Electron.*, 2014, To be published.

[96] M. Trabelsi, M. Boussak, M. Gossa. PWM-Switching pattern-based diagnosis scheme for single and multiple open-switch damages in VSI-fed induction motor drives. ISA Transactions; 51:333-344.

[97] Salehifar M, Arashloo R S, Moreno M, Sala V. Open Circuit Fault Detection Based on Emrging FCS-MPC in Power Electronics Systems," 15th European Conference on Power electronics and Applications (EPE);

2013.

[98] M. Preind, and S. Bolognani, “Model Predictive Direct Speed Control with Finite Control Set of PMSM Drive Systems,” *IEEE Trans. Power Electron.*, vol. 28, no. 2, pp. 1007-1015, Feb. 2013.

[99] S. Kouro, P. Cortes, R. Vargas, U. Ammann, and J. Rodriguez, “Model Predictive Control - A Simple and Powerful Method to Control Power Converters,” *IEEE Trans. Ind. Electron.*, vol. 56, no. 6, pp. 1826-1838, Jun. 2009.

[100] P. Lezana, R. Aguilera, and D. Quevedo, “Steady-state issues with finite control set model predictive control,” in Industrial Electronics, 2009. IECON ’09. 35th Annual Conference of IEEE, 2009, pp. 1776–1781.

[101] T. Geyer, “A Comparison of Control and Modulation Schemes for Medium-Voltage Drives: Emerging Predictive Control Concepts Versus PWM-Based Schemes,” *IEEE Trans. Ind. Appl.*, vol. 47, no. 3, pp. 1380 – 1389, Jun. 2011.

[102] J. Rodriguez, M. P. Kazmierkowski, J. R. Espinoza, P. Zanchetta, H. Abu-Rub, Hector A. Young, and C. A. Rojas, “State of the Art of Finite Control Set Model Predictive Control in Power Electronics,” *IEEE Trans. Ind. Inform.*, vol. 9., no. 2, pp. 1003-1016, May 2013.

[103] R. P. Aguilera, P. Lezana, D. E. Quevedo, “Finite-Control-Set Model Predictive Control with Improved Steady-State Performance,” *IEEE Trans. Ind. Inform.*, vol. 9, no. 2, pp. 1003-1016, May 2013.

[104] Marco Rivera, Venkata Yaramasu, Ana Llor, Jose Rodriguez, Bin Wu, and Maurice Fadel, “Digital Predictive Current Control of a Three-Phase Four-Leg Inverter,” *IEEE Trans. Ind. Electron.*, vol. 60, no. 11, pp. 4903-4912, Nov. 2013.

Appendix

CONTENTS:

A.1. Test bench

In order to evaluate the different contributions presented in this thesis work, different experimental arrangements have been used.

To validate the theory, experimental results presented are conducted on a five-phase BLDC motor; block diagram of the experimental setup is shown in Fig. A.1(a). Also, experimental setup is shown in Fig. A.1(b). As it can be seen, the five-phase motor is coupled with a commercial three-phase PMSM which serves as the load motor. The load motor is supplied with an independent AC SIEMENS drive (known as SINAMICS-S120). A national instrument card known as Compactrio is used as interface between the three phase PMSM drive and the host PC. The torque and speed references of the load motor can be set from the host PC. Also, torque and speed values of the setup are measured by a torque sensor and an encoder included in the test bench. Sensor outputs are sent to the analog inputs of the NI card.

The five-phase motor parameters are shown in table A.1. It has an outer rotor in-wheel structure; this configuration is useful for electric vehicles. The control algorithm, and FD method of the five-phase motor are implemented in a dSPACE control board model ds1005. The motor is supplied with a five-phase two-level VSI. The sampling frequency of the phase currents is 4 kHz. The dc link voltage of the VSI is 24 V; the switching frequency is 4 kHz. Besides, output current of the motor are measured by Hall Effect sensors and converters to valid voltage signals by a simple condition monitoring circuit. After that, the suitable signals are sent to dSPACE analog inputs.

Besides, due to its high number of input-outputs and high processing speed, a separate FPGA board was designed to implement the FD algorithm. The FD algorithm was implemented on an EP4CE22F17C5N FPGA Cyclone IV from Altera Company available on DE0_Nano board. The motor phase currents are sent to a signal conditioning circuit on FPGA board. The combination of Verilog and VHDL programming language with schematics are used to implement the FD algorithm.

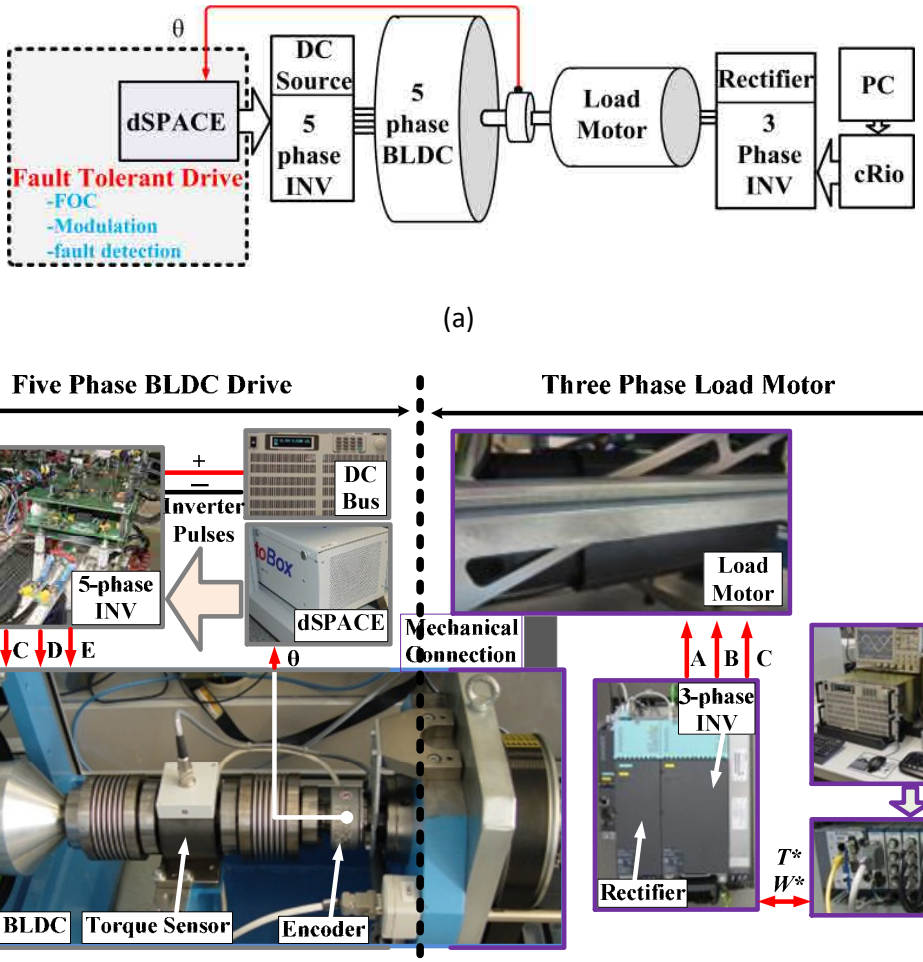

Fig. A.1. Test bench (a) Block diagram of the test bench. (b) Experimental setup.

TABLE A.1. Motor parameters

Number of Pole Pairs		26
Stator Resistance		0.1 Ω
Stator Inductance	Laa	408 µH
	Lab	15 µH
	Lac	18 µH
Nominal Torque		8 Nm
Nominal Power		350 (Watt)
Nominal Phase Current		5 (A-rms)
Nominal Phase Voltage		16 (V-rms)
Nominal Speed		400 rpm
Permanent Magnet Flux		0.48 Wb
Moment of Inertia		235 µkgm2

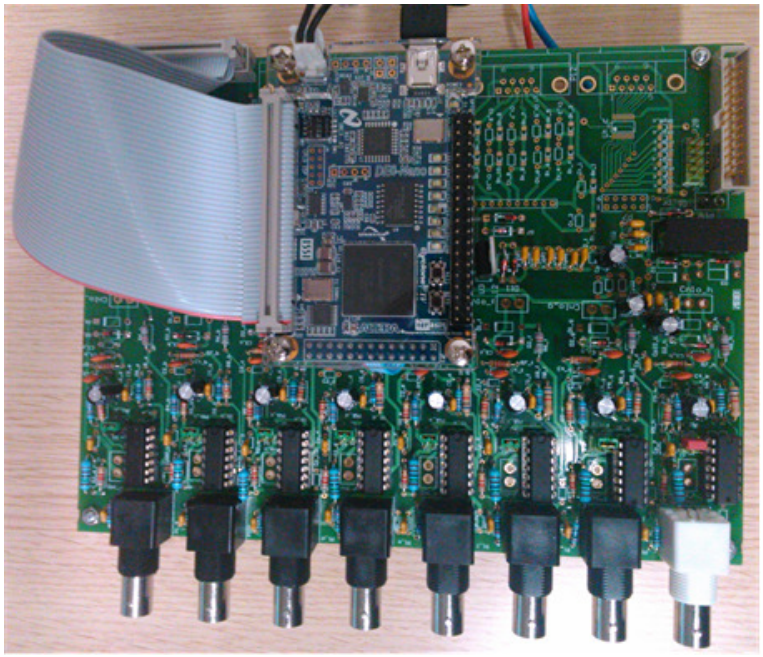

Fig. A.2. FPGA board

UNIVERSITAT POLITÈCNICA DE CATALUNYA
BARCELONATECH
Departament d'Enginyeria Electrònica